Detector Electronics and Trigger Systems – Status and Challenges

Helmuth Spieler

Physics Division
Lawrence Berkeley National Laboratory

Outline

Background and Status
Silicon Front-End Electronics for ILC and SLHC
Trigger Systems
Bolometer Readout

Original Title:

Modern Detector and Trigger Electronics

What is "modern"?

One definition ...

If it works, it's obsolete.

Marshall McLuhan

Back to reality:

If it works, it doesn't always work.

H.S.

HEP detector systems push the envelope, but we build BIG systems, so we're concerned about

1. Feasibility of large-scale construction
2. Reliable designs
3. Powerful technology (to accommodate surprises)
4. Cost

"Modern Electronics" Can't Work Miracles

"Modern Electronics" utilize circuit topologies that have been established for many years.

Under power constraints new technologies will not provide lower amplifier noise parameters, but reduction in sensor capacitance can reduce equivalent noise charge.

Smaller feature sizes reduce size of circuitry (although not necessarily in analog applications), which allows for additional circuitry to correct for shortcomings.

Examples: Small feature sizes tend to increase threshold mismatches, but facilitate compact trim DACs to correct for this.

Radiation damage shifts operating points, but digital control of bias circuitry can compensate.

However, smaller feature sizes impose smaller supply voltages, which reduce dynamic range and place constraints on circuit topology.

Major challenges unchanged:
- Isolation of digital from analog input
- Immunity to ext pickup
  - e.g. power supply noise rejection
- Packaging (detector modules)
- Power
- Material

"Modern" electronics largely adapt existing techniques to new technologies.

Monolithic technology evolves, but key techniques remain the same.

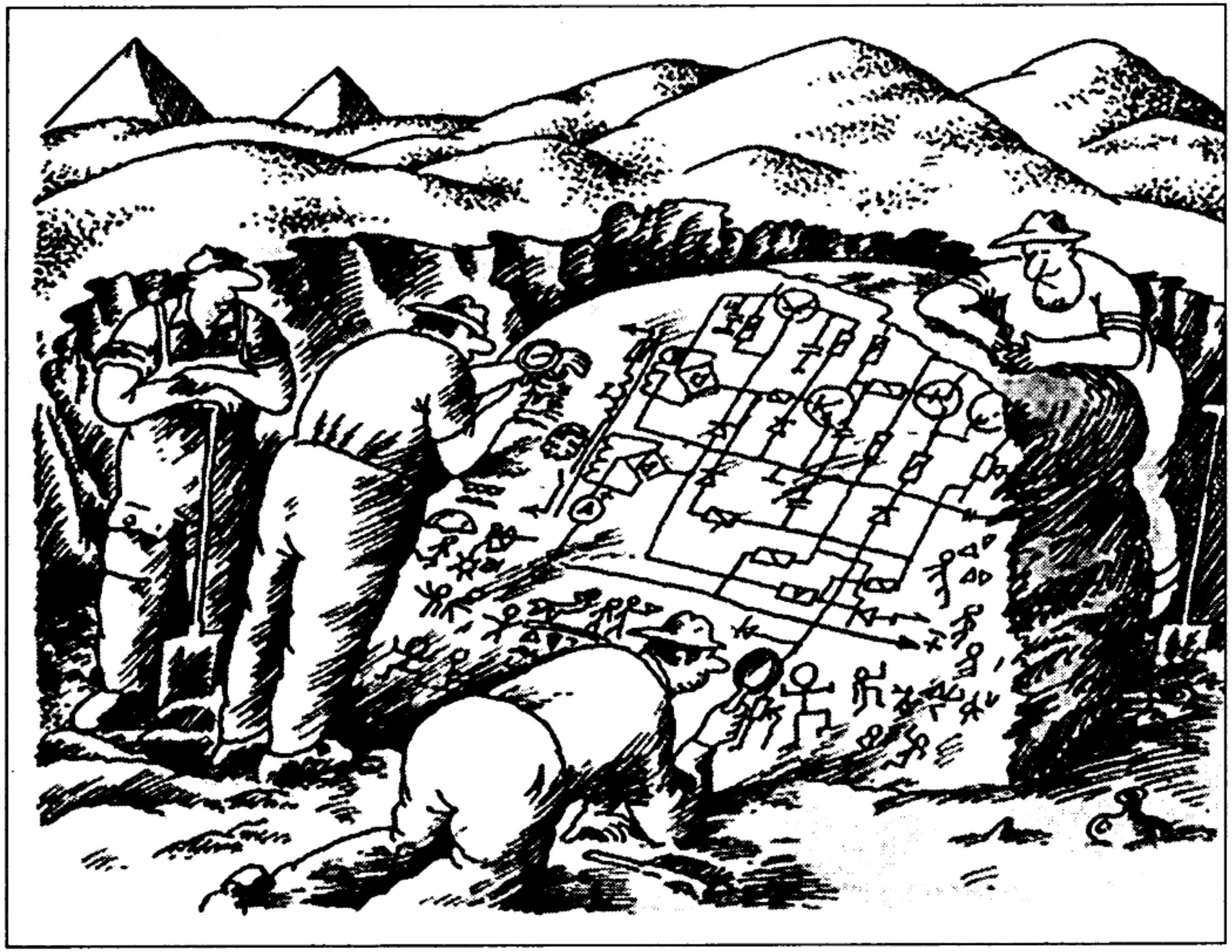

Front End IC Geneology

Microplex (S. Parker and T. Walker, ~1984)

First front-end IC designed to read out strip detectors

Architectural elements common to many subsequent designs

a) charge-sensitive amplifier

b) correlated double-sampling

c) output multiplexing

First full-custom IC designed with intimate involvement by a high-energy physicist

– set precedent for subsequent designs performed at high energy physics labs

Custom ICs brought about a major paradigm shift from discrete circuits:

Circuit topologies

Ability to tailor transistors to specific needs.

IC Family Tree

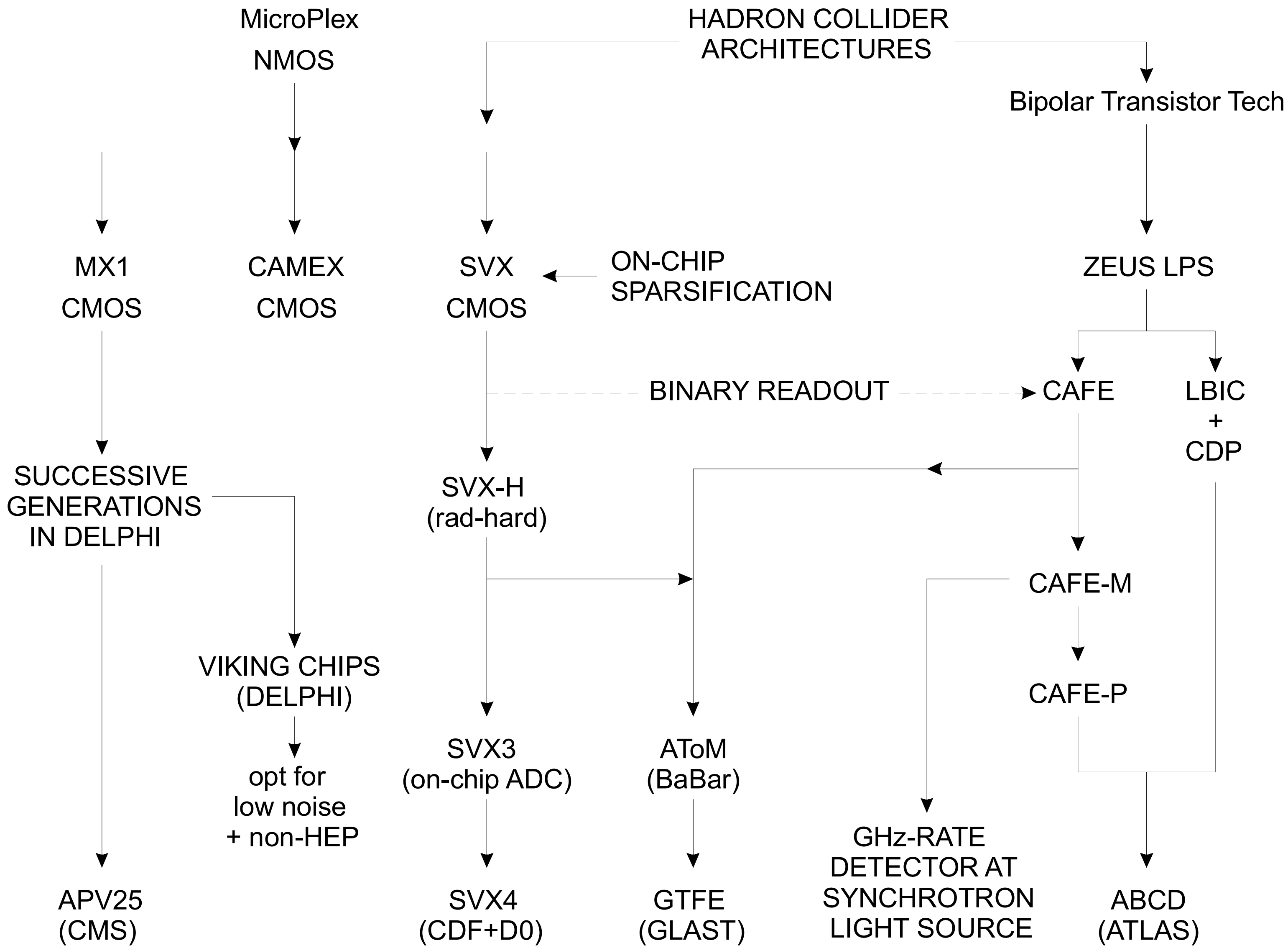

Descendents of Microplex (1984)

MX1 (1988, RAL)
- 50 μm pitch, 128 channels per chip

CAMEX (1988, MPI Physik, Fraunhofer Inst. Duisburg, Univ. Pavia)
- 50 μm pitch, 127 channels per chip + 1 reference channel
- added flexibility in pulse shaping (multiple sampling)
- 100 μm pitch version used in ALEPH: double –sided detector

SVX (1988, LBNL)
- 50 μm pitch, 128 channels per chip
- added: on-chip sparsification (zero suppression)
- first chip for hadron collider
- subsequent versions
  - rad-hard process (SVX-H)
  - on-chip analog-to-digital conversion (SVX3, 4)

APV25 (1992 – 2001)
- uses deconvolution to retrieve timing

Viking chips (CERN, Oslo)
- designed for very low noise + non-HEP applications

A major distinction between the Microplex and subsequent designs was the process:

Microplex:	NMOS
MX1, CAMEX, SVX:	CMOS

The Microplex dissipated ~10 mW per channel and required pulsing the power supply – a theme that has reappeared in ILC chip designs.

The MX1, CAMEX, and SVX reduced power by an order of magnitude.

This is commonly attributed to the use of CMOS, but this doesn't apply to analog circuitry as strongly as to digital circuits.

High power in Microplex strongly driven by excessive speed in preamplifier.

Reasoning: fast detectors require fast preamps, but this isn't true.

Front-end can be much slower than detectors, as charge is initially stored on the detector capacitance.

Conclusions: Think hard about what you REALLY need.

Buzzwords trump physics!

"Deep" Submicron CMOS

Strong decrease of MOS threshold shifts in thin oxides demonstrated in early 1980s

CERN group (Marchioro et al.) recognized potential for rad-hard electronics.

Initiated collaboration with IBM

Radiation resistance to >100 Mrad demonstrated

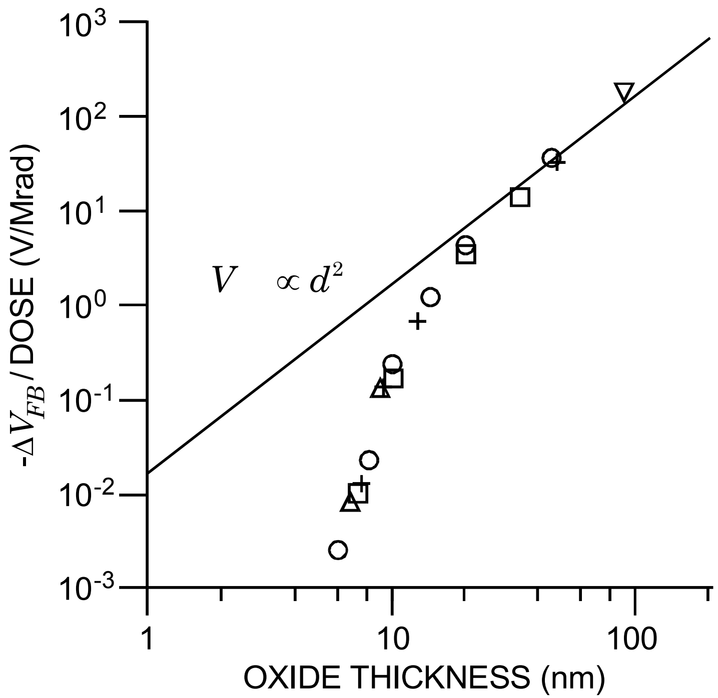

Saks et al. (1984)

Rescued APV25 (CMS tracker chip)

ATLAS pixels (prohibitive price increase by rad-hard vendor)

Crash design program provided working chips

Excellent yields

Conclusion: Possible because CERN group not bound to project timelines

US funding project-driven $\Rightarrow$ inhibits innovation

Where are we now?

CMS Silicon Tracker Front-End IC

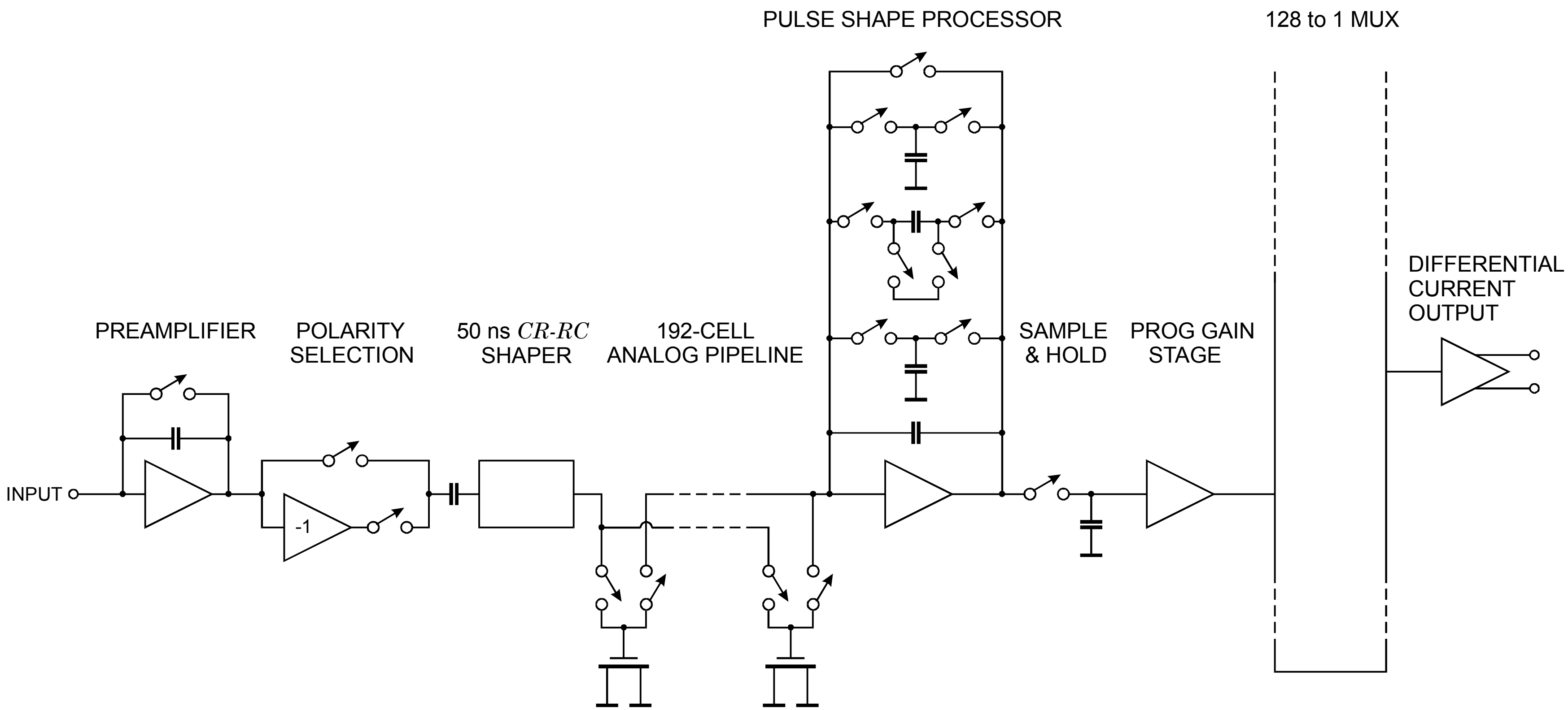

0.25 μm CMOS, Analog Readout, 1.8 mW/ch, Q_n = 396 e + 59.4 e/pF
Deconvolution shaper to allow 25 ns time stamping

ATLAS SCT Silicon Strip Front-End IC

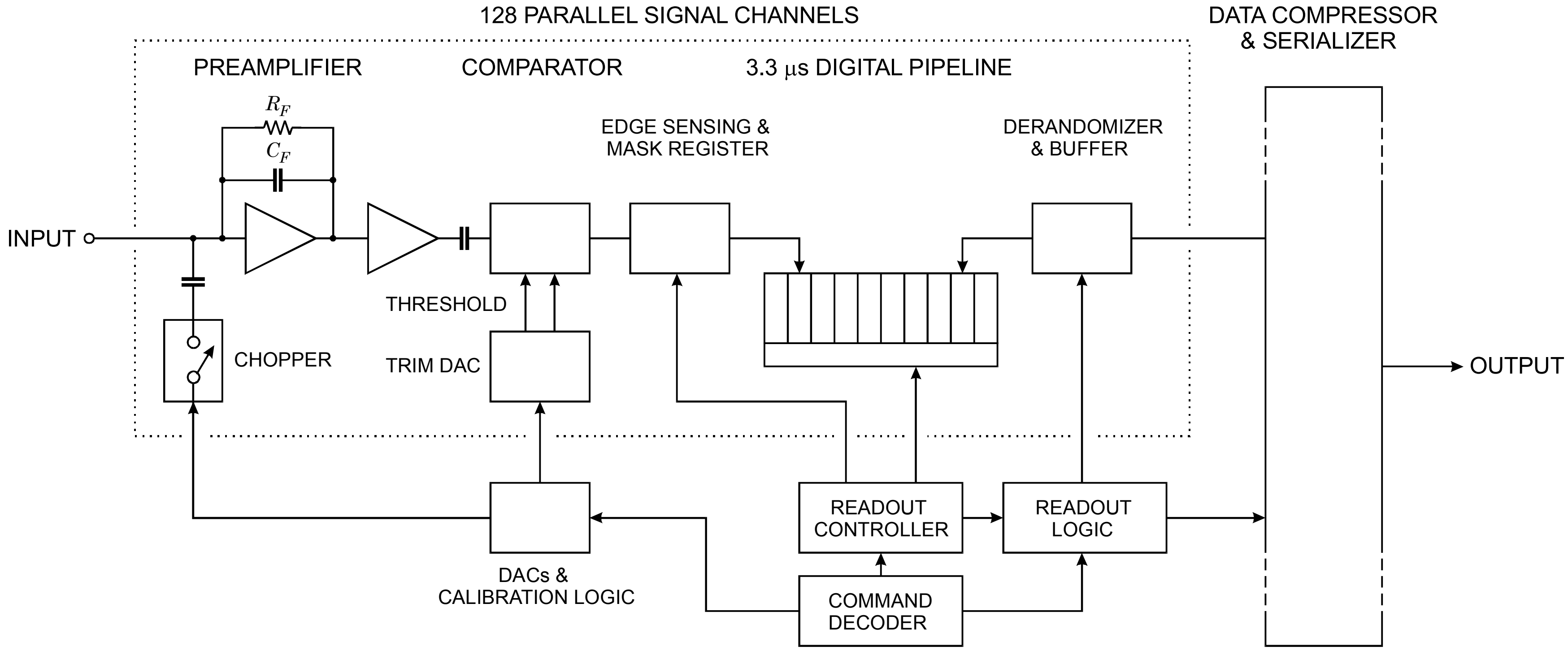

DMILL BiCMOS, 1.3 – 1.8 mW/ch, Q_n < 1500 e (12cm strips), **Binary Readout**

↑

Dead End

ATLAS Pixel Detector

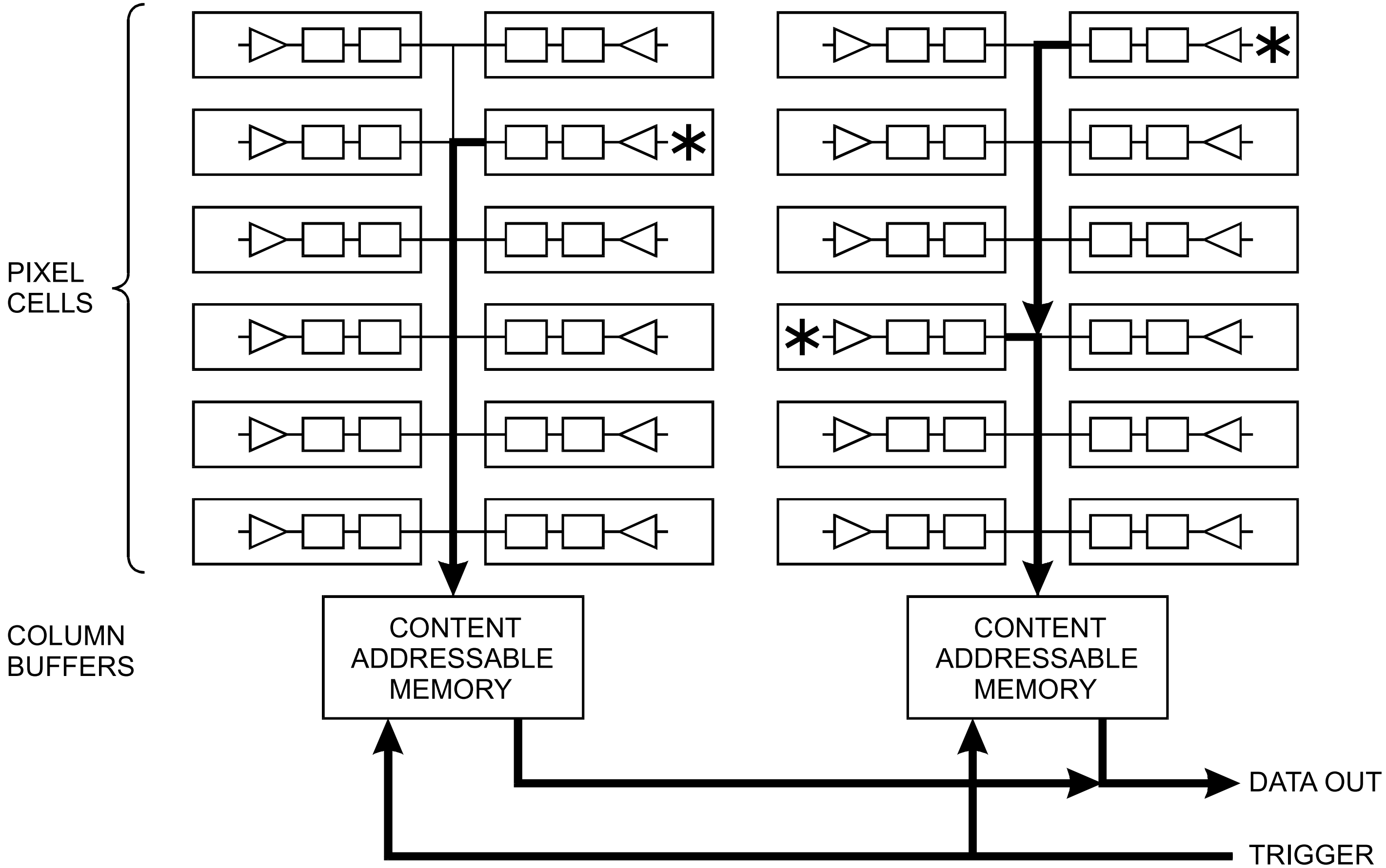

Pixels continuously active, but don't send signals until struck (self-triggered).
Time stamp for struck pixels stored immediately in Content Addressable Memory
Data stored in pixel until Level 1 trigger received for stored time stamp.

ATLAS Pixel Cell

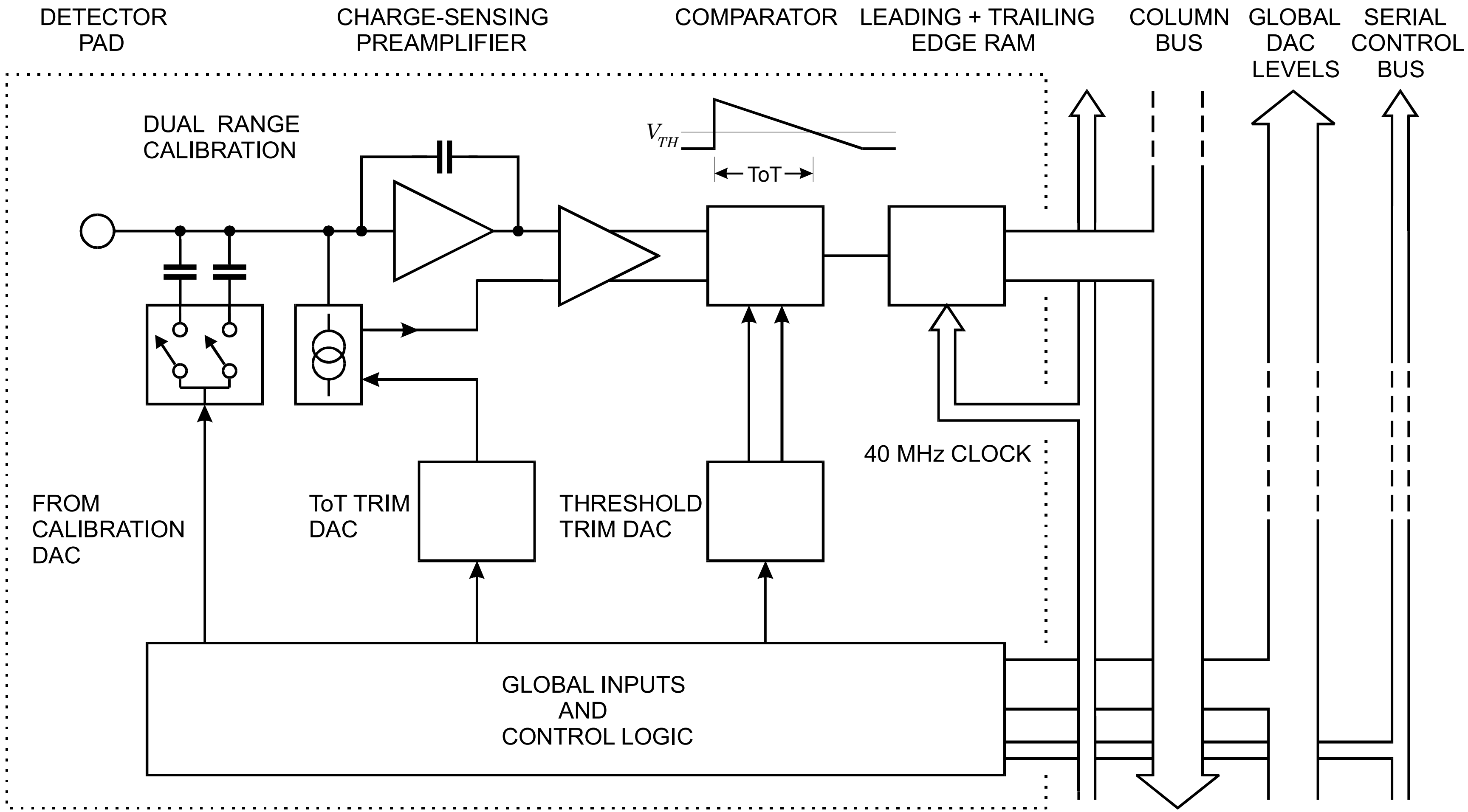

0.25 μm CMOS, $Q_n \approx 170$ e

40 μW per cell; total power for 2880 pixels: 200 mW (incl. peripheral circuitry)

Threshold dispersion must be smaller than noise.
Small feature sizes ⇒ large threshold dispersion ⇒ correct with trim DAC

Threshold dispersion before and after trimming

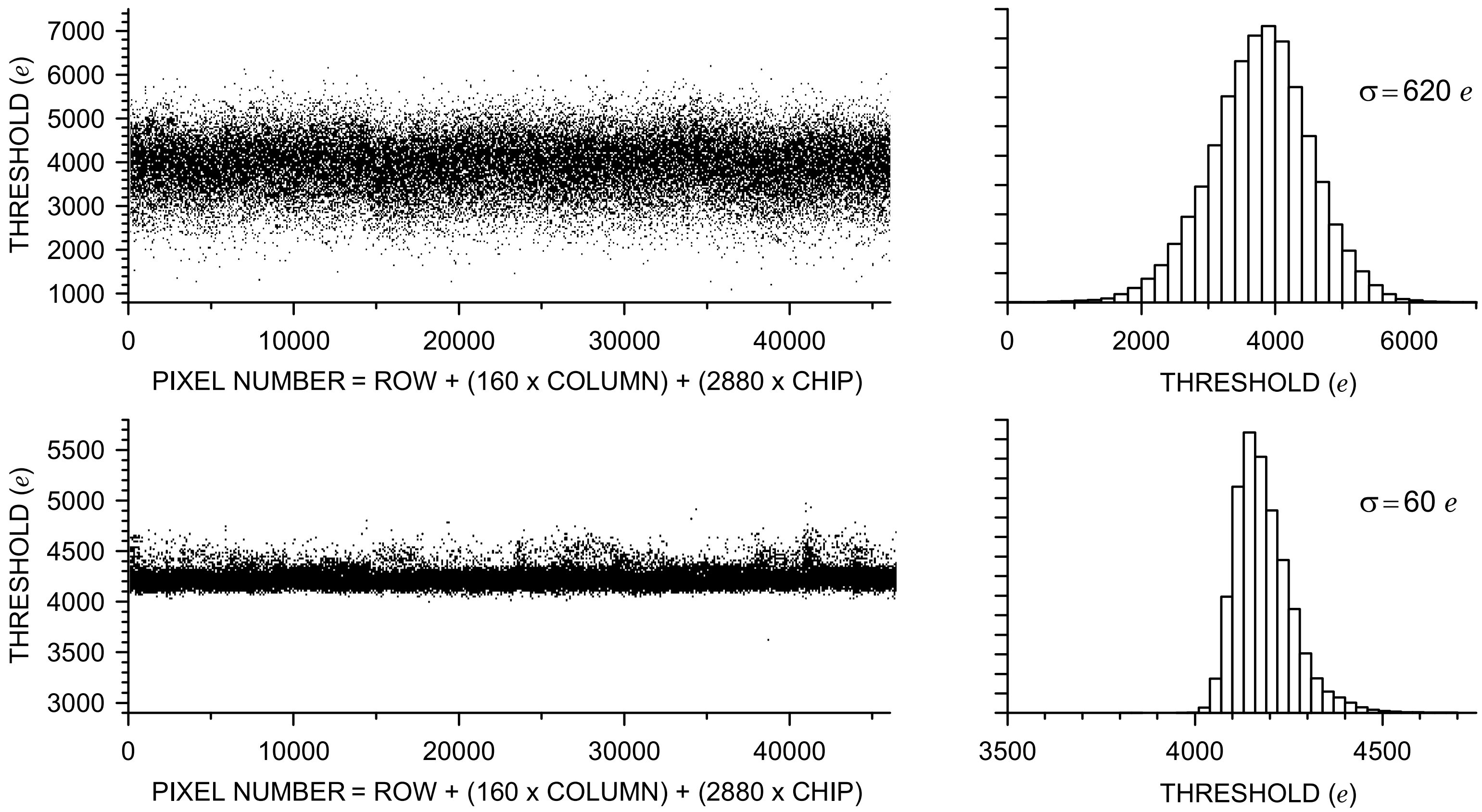

Where are we Going?

ILC: μm position resolution in vertex detector (1 – 5 μm)

⇒ ~20 μm pixels

Jet (multi-track) resolution

Minimal mass

⇒ monolithic pixel devices
(CCDs, MAPs, DEPFETs, multi-tier ICs?)

⇒ low-mass power distribution, cooling

SLHC: 10-fold luminosity

$\Rightarrow$ radiation hardness limited primarily by sensor

Charge trapping in the sensor $\Rightarrow$ reduced signal

To maintain S/N we can

a) reduce electronic noise

$\Rightarrow$ increased power (front-end power $\propto (S/N)^2$)

and/or

b) reduce sensor capacitance

pixels (material, power, cost)

reduce strip length

$\Rightarrow$ more readout ICs per unit area

$\Rightarrow$ low-mass power distribution, cooling

ICs: Reduce power: SiGe BiCMOS?

Reduce size per cell: multi-layer electronics?

Hybrid pixels allow optimization of sensor and readout, but at the expense material and cost.

Simplifications?

Next-Generation Pixel Devices

Monolithic Active Pixel Sensors (MAPS)

Utilize epi layer of "standard" CMOS as sensor

Charge collection by diffusion ⇒

limits speed, radiation resistance

OK for ILC

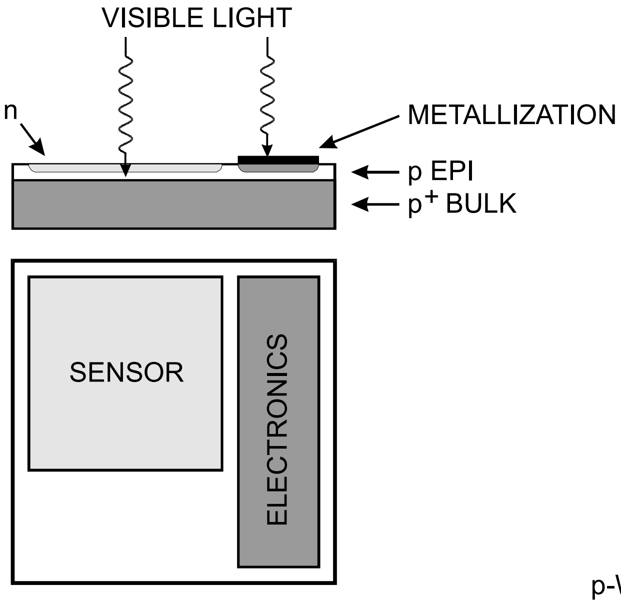

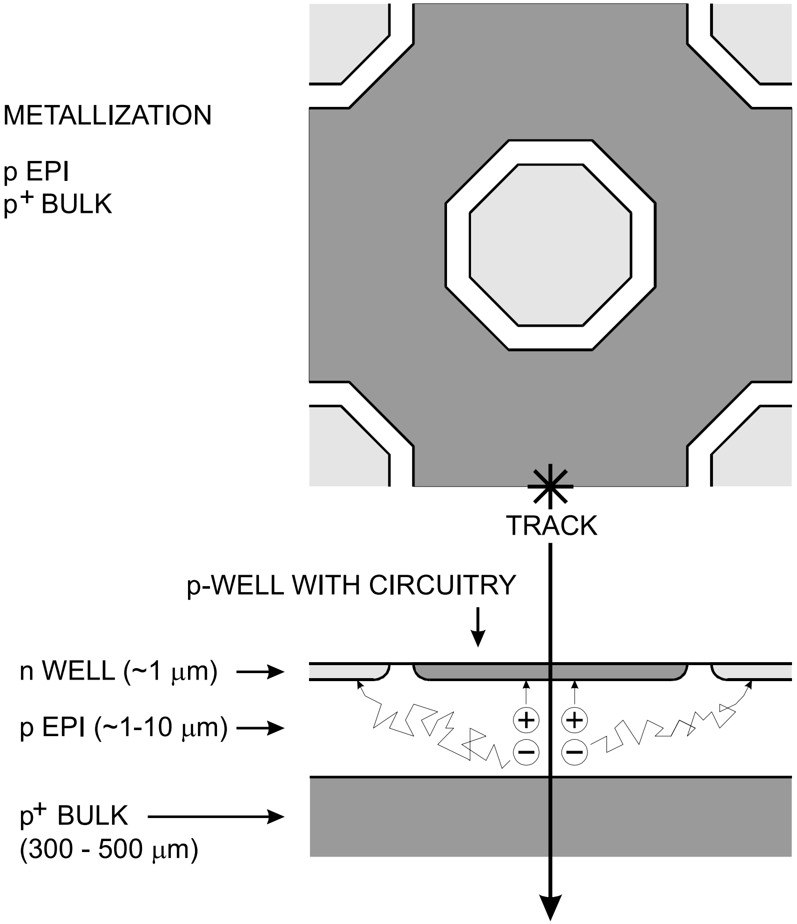

Designs with ~90% active area (see posters)

Chips can be thinned to ~50 μm to reduce material. (Battaglia et al.)

Simple MAPS Output Circuit

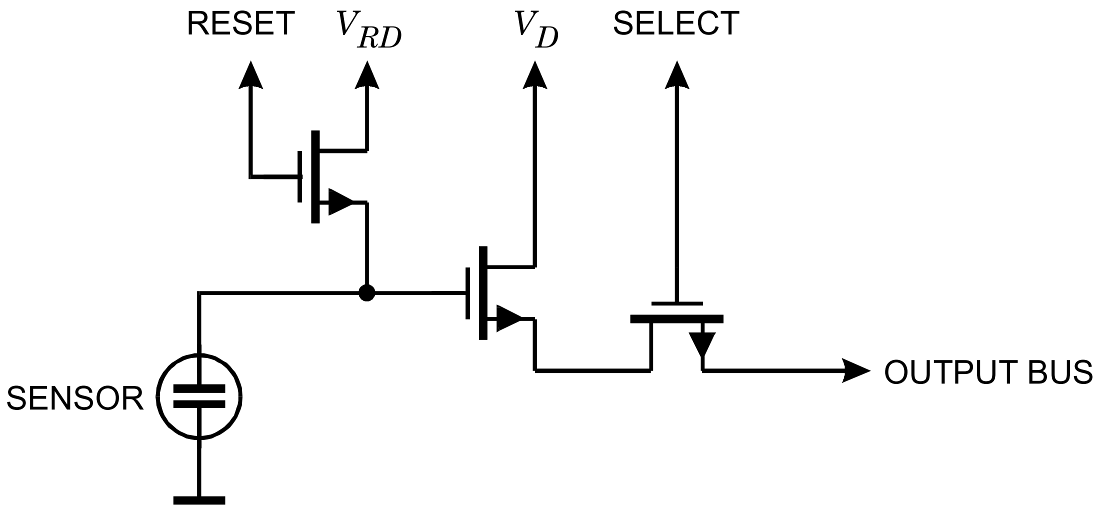

Some designs implement correlated double sampling on each pixel.

Requires that all pixels be read out, so readout time extends over many beam crossings. Frame rate determines shot noise contribution to Q_n.

Reduce readout time: Full processing chain (preamp, shaper, comparator) required to implement on-chip sparsification.

e.g. see poster by Traversi et al.: 0.13 μm CMOS, 25 μm pixel, but threshold dispersion ≈ elec. noise

Multi-Tier Electronics (aka “SOI” or “3D”)

CMOS Circuitry

Isolation Oxide

Sensor Layer

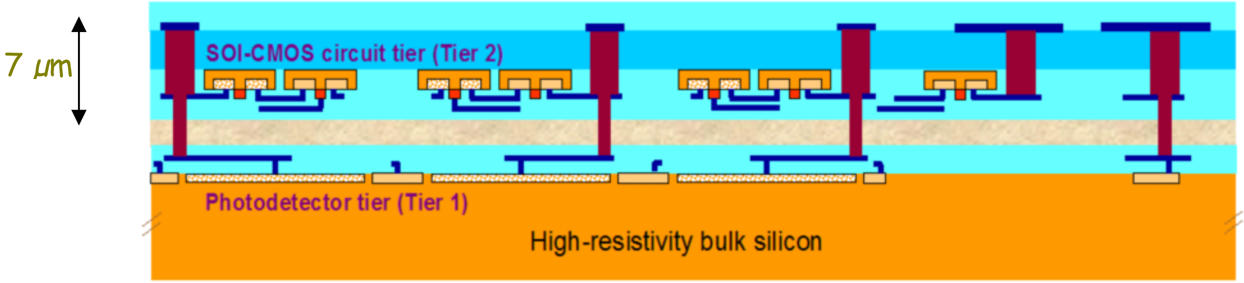

MIT Lincoln Lab

3-Tier Design (FNAL)

3 transistor levels
11 metal layers

Accommodate additional circuitry for given pixel size.

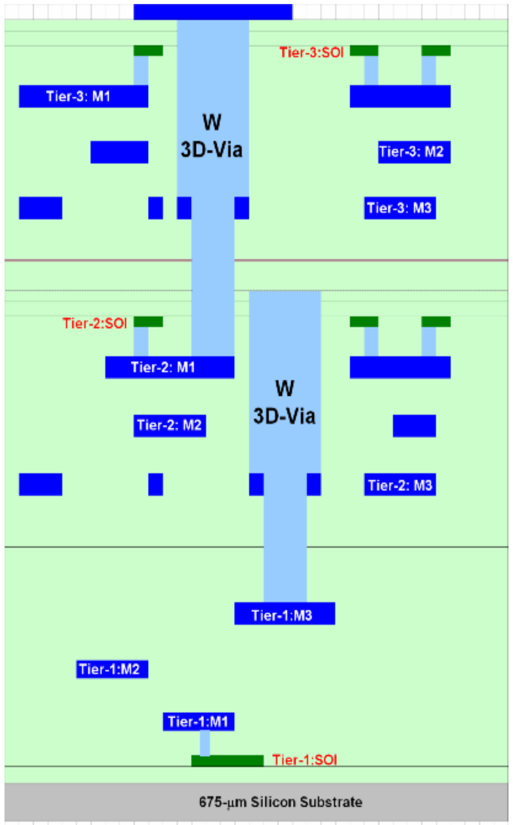

(R. Lipton, STD6)

Test Chips designed at KEK (Arai et al.)

Fabricated by OKI

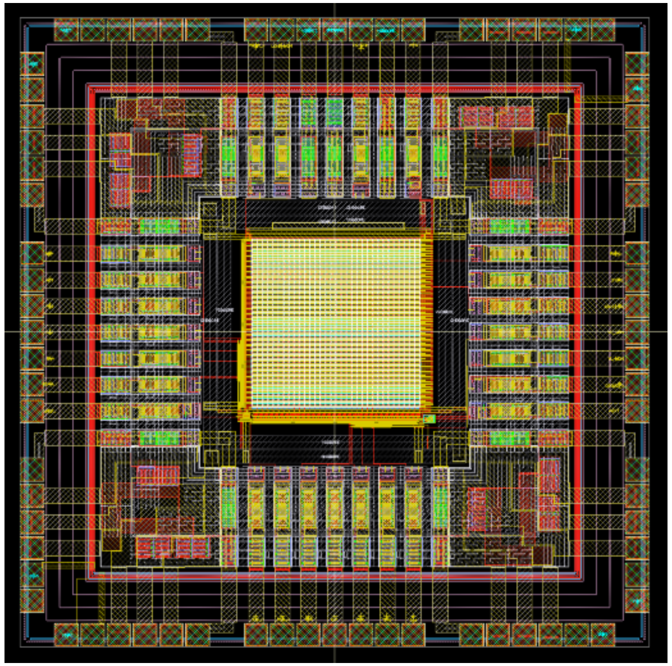

Image (20 μm pixels)

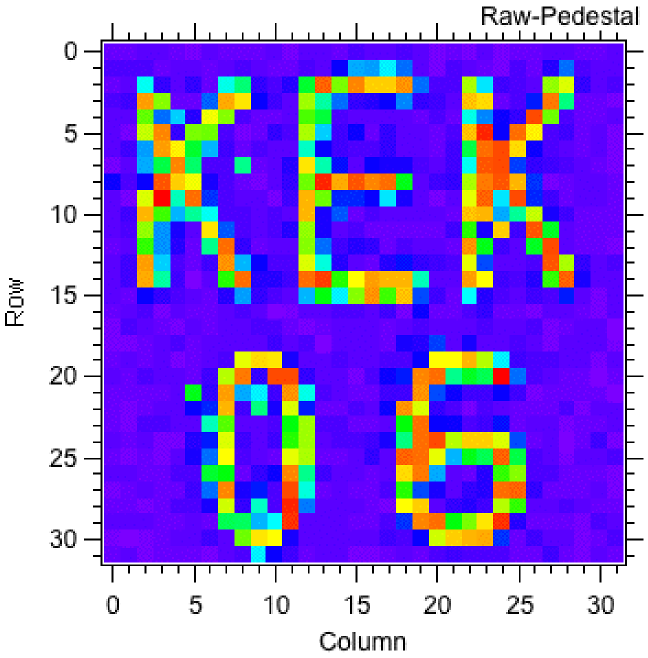

High resistivity substrate (1 kΩ cm CZ) thinned to 350 μm.
(see talk T6.9 by Tsuboyama et al.)

Radiation resistance of sensor layer in industrial processes inadequate for SLHC, but suitable for ILC.

Both ILC and SLHC drive developments towards higher levels of segmentation.

ILC: micron-resolution pixel detectors for vertexing.

SLHC: short strips and pixel detectors to increase radiation resistance.

However, power constraints remain

Cooling (material)

Cabling (material + heat due to I^2R losses $\rightarrow$ cooling)

Material in ATLAS Silicon Tracker Barrel

Total material per layer:
3% X_0.

Half is services:
- cooling
- cabling
- carbon fiber support

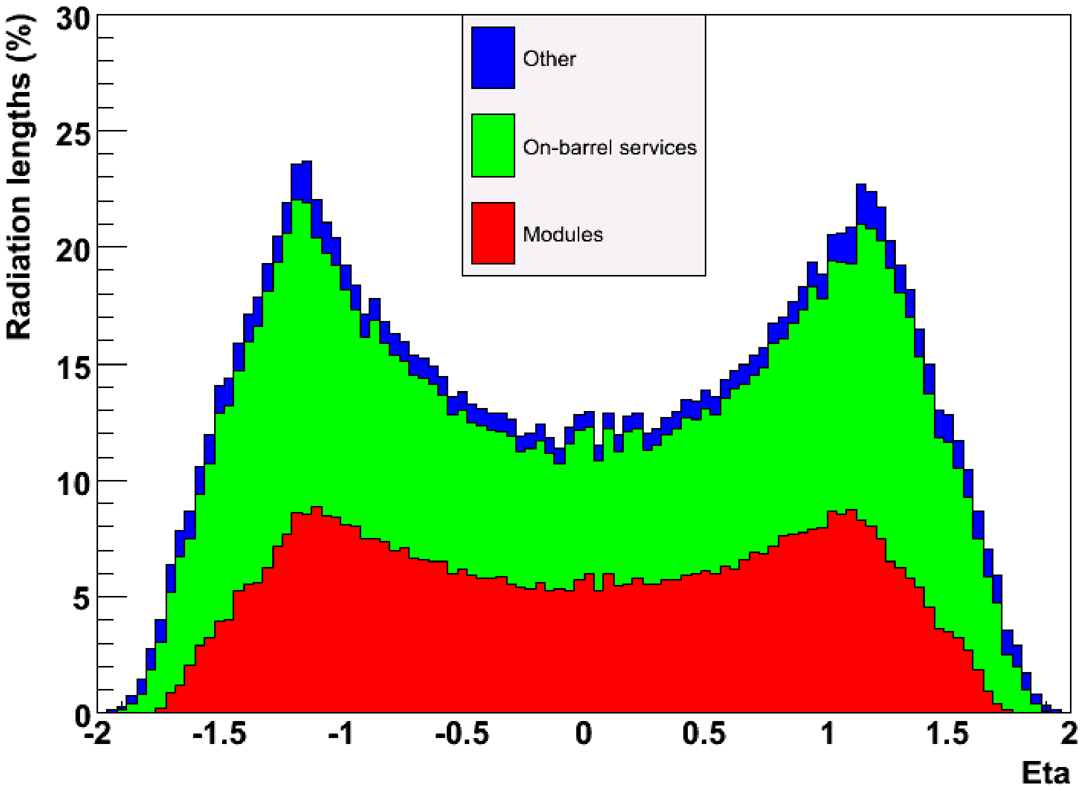

(see http://www.hep.phy.cam.ac.uk/~cpw1/atlas.html)

ATLAS Pixel Detector:		
	Total (3 layers)	10.7% X_0
	Hybrids + Cables	1.3% X_0
	Support + Cooling	6.9% X_0

Goal: Increase power efficiency

Digital circuitry:

Reduced voltage swings and circuit capacitance reduce power consumption

$$P = fCV^2$$

Smaller CMOS feature sizes reduce both the voltage swing V and capacitance C, so for a given switching rate f power decreases.

Analog front-end:

Equivalent Noise Charge: $Q_n^2 \approx i_n^2 T_S + e_n^2 C_d^2 \frac{1}{T_S}$

T_S	Shaping Time			
i_n	Spectral noise current density	$i_n^2 = 2eI_{bias}$	$\propto$	strip length
C_d	Detector capacitance		$\propto$	strip length
e_n	Amplifier spectral noise voltage density	$e_n^2 \approx \frac{1}{g_m}$		

In analog circuitry the current draw is driven by the requirements of noise and speed.

Both depend on transconductance $g_m = \dfrac{dI_C}{dV_{BE}}$ (BJT) or $g_m = \dfrac{dI_D}{dV_{GS}}$ (FET).

Transconductance in a bipolar transistor (BJT) depends only on current, not on geometry (determined by basic physics):

$$g_m = \frac{I_C}{kT/e} = 38.5 \cdot I_C$$

FET transconductance is a non-linear function of current (W=100, L= 0.8 μm):

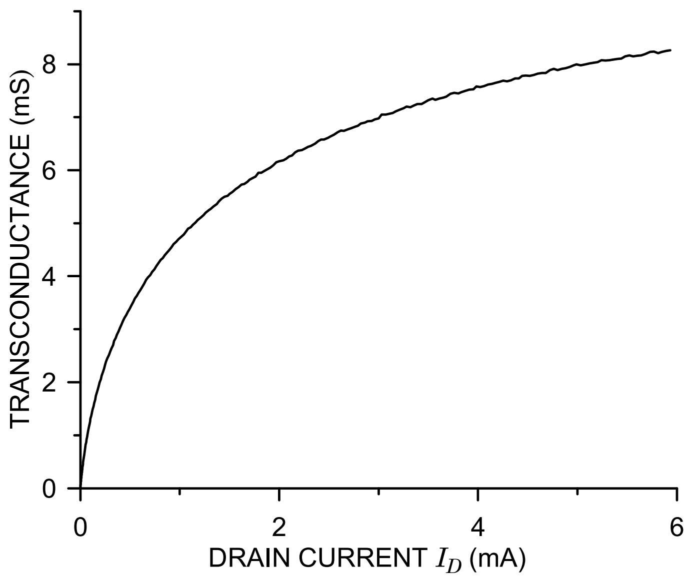

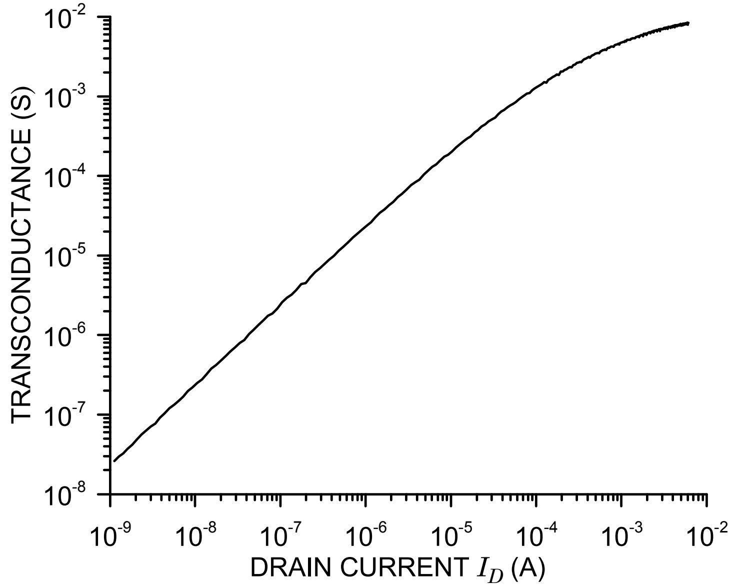

Power efficiency depends on transconductance per unit current g_m / I_D

Measurements on 0.8 μm process

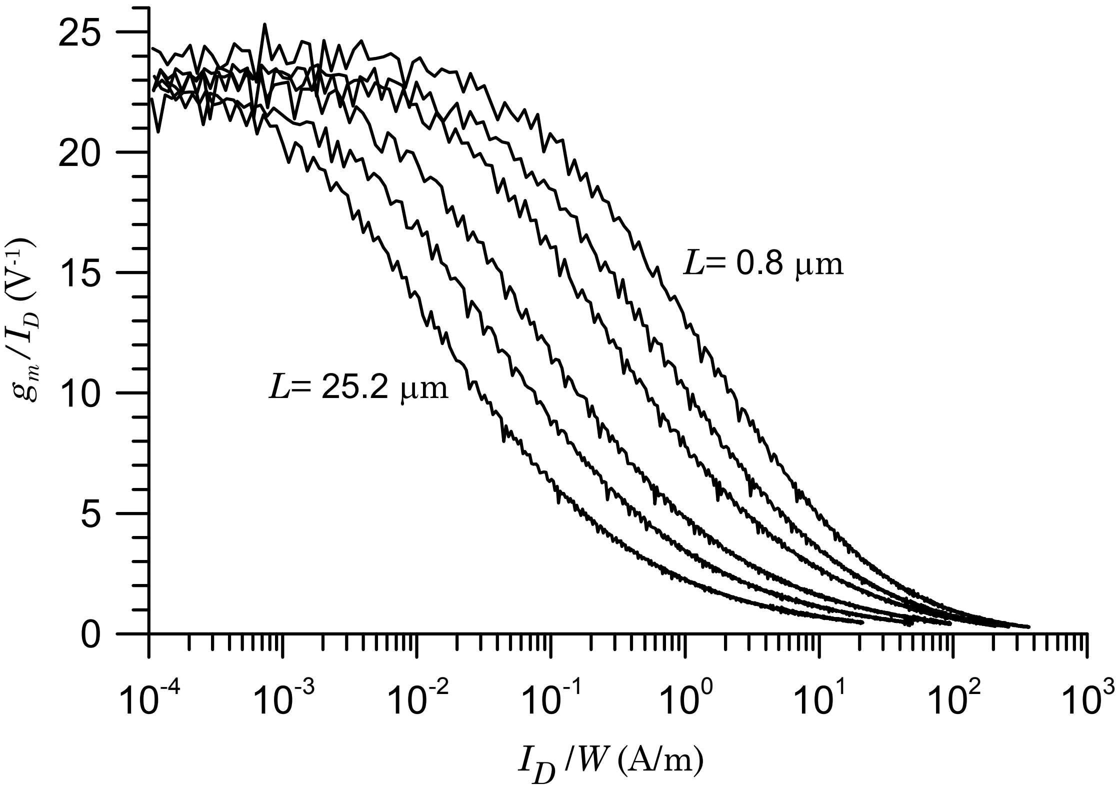

↑ weak inversion ↑ strong inversion

In weak inversion the transconductance depends only on current, not geometry!
Independent of feature size!

Historical development from 3 micron (early ‘80s) to 0.8 micron CMOS (~1998)

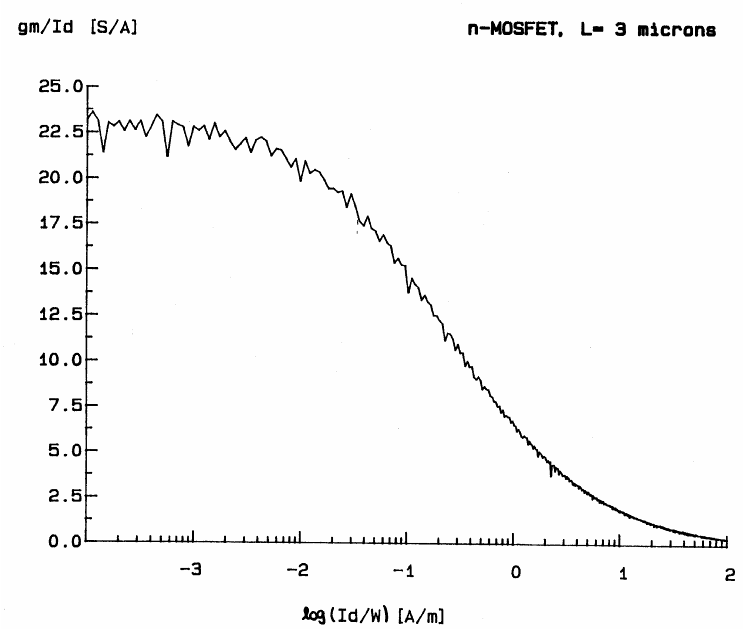

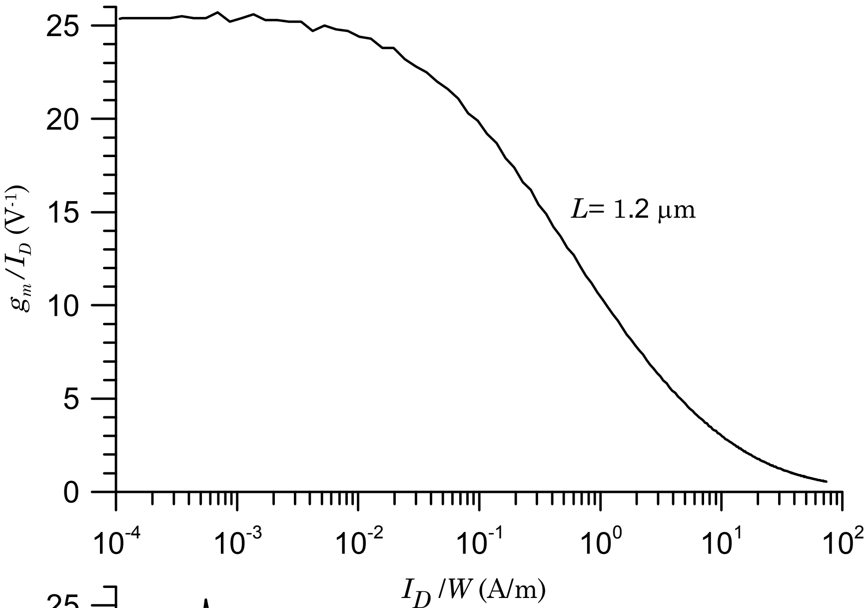

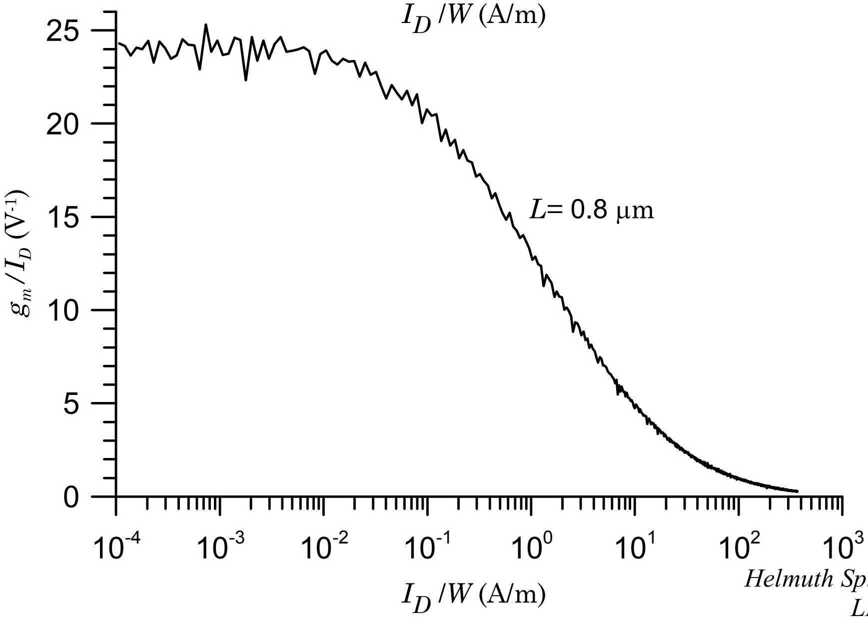

Example:
For I_D / W = 1 the reduction in feature size increases the transconductance per unit drain current:

$$L = \quad 3\ \mu\text{m} \rightarrow 1.2\ \mu\text{m} \rightarrow 0.8\ \mu\text{m}$$
$$g_m / I_D = 6.5 \quad \rightarrow 10 \quad \rightarrow 14\ \text{V}^{-1}$$

Processes with reduced feature size do not necessarily improve power efficiency.

Comparison of 0.8 μm and 0.25 μm CMOS processes

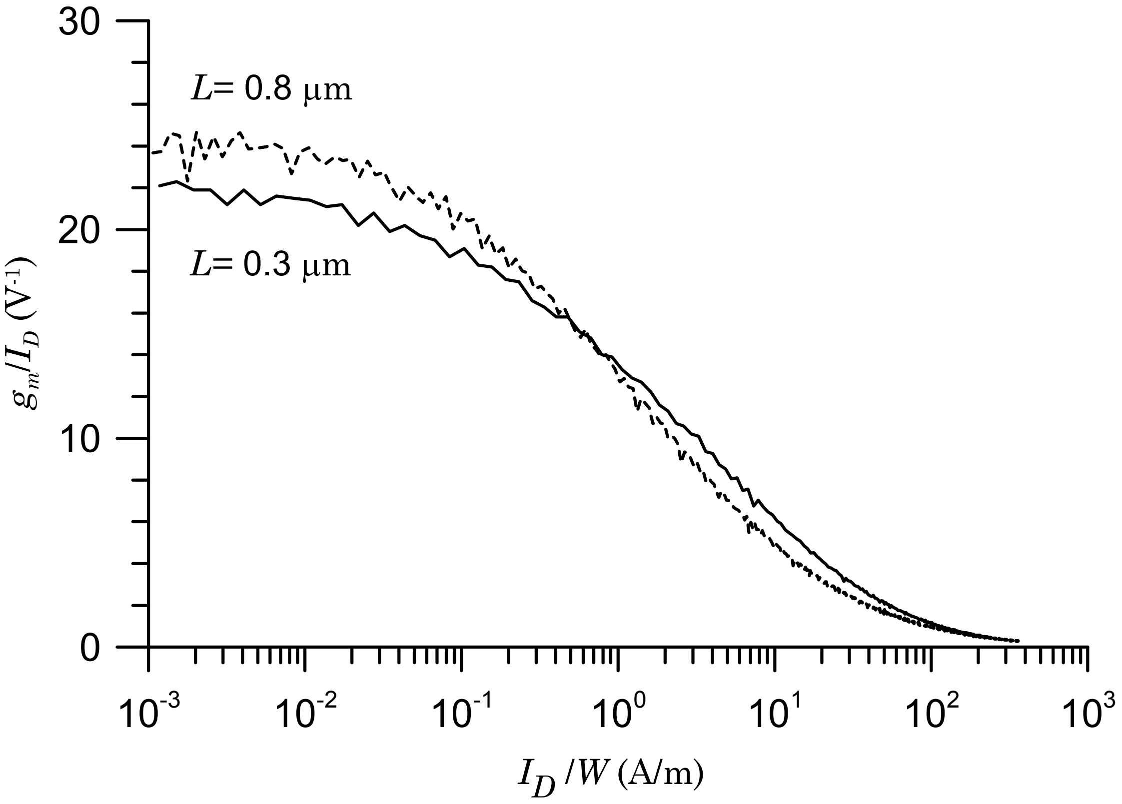

In “deep submicron” CMOS weak inversion operation possible in many detectors.

However, bipolar transistors superior by at least factor 1.6.

⇒ “Optimal” process: BJT for analog, CMOS for digital circuitry

Radiation resistance

0.25 μm CMOS shown to be usable to >100 Mrad (p fluence $\Phi > 3{\cdot}10^{15}$ cm^{-2})

Bipolar transistors limited by degradation in DC gain $\beta_{DC} = I_C / I_B$

$$\frac{1}{\beta_{DC}} = \frac{1}{\beta_0} + K\Phi$$

BJT Optimum noise: $Q_n^2 \approx 4kT \dfrac{C_d}{\sqrt{\beta_{DC}}}$ (C_d = detector capacitance)

Current gain often degraded by radiation effects in isolation structures:

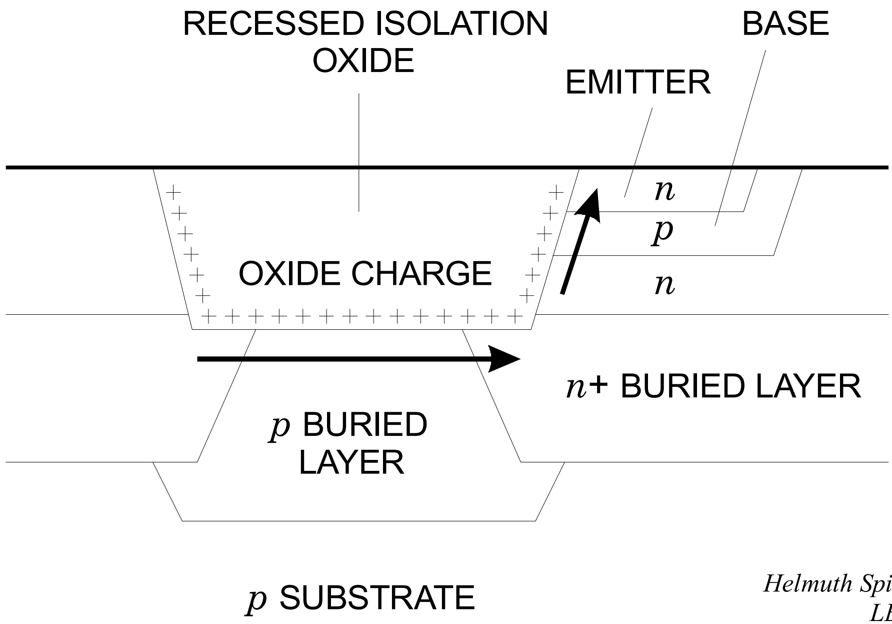

SiGe heterostructure BJTs used together with high density CMOS (BiCMOS).

Measured DC gain vs. fluence (Grillo et al., UC Santa Cruz) for various emitter sizes (all devices at the same emitter current density of 10 $\mu A/(\mu m)^2$)

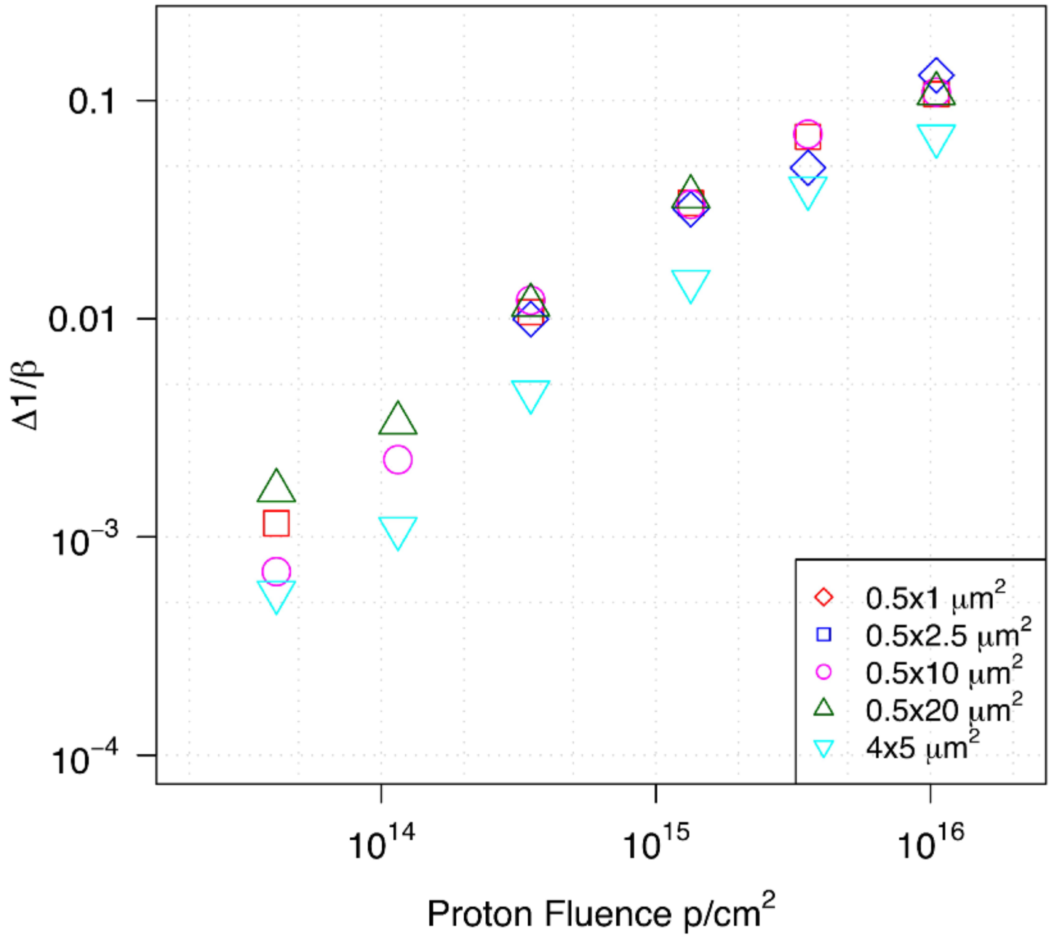

Gains in electronic noise vs. power are limited.

Alternatives?

Assume reduced signal charge S_{rad} / S_0 due to trapping:

Under optimum scaling to maintain signal-to-noise ratio,

input transistor power (≈ preamp power) scales with $(S_0 / S_{rad})^2$.

see Spieler, *Semiconductor Detector Systems*, Ch. 6

Best to scale strip length by S_{rad} / S_0.

Increases number of readout ICs by S_0 / S_{rad}

Increases power by S_0 / S_{rad}

Power services already major contribution to tracker material.

How to provide power more efficiently while reducing material?

Power Distribution

Both SLHC and ILC require more efficient power distribution schemes than existing designs.

1. Material in ILC critical, so material in power cabling must be minimized.

   Vertex detector requires pixels of ~20 μm size ⇒ ~10^8 channels.

2. ~10-fold particle flux at SLHC imposes shorter strips in tracker.

3. Deep submicron processes operate at reduced supply voltages

Examples:	180 nm	Logic supply	1.8 V	max
	130 nm		1.2 V	max

Voltage drops in power cabling must be well-controlled

Failure of one detector module, for example, must not raise voltage too much.

Key circuit parameters (e.g. transconductance, switching power) define current (not voltage), so current cannot be reduced arbitrarily.

Power conversion circuits allow supply at higher voltage (and reduced current).

⇒ reduced current and higher allowed ΔV allow less material in cabling.

Two Powering Schemes

1. Serial connection of detector modules

   Local regulators maintain module voltage with varying loads

2. Local voltage step-down regulators

   a) Pulse-width regulators

   b) Switched charge-pump circuits can operate at high efficiency

      No inductors needed

In addition, at ILC the beam duty cycle allows powering off of electronics between pulse trains.

$\Rightarrow$ forced air cooling probably practical

1. Serial Powering

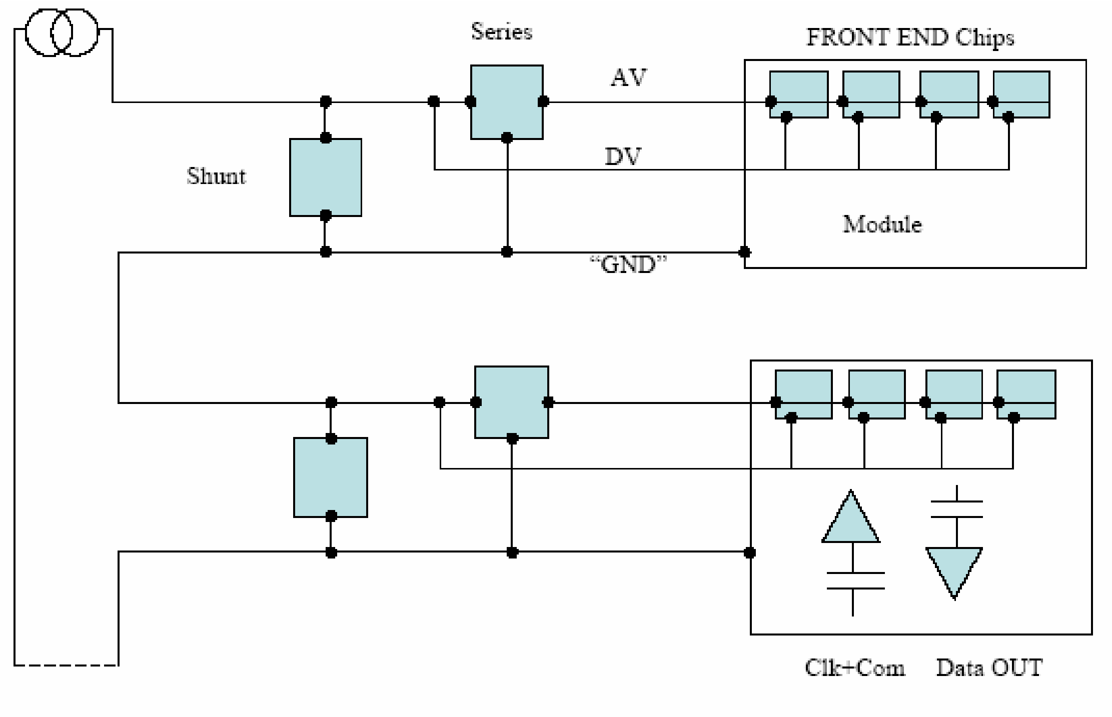

Carl Haber

Constant current through all modules.

Local regulators either on chip or module generate voltages.

Initiated at Univ. Bonn (see Ta *et al.* NIM A557 (2006) 445).
Studies at at Bonn, RAL, LBNL show little or no degradation of electronic noise using ATLAS pixel and SCT ICs.

2. Parallel powering with local switching regulators to convert high supply voltage to low voltage for ICs

2a. Pulse width modulation

Proof of Principle:
Commercial parts available, but not rad-hard

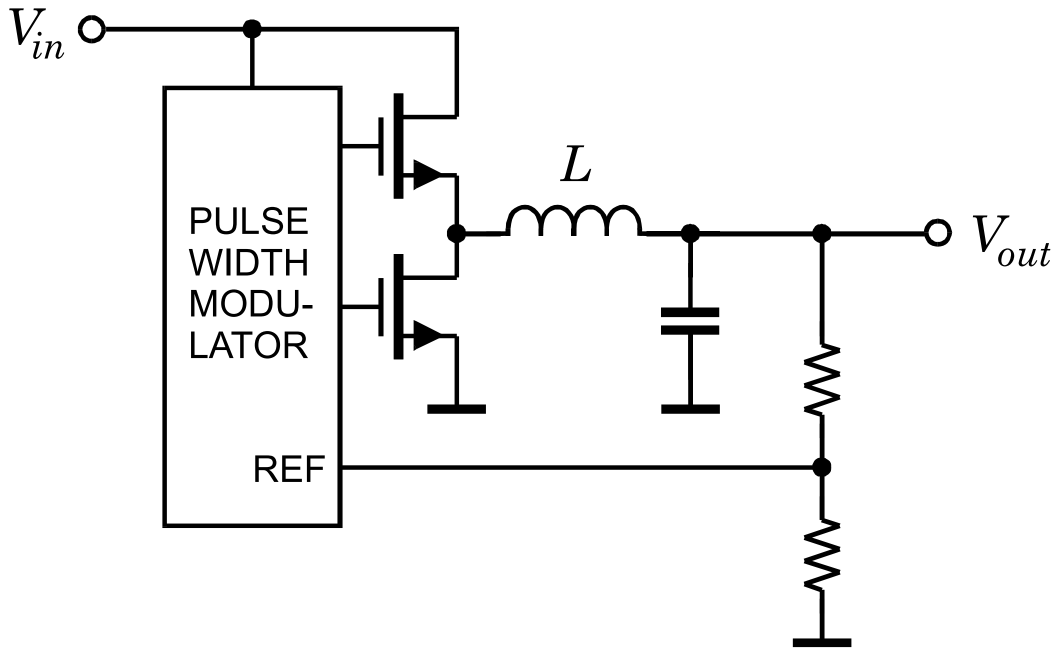

Example:	LTC 3415
Input range	2.25 – 5.5 V
Output	1.8 V, 7 A
Frequency	~1.5 MHz
Inductor L	200 nH (air core)
Efficiency	~85% (0.1 – 7 A)

Output noise (spread spectrum) ~50 mV (see work by S. Dhawan, Yale)

Front-end ICs typically have poor power supply noise rejection (typically gain).

Requires special post-regulator effective at high-frequencies.

2b. Charge Pump

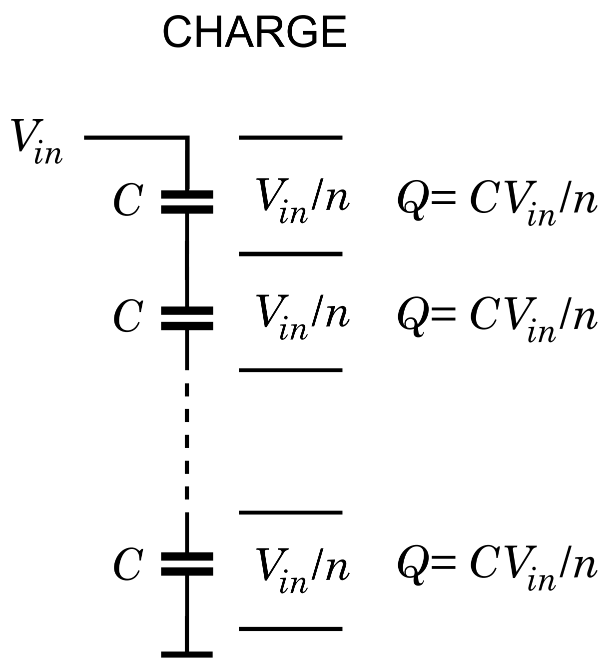

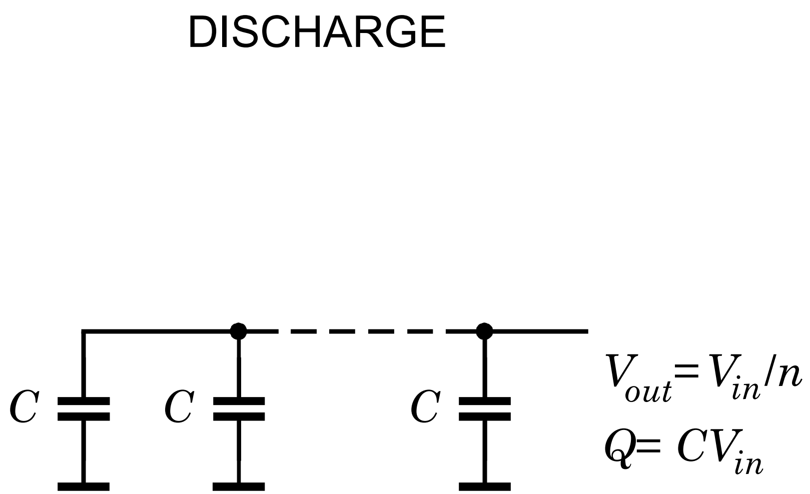

Use MOSFET switches to rearrange connections

Losses: on-resistance of MOSFETs

$$P = fCV^2 \quad (f = \text{switching frequency})$$

Lower ripple than pulse-width regulator

Simple in principle, but practical implementation more complicated:

Design by P. Denes (LBNL)

V_{in} = 12.4V
V_{out} = 2.23 V

2 MHz clock: 65% eff.

5 MHz clock: 57% eff.

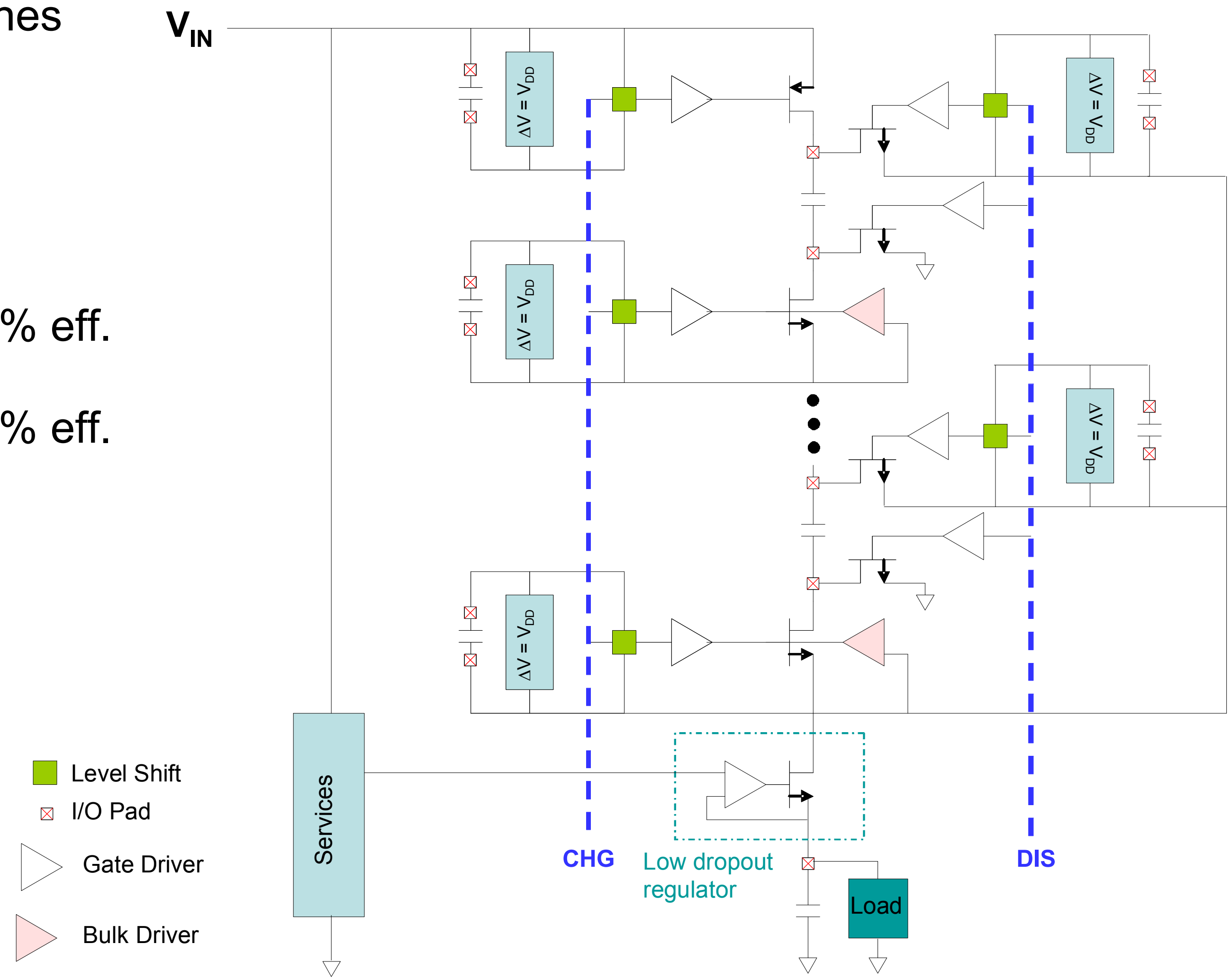

Power Cycling

At the ILC the time between bunch trains is long enough that substantial power savings are possible by switching the electronics off between bunches.

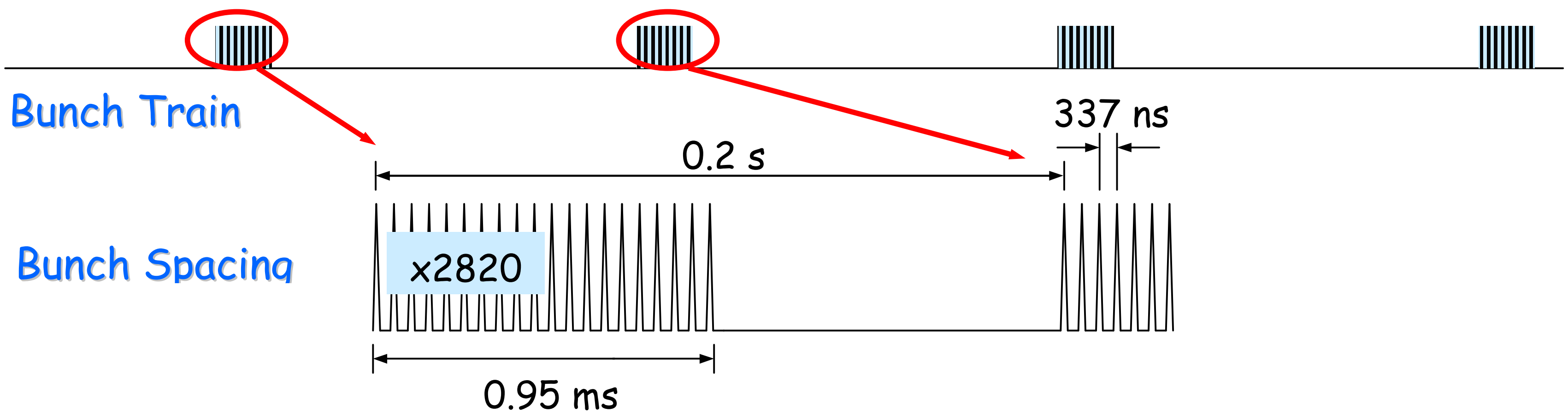

Figure: Ingrid-Maria Gregor

Power cycling measured on strip det IC with 1.2 μs shaping time
(B. Schumm, UCSC)

Power

Preamp Output

Shaper Output

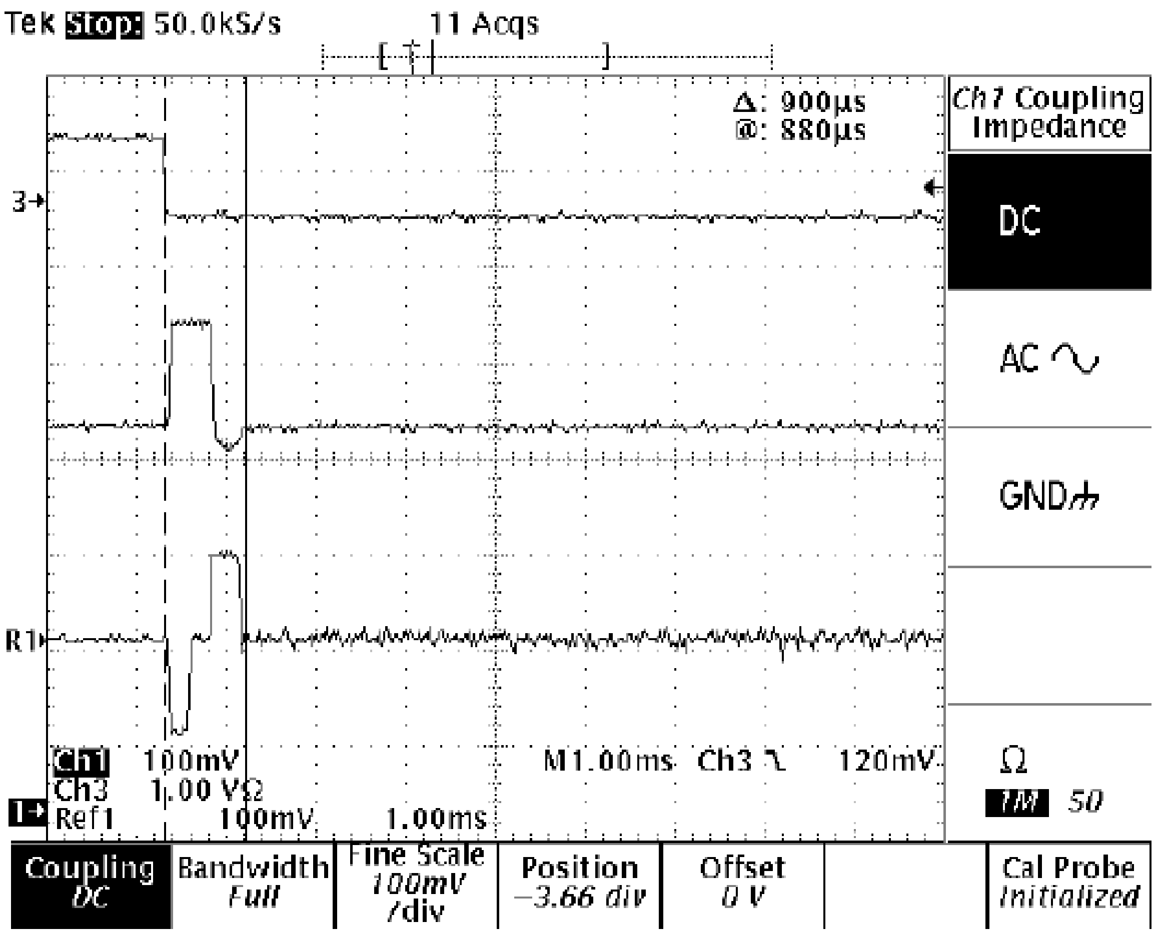

Trigger Systems

Example: ATLAS

High P_T trigger formed from regional calorimeter data and muon trigger detectors

Silicon Tracker is read out upon receipt of Level 1 trigger.

Latency is sum of Level 1 processing time and round trip cable delays from the detector to the electronics gallery.

see Poster B9
Berge,
ATLAS L1 Trigger

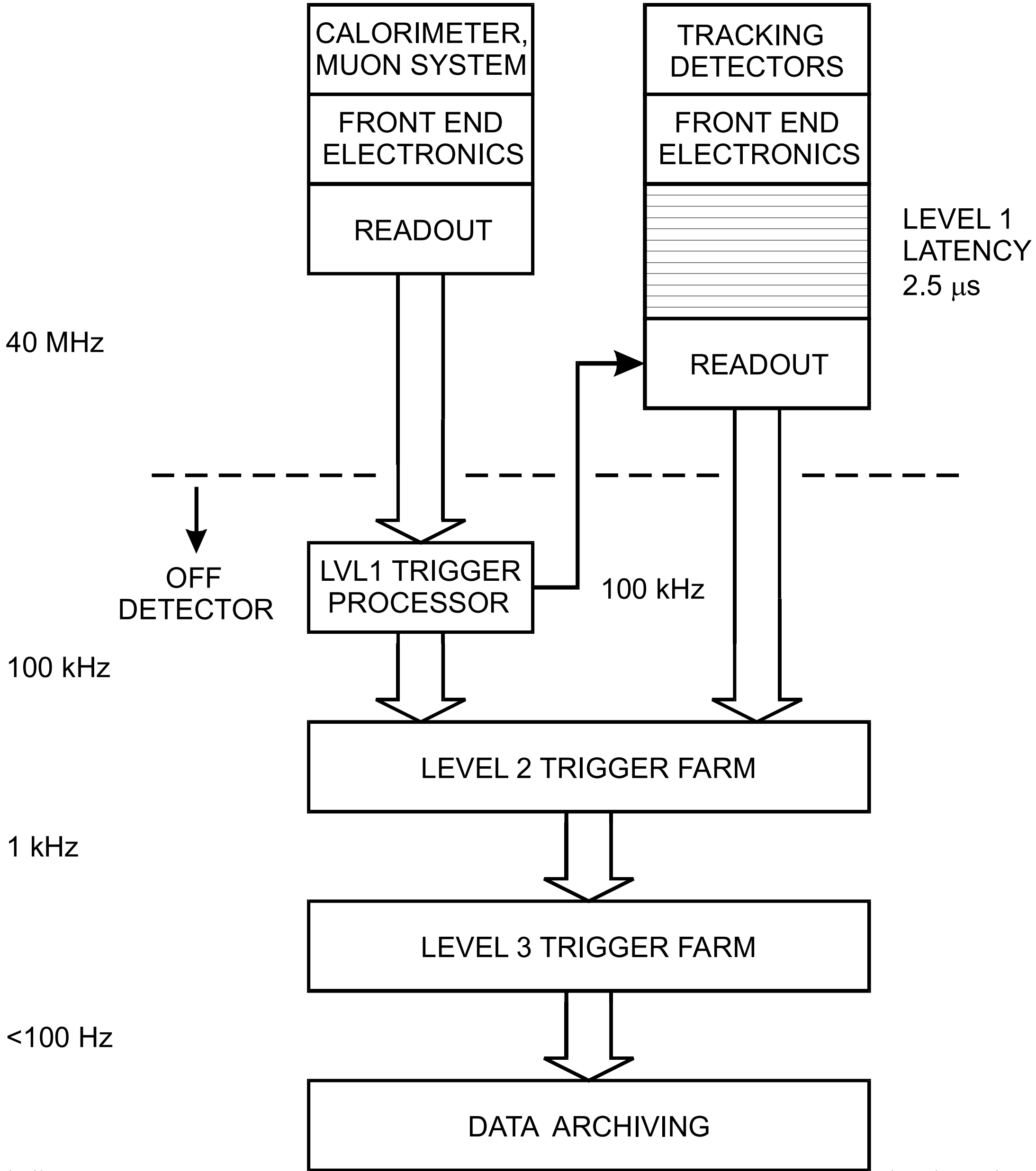

Triggers are filters that improve the ratio of desired events to background hits.

Filters are not perfect: typical trigger efficiencies 20 – 70%

Compromise between efficiency and processing time

Trackers have too many channels to read out everything for each bunch crossing (power constraints), so data are stored in the front-end chip and read out upon receipt of a Level 1 trigger.

ATLAS strip and pixel systems employ on-chip sparsification to exploit the available readout bandwidth.

The ATLAS SCT further increases readout efficiency by utilizing a binary readout (i.e. only hit/no-hit)

The readout rate for tracking systems is limited, so it cannot be increased with luminosity.

$\Rightarrow$ Desirable to increase trigger efficiency

Example:
CDF hardware vertex trigger

See Poster B18

Silicon detector still read out with Level 1 trigger, but a dedicated hardware vertex trigger utilizes ASICs and FPGAs to find displaced vertex events.

Improves rate of "good" events by factor 10 – 30.

FPGA computational density roughly doubles per year.

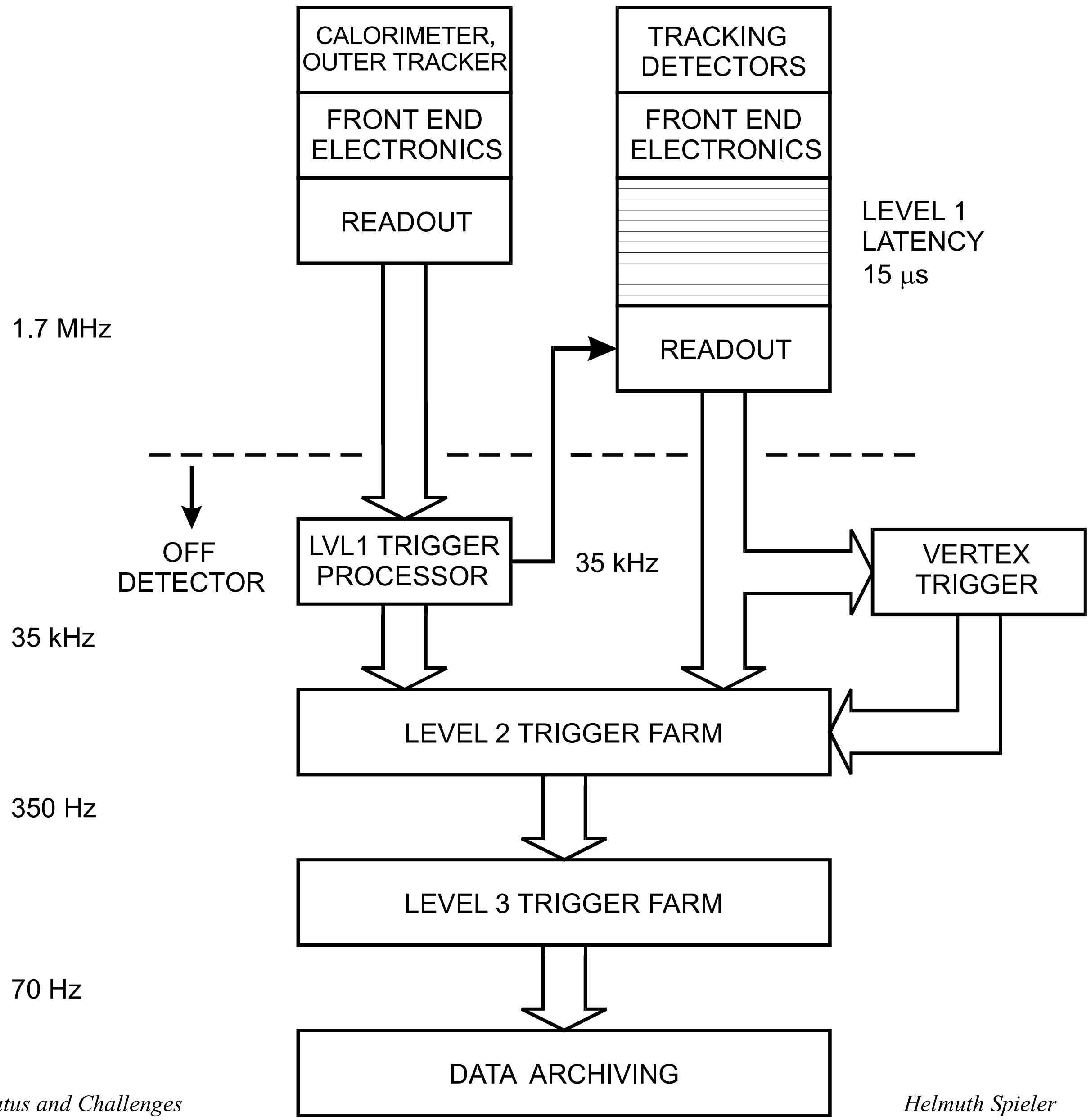

Summary: Complex systems require mature designs.

The chips we have today resulted from a complex multi-branch evolutionary process.

They required

Multiple development paths,

The work of many independent efforts, and

Extensive detector R&D in Europe, Japan and the US.

Functioning system requires more than “headline specs”: noise, speed, power

Important to consider pickup immunity (e.g. power supply rejection ratio),
signal return paths,
tolerance to parameter variations, etc.

Modern technology cannot work miracles, but we can improve the trade-offs.

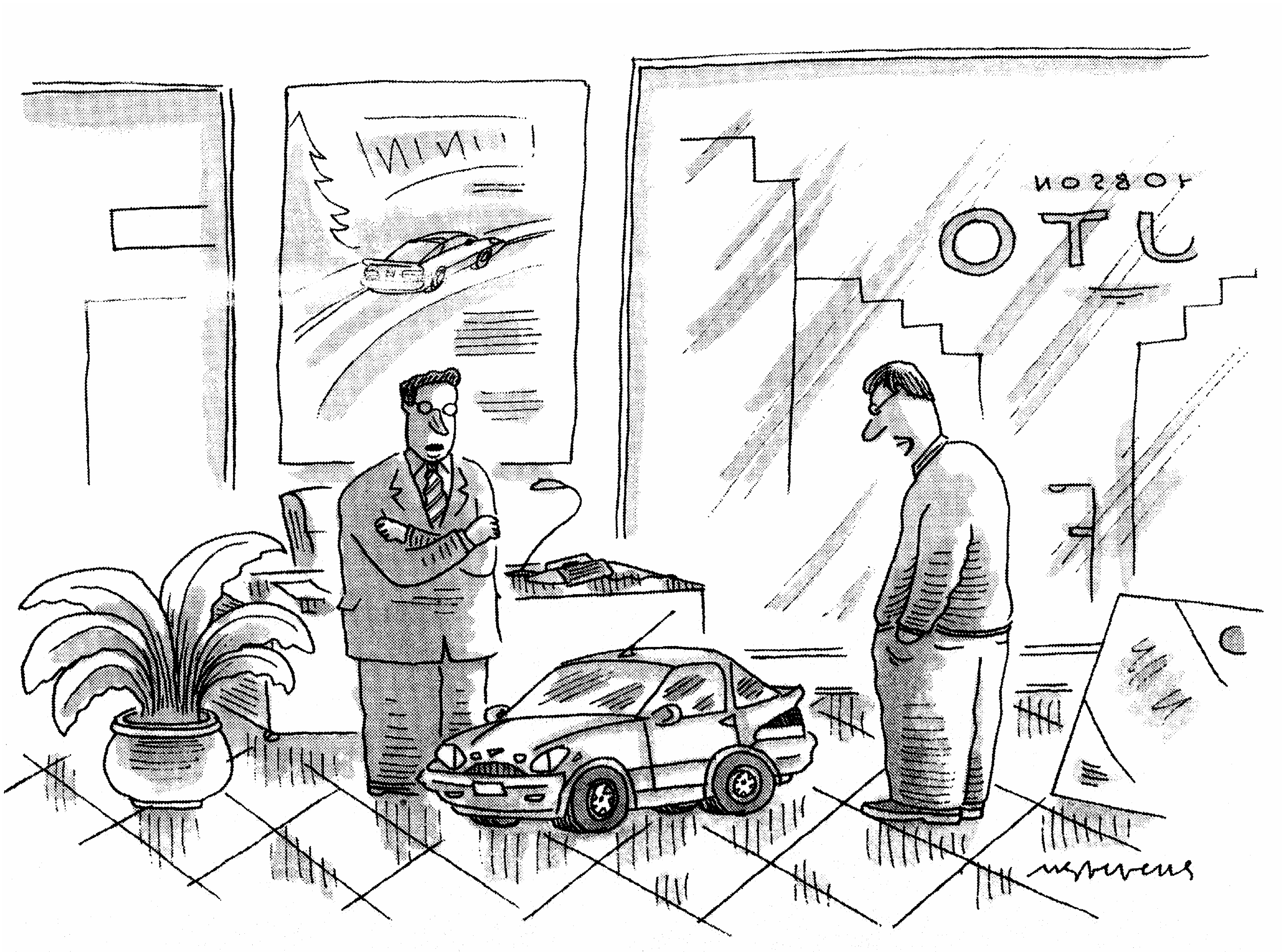

"Naturally, there's a trade-off for its exceptional fuel economy."

Bolometer Readout Electronics

William Holzapfel (UCB)
Adrian Lee (LBNL,UCB)
Paul Richards (UCB)
Helmuth Spieler (LBNL)

John Clarke (LBNL,UCB) SQUIDs

John Joseph (Eng. Div. LBNL)
Chinh Vu (Eng. Div. LBNL)

Brad Benford (UCB)
H.-M. "Sherry" Cho (UCB)
Matt Dobbs (LBNL
– now McGill Univ.)
Nils Halverson (UCB
– now Univ. Colorado)
Huan Tran (UCB SSL)

+ 15 graduate students

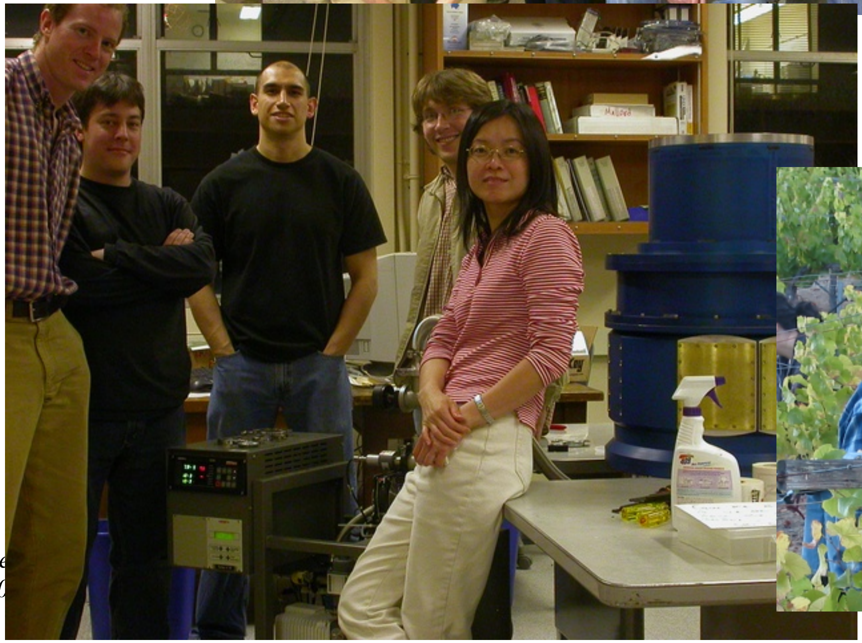

Funding: NSF, NASA, DoE

Cosmic Microwave Background has a near perfect black body spectrum (T = 2.7K)
– measurements within 1% of theoretical spectrum

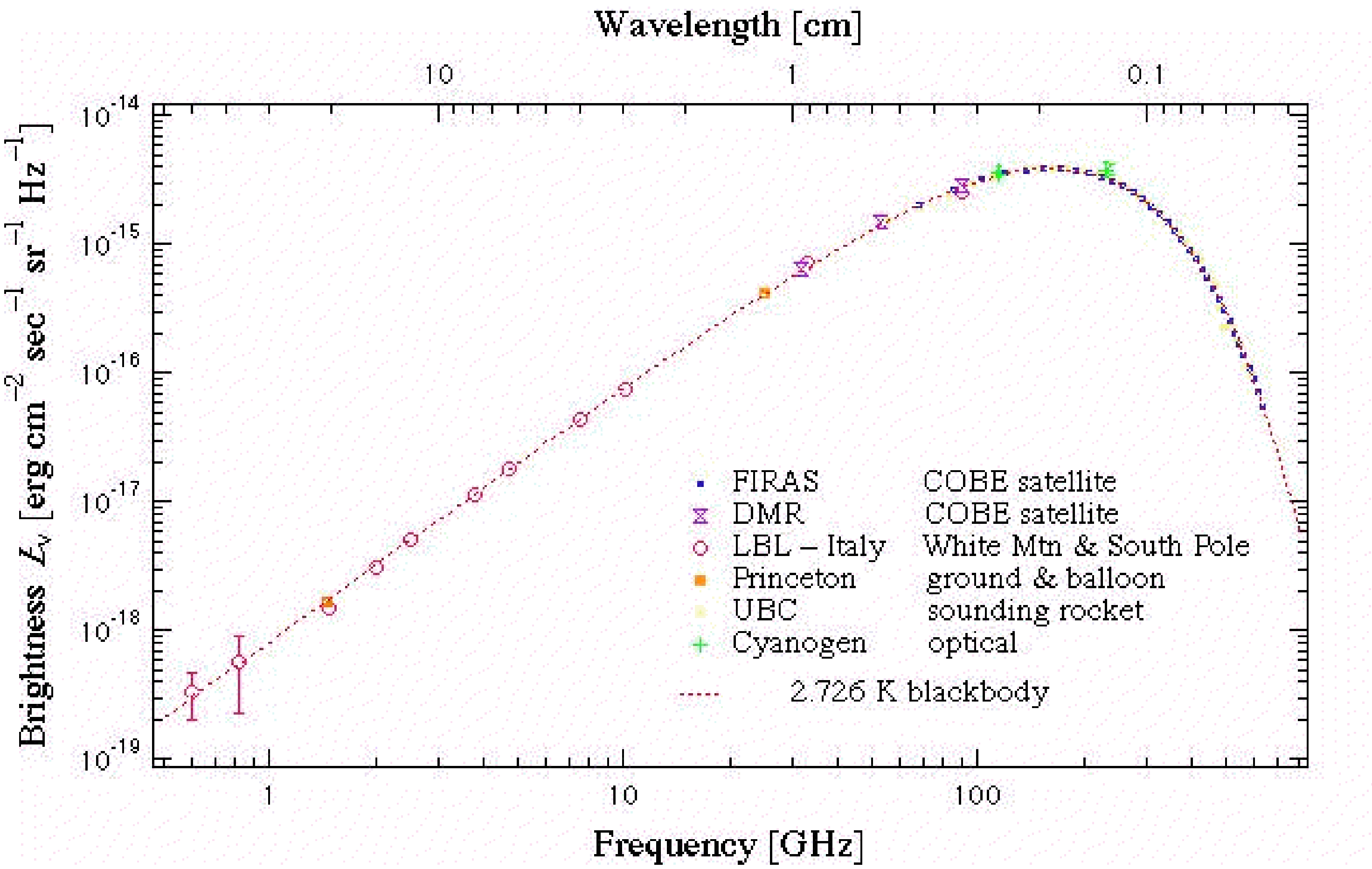

Spectrum peaks at about 200 GHz.

CMB very well understood – has provided precision data on key cosmological parameters.

Map Temperature of Sky:

Data from WMAP

Temperature anisotropy ~10^{-5}

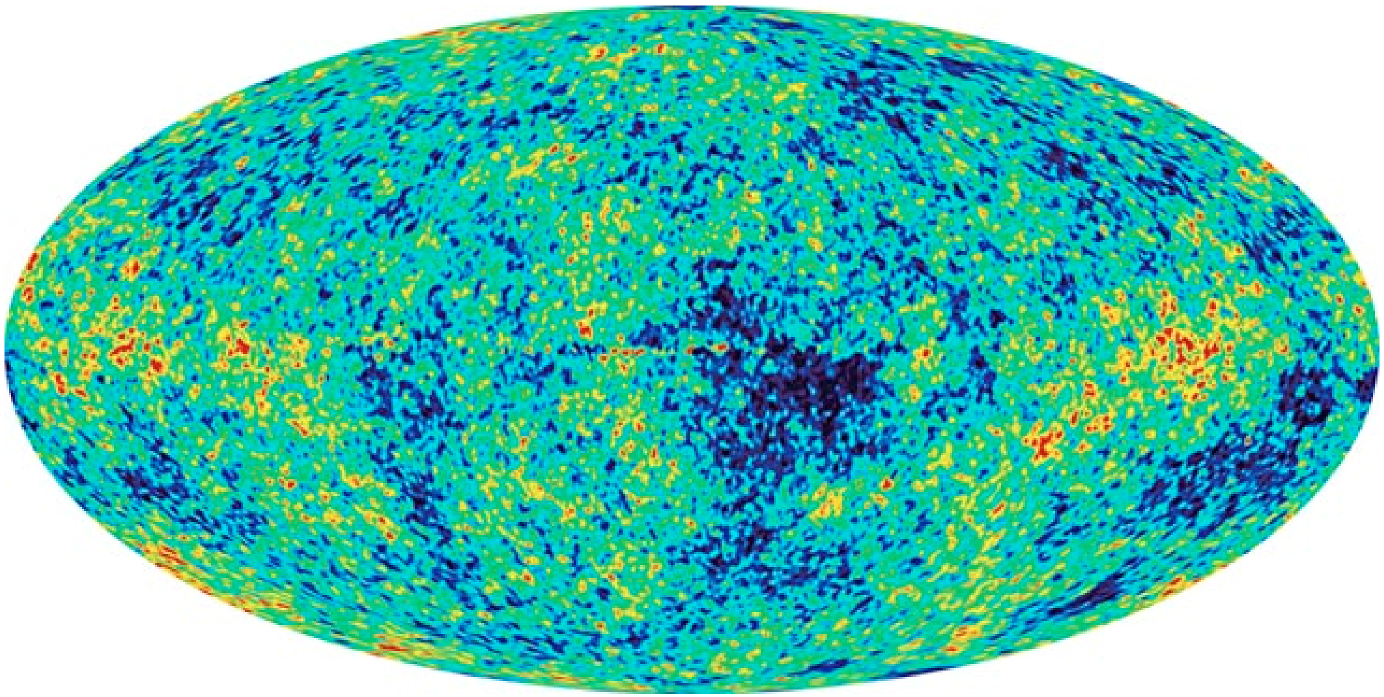

- CMB measurements provide constraints on fundamental cosmological parameters
- CMB spatial distribution largely unaffected since 300k yrs after Big Bang
- Supernova and CMB data *together* give best constraints on mass and energy density of the universe
- Also consistent with Ω_m from Large Scale Structure data

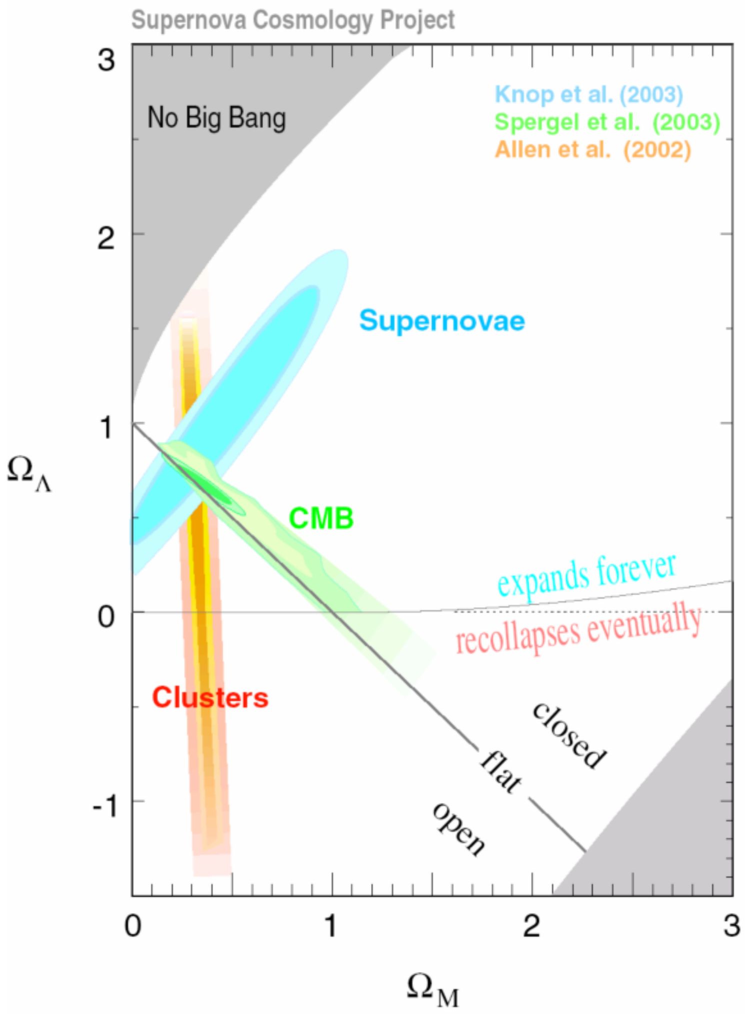

Cosmology relies on combined data from different techniques.

Today we use CMB as a tool:

Map large-scale structure:

use Sunyaev-Zel'dovich Effect in galaxy cluster search $\Rightarrow$ w, Ω_m

Inverse Compton scattering: Hot gas bound to clusters of galaxies scatters CMB

$\Rightarrow$ distorts black-body spectrum – shifts to higher frequencies:

Clusters appear as dark spots in CMB sky

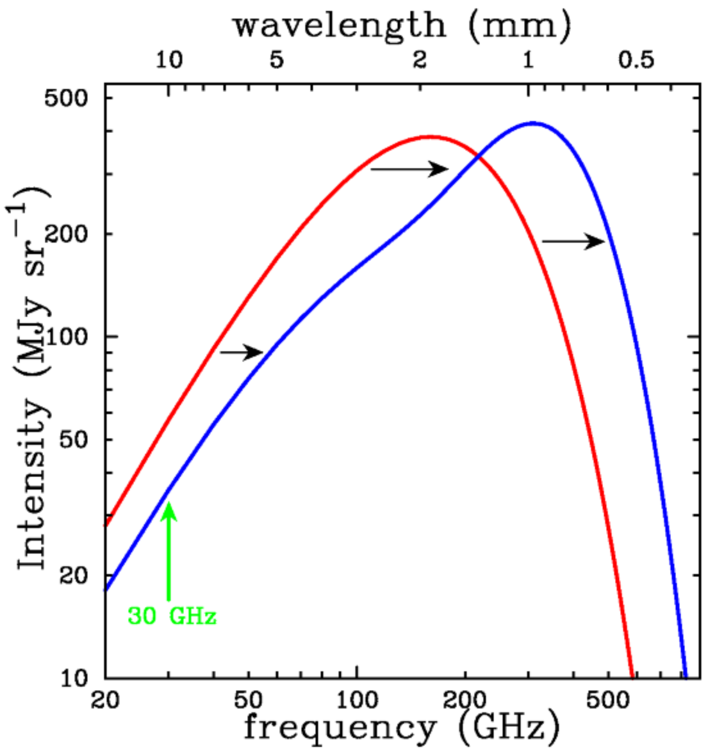

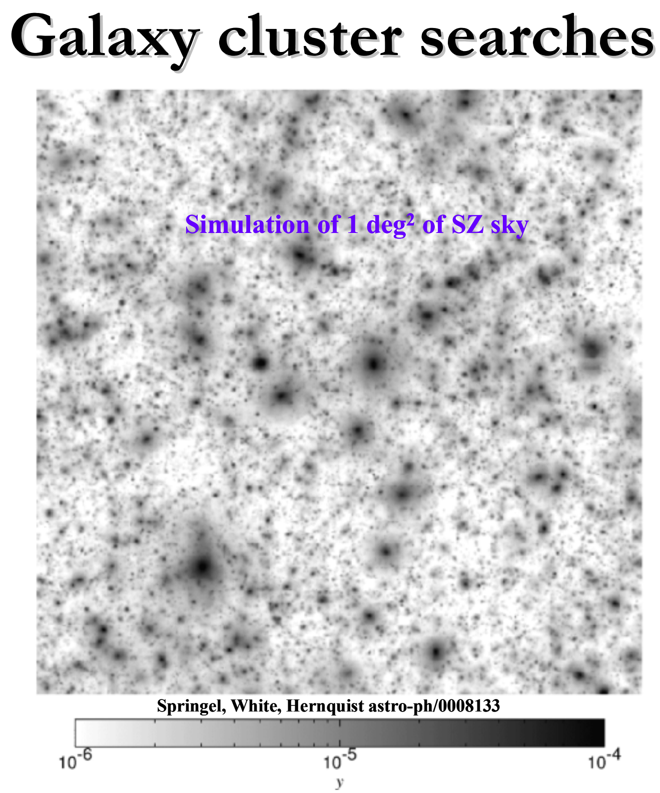

SZ signal independent of redshift z

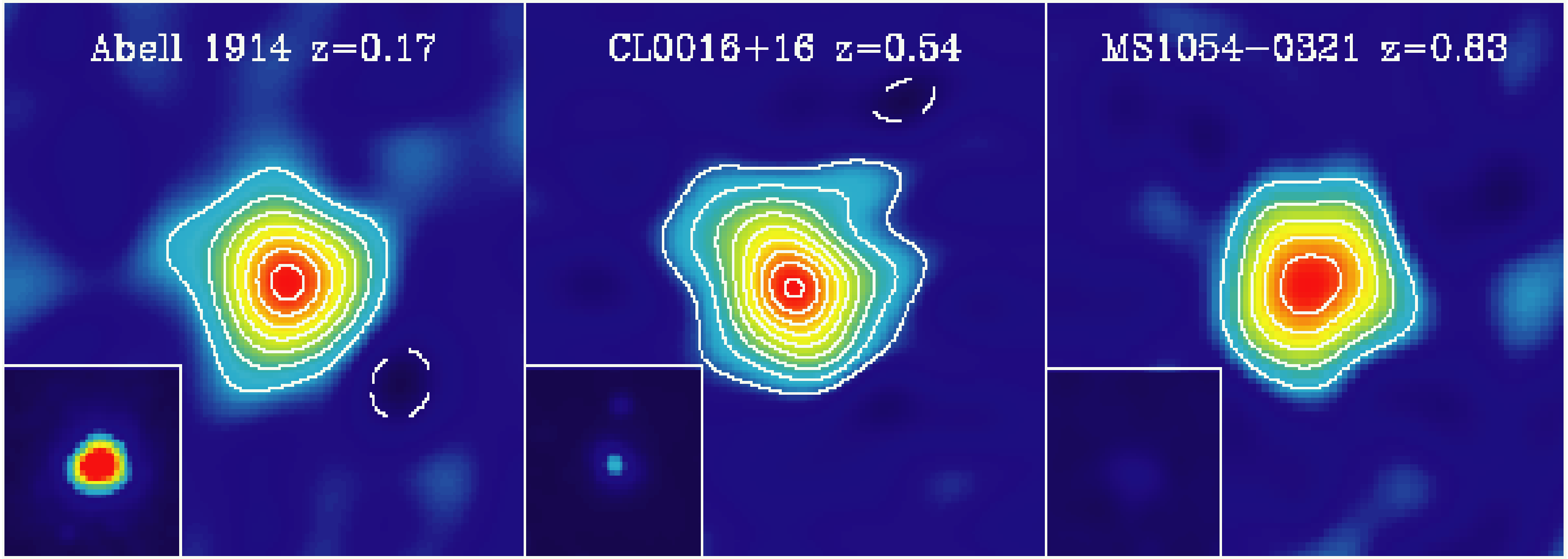

(Holzapfel et al.)

In contrast to x-rays (insets), SZ surface brightness is independent of redshift, so clusters can be seen at any distance.

However, optical data needed to determine redshift.

Emerging technique that requires greatly improved arrays.

Cluster densities at z > 1 sensitive to cosmological parameters

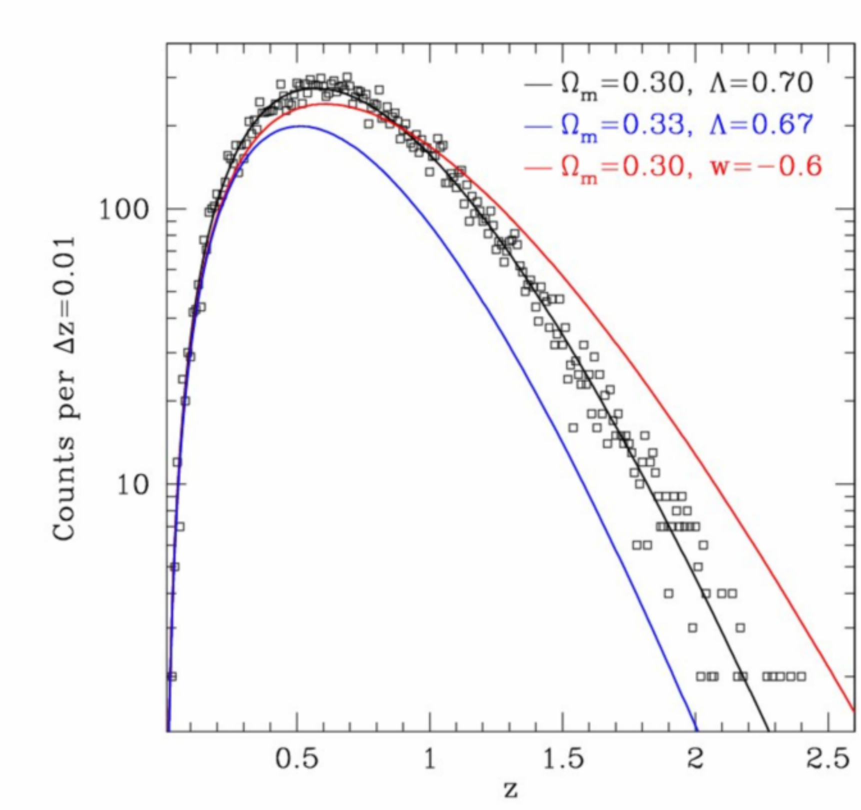

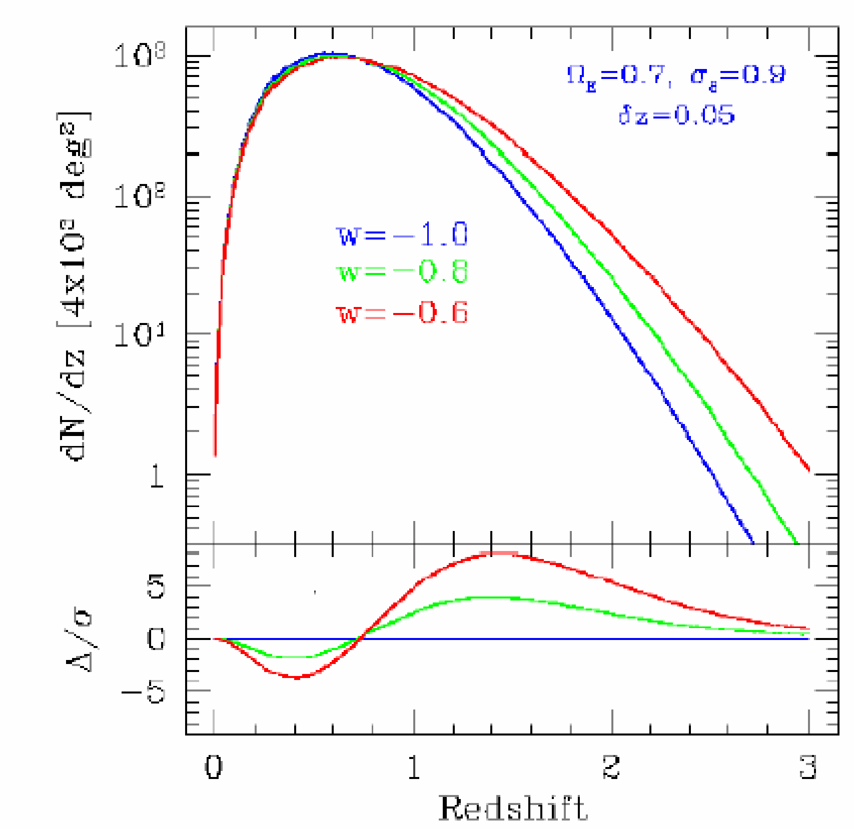

DETECTED SIGNAL

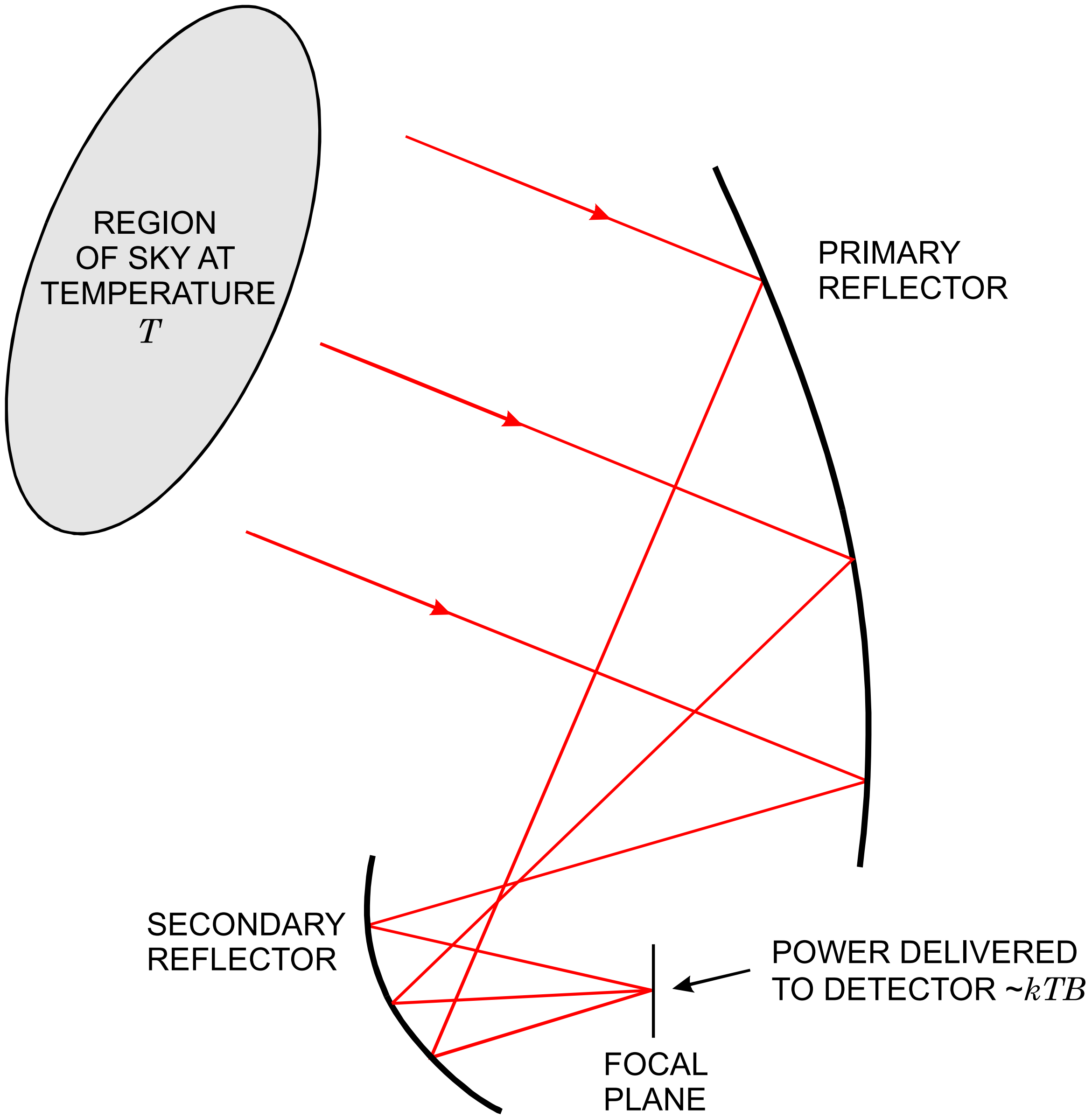

- View region of sky with temperature T
  (CMB: $T \approx$ 3K)
- Measured signal proportional to kTB
  (B = bandwidth)
- The signal is noise.

Example Optics and Focal Plane (South Pole Telescope)

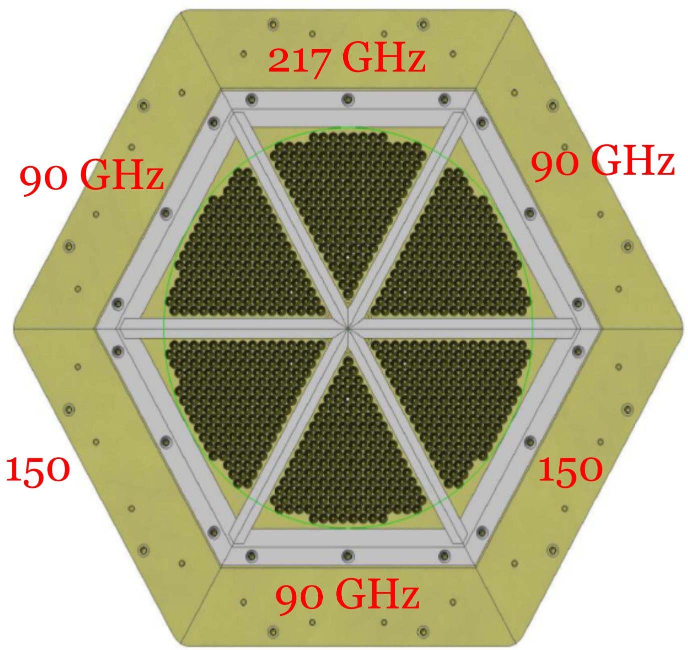

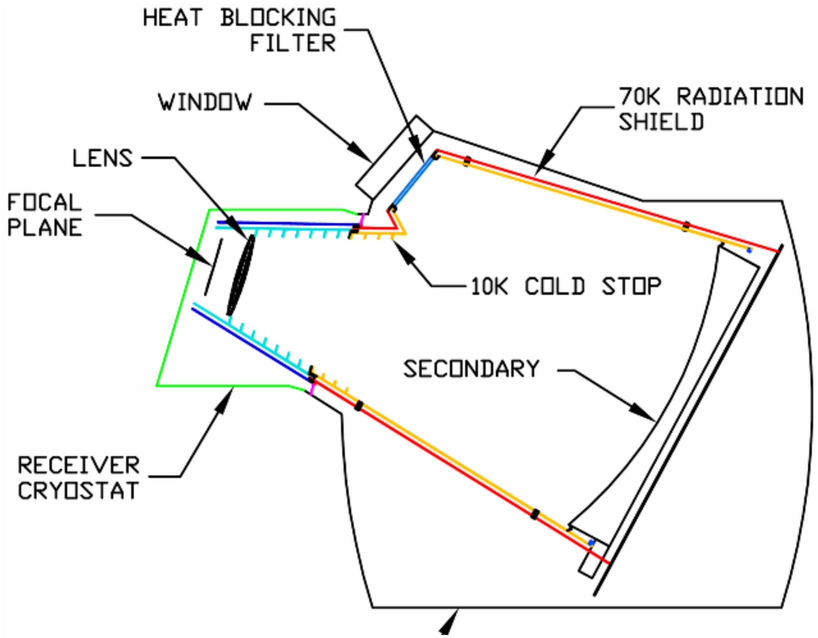

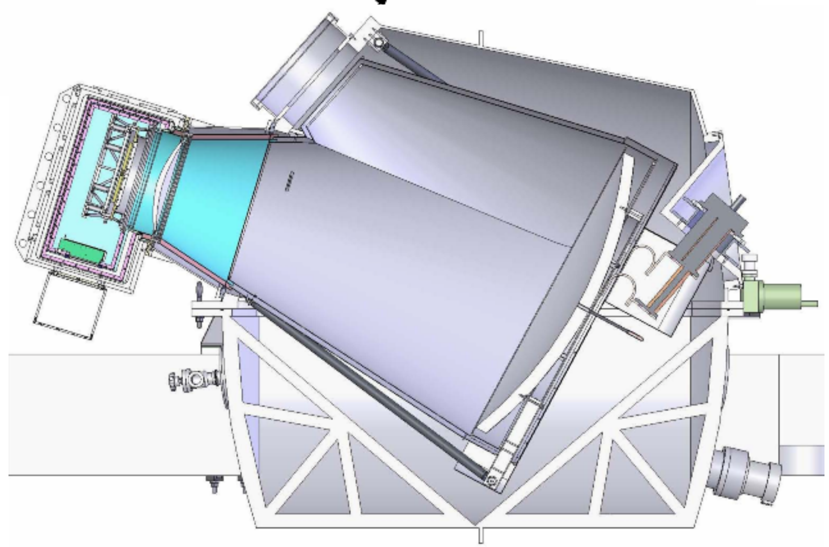

Why Bolometers?

Amplifiers (phase coherent systems) subject to quantum noise limit.

Minimum spectral noise power density: $\frac{dP_n}{d\omega} = \hbar\omega$

Follows from uncertainty principle.

see H.A. Haus and J.A. Mullen, Phys. Rev. 128 (1962) 2407-2413

For a simple derivation see Spieler, *Semiconductor Detector Systems*, p.132-133
or at www-physics.LBL.gov/~spieler go to Heidelberg Lectures.

Bolometers do not preserve phase, so not subject to quantum noise limit.

COUPLING TO BOLOMETER

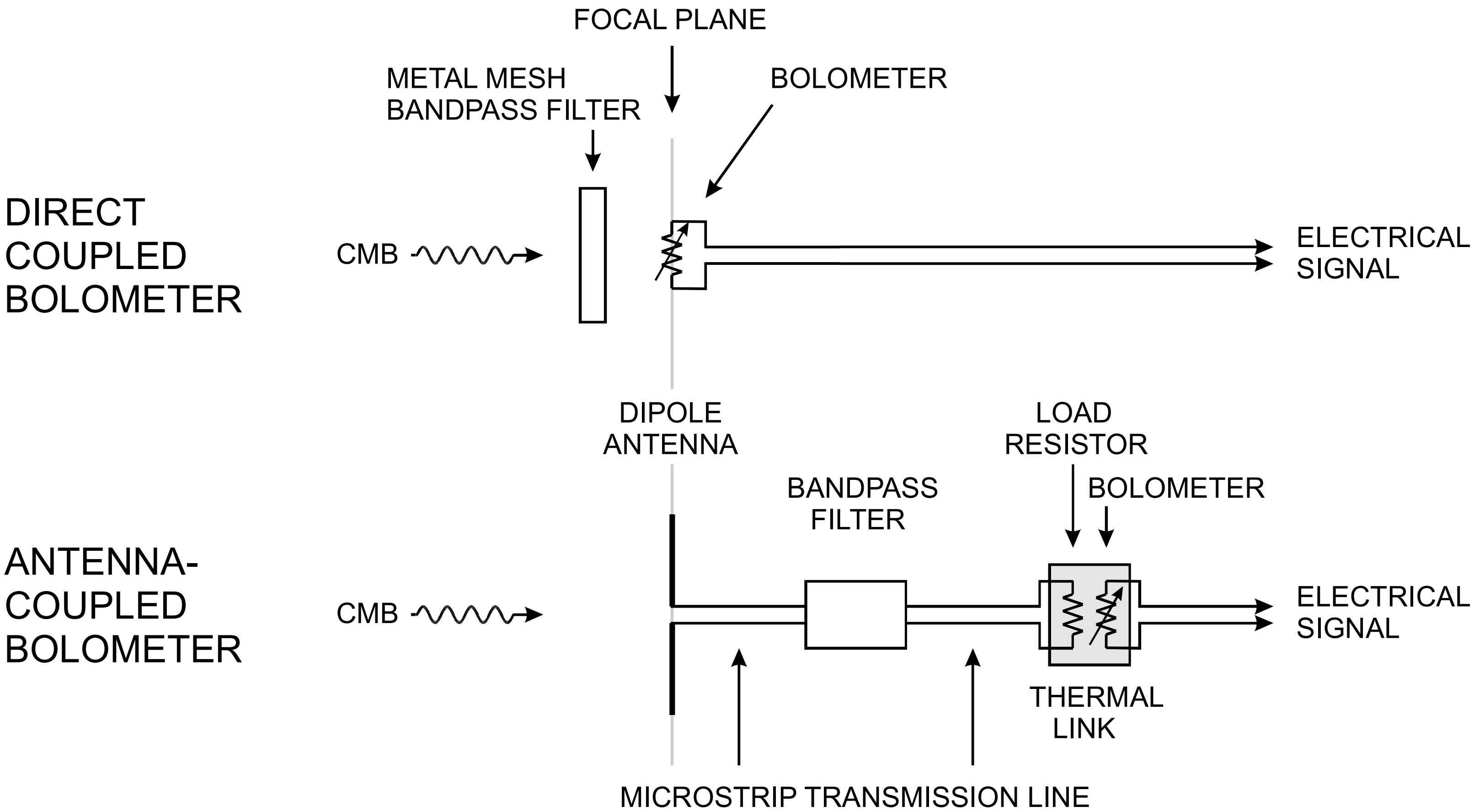

Antenna-coupling provides inherent polarization sensitivity. Possibly detect signature of gravity waves from Big Bang and measure energy scale of inflation.

Signal Spectrum in Galaxy Cluster Search

Antenna beam width: 1' FWHM Scan speed: 10'/s

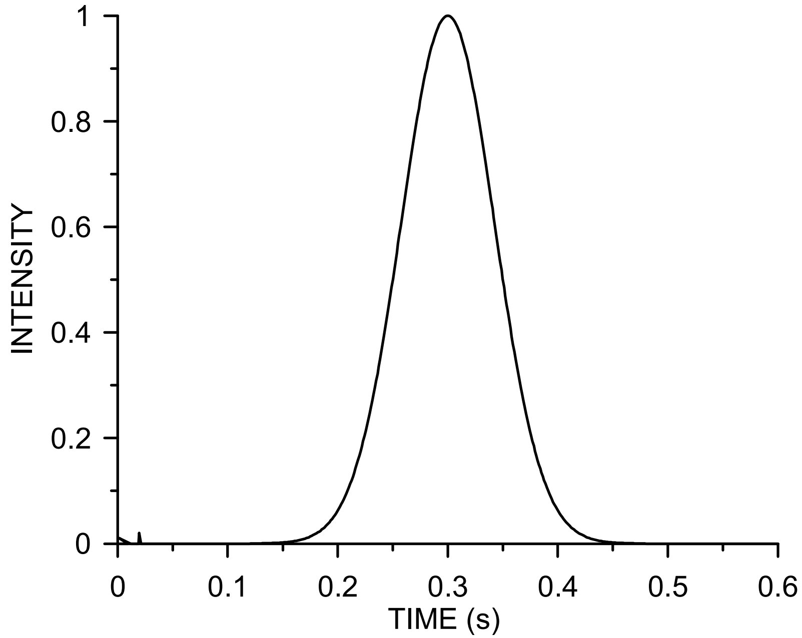

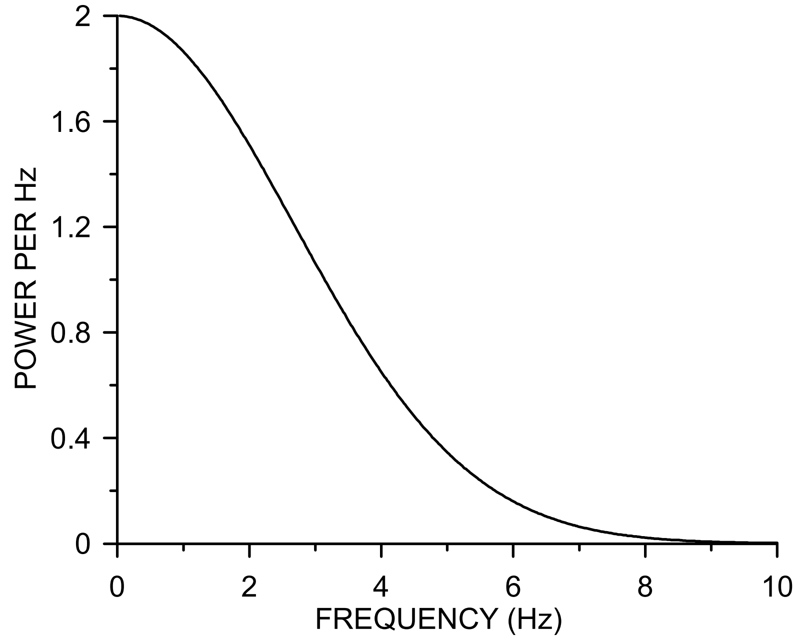

(W. Lu, CWRU)

⇒ Maintain Gain Stability + Noise Level down to ~0.1 Hz

Some Next Generation Cluster Search Experiments:

Ground-based experiments. Suitable sites are high and dry.

a) APEX-SZ

UCB, LBNL, MPIfR, Colorado, McGill

12 m on-axis telescope (ALMA prototype) on Atacama Plateau, Chile, 5000m

~300 pixels

Shared with many other experiments, so CMB observing time limited to few weeks

APEX-SZ first light Dec 2005

b) South Pole Telescope

Univ. Chicago, UCB, LBNL, CWRU, CfA, Univ. Colorado, McGill, Univ. Illinois

10 m off-axis telescope

Installation: 2006-2007, First Light Feb. 16, 2006

~1000 pixels, dedicated to CMB measurements

Optical followup with DES

Test assembly in Texas (August 2006)

January 3, 2007 at South Pole

SPT final configuration with ground shield (Jan 2008)

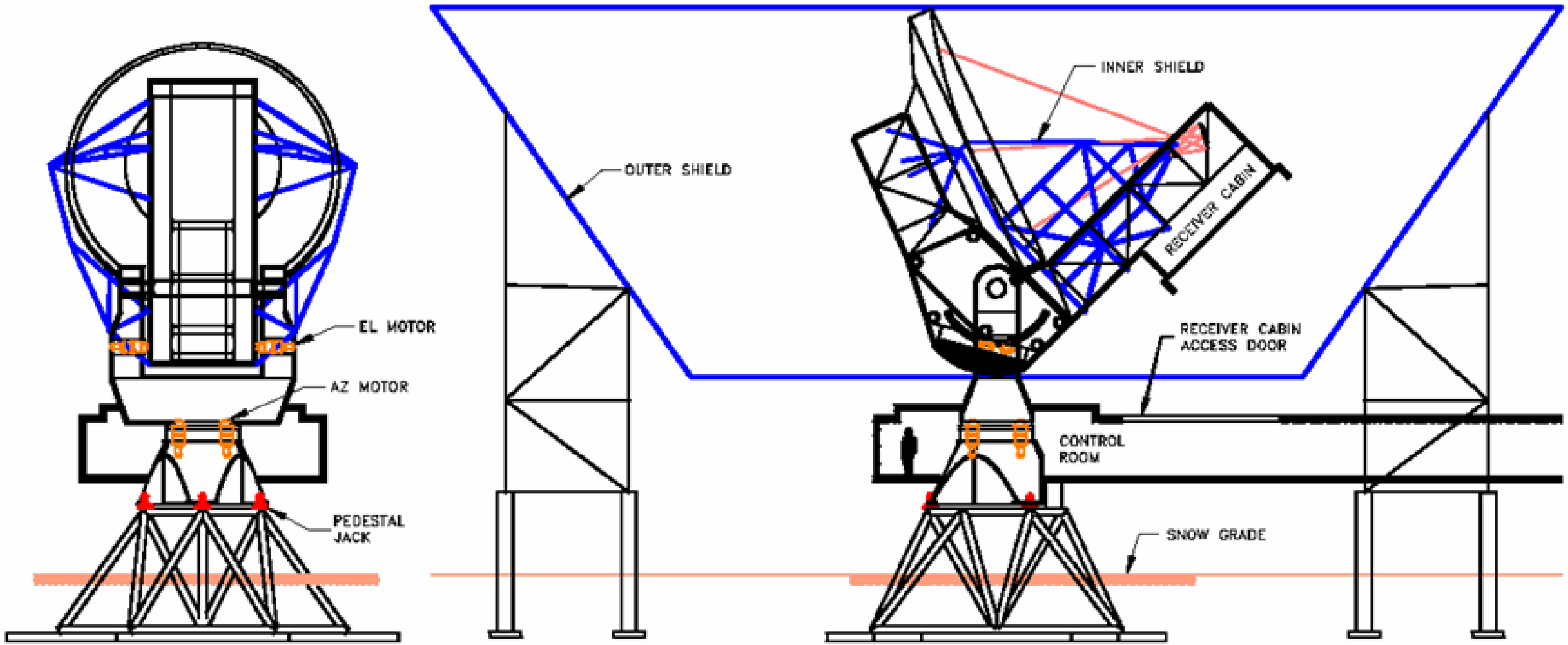

All of these experiments require a major step up in sensitivity

Bolometers today are so sensitive that we are limited by the shot noise of the CMB photons.

Increase sensitivity by

performing many measurements simultaneously

⇒ bolometer arrays (100s to 1000s)

extending observation time

⇒ ground-based experiments
eventually space-based

Bolometer array technology:

Wafer-scale monolithic fabrication ("radiometer on a chip")

Cold multiplexing on 0.25K stage (reduce heat leaks through wiring)

Cryogen free system: pulse tube cooler + $^4He/^3He/^3He$ sorption fridge
(remote operation with minimal on-site staff)

Thermal Detectors

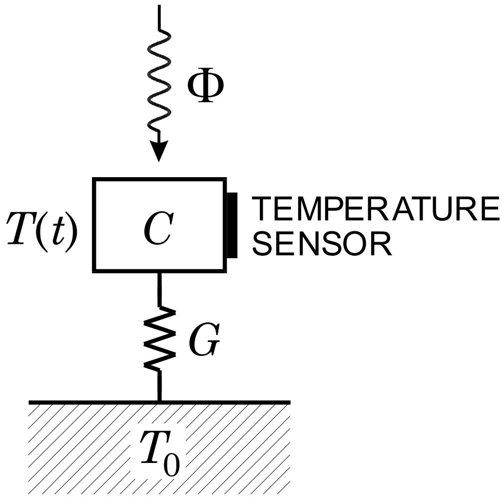

Basic principle:

Assume thermal equilibrium:

If all absorbed Energy $E = \Phi \Delta t$ is converted into phonons, the temperature of the sample will increase by

$$\Delta T = \frac{E}{C} \ ,$$

where C is the heat capacity of the sample (specific heat x mass).

After absorption of an energy packet E the heat flows through the thermal conductance G and the bolometer temperature decays as

$$T - T_0 = \frac{E}{C} e^{-t/\tau}$$

with the thermal time constant

$$\tau = \frac{C}{G} \ ,$$

analogous to a capacitor discharged through a resistance.

Bolometers

Superconducting transition edge sensors:

- Bias thin film superconductor at transition from super- to normal conducting

⇒ Large change in resistance with absorbed power

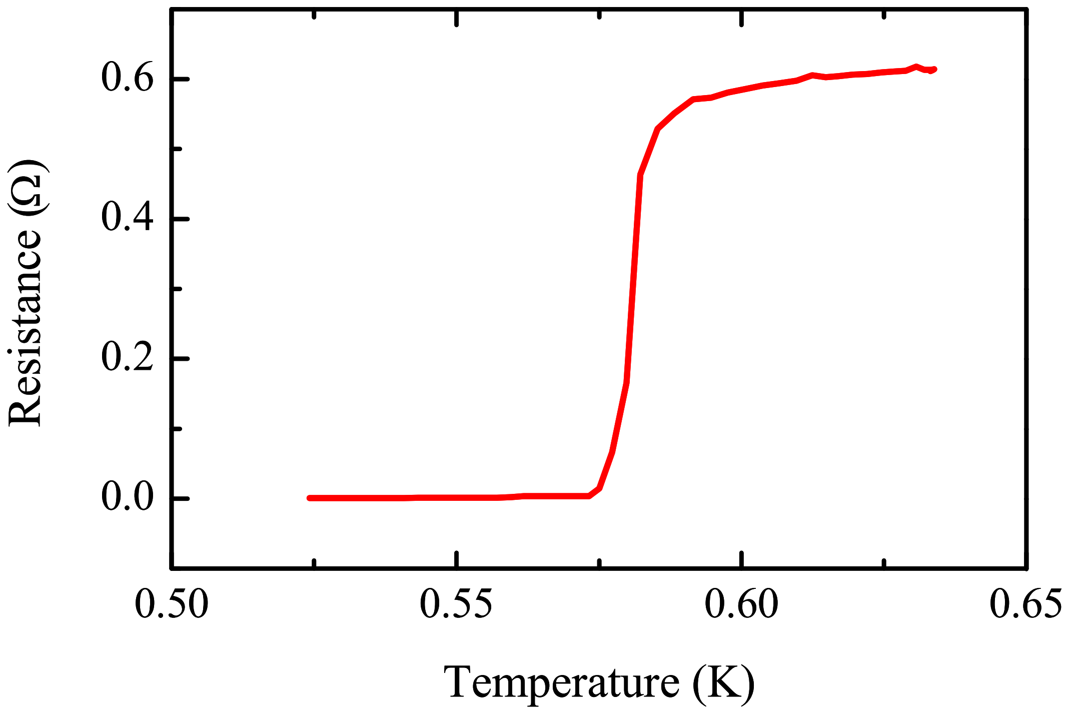

- Thin bi-layers (e.g. Al – Ti) allow tuning of transition temperature

Voltage-Biased Transition-Edge Sensors

Required power is of order pW, i.e. voltage of order μV
current of order μA

Simplest to bias device with a constant current and measure change in voltage

Problem: power dissipated in sensor $P = I^2 R$

Increasing R $\Rightarrow$ Increasing P $\Rightarrow$ Increasing R $\Rightarrow$ Increasing P

$\Rightarrow$ **thermal runaway**

When biased with a constant voltage $P = \dfrac{V_b^2}{R}$

Increasing R $\Rightarrow$ Decreasing P $\Rightarrow$ Decreasing T $\Rightarrow$ Decreasing R

$\Rightarrow$ **negative feedback**

stabilizes operating point

Analogous to op-amp:

Bolometer time constant corresponds to amplifier cutoff frequency.

Subject to constraints of feedback theory!

- Operate with constant voltage bias

⇒ Electrothermal negative feedback

⇒ Stabilize operating point + predictable response

⇒ **“Constant power operation”:**
Change in absorbed power is balanced by change in electrical power: $\Delta I / \Delta P = 1 / V_{bias}$

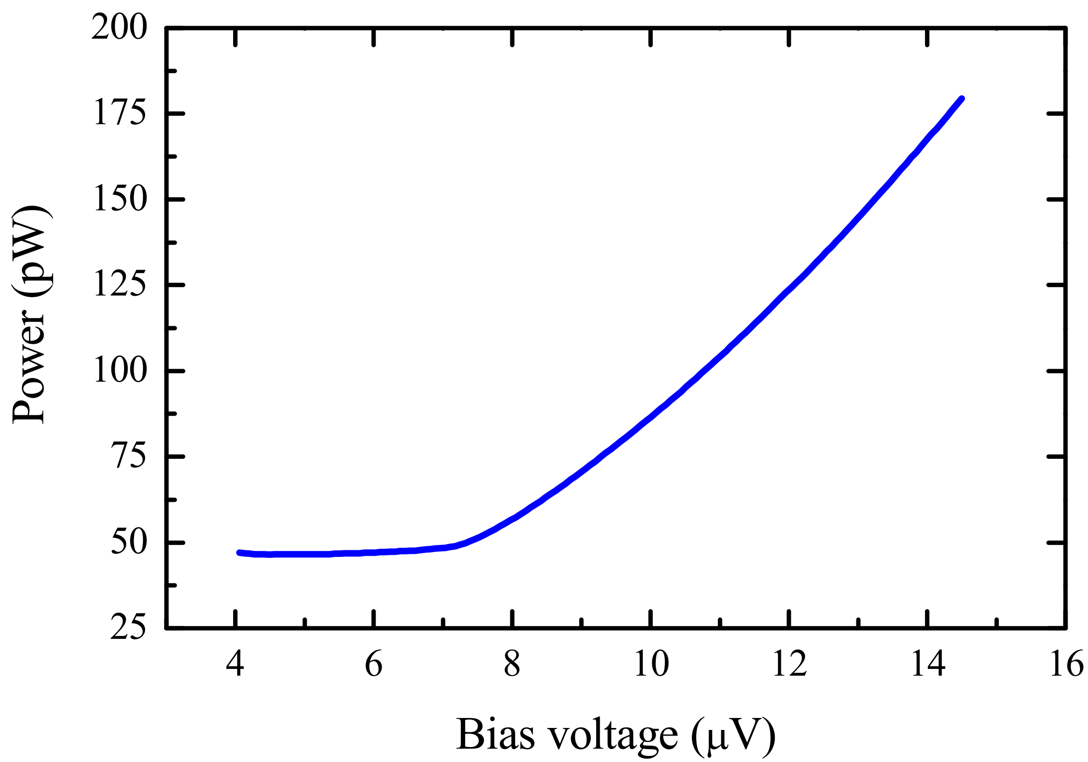

APEX Focal Plane (Jared Mehl)

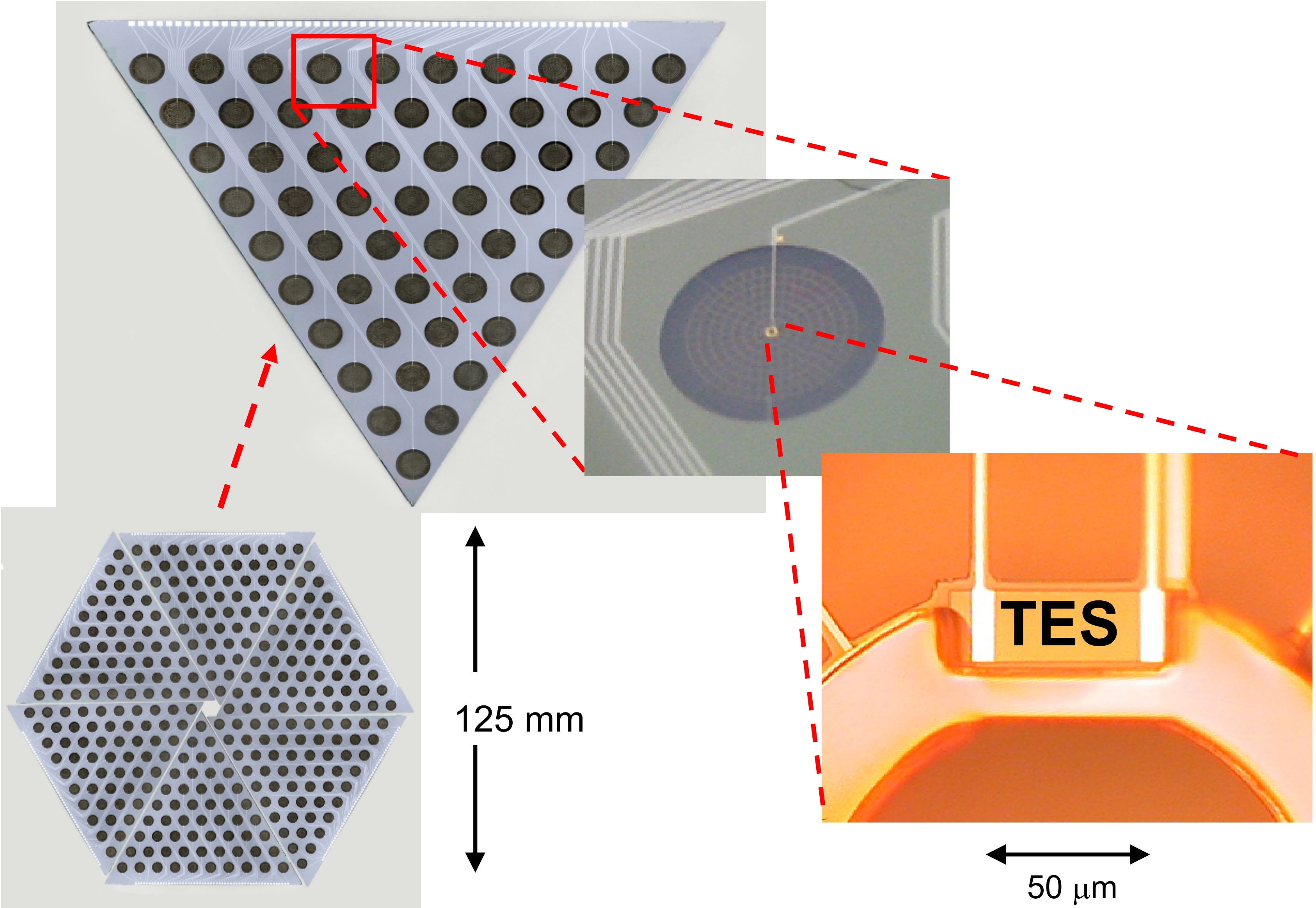

Close-up of spiderweb bolometer

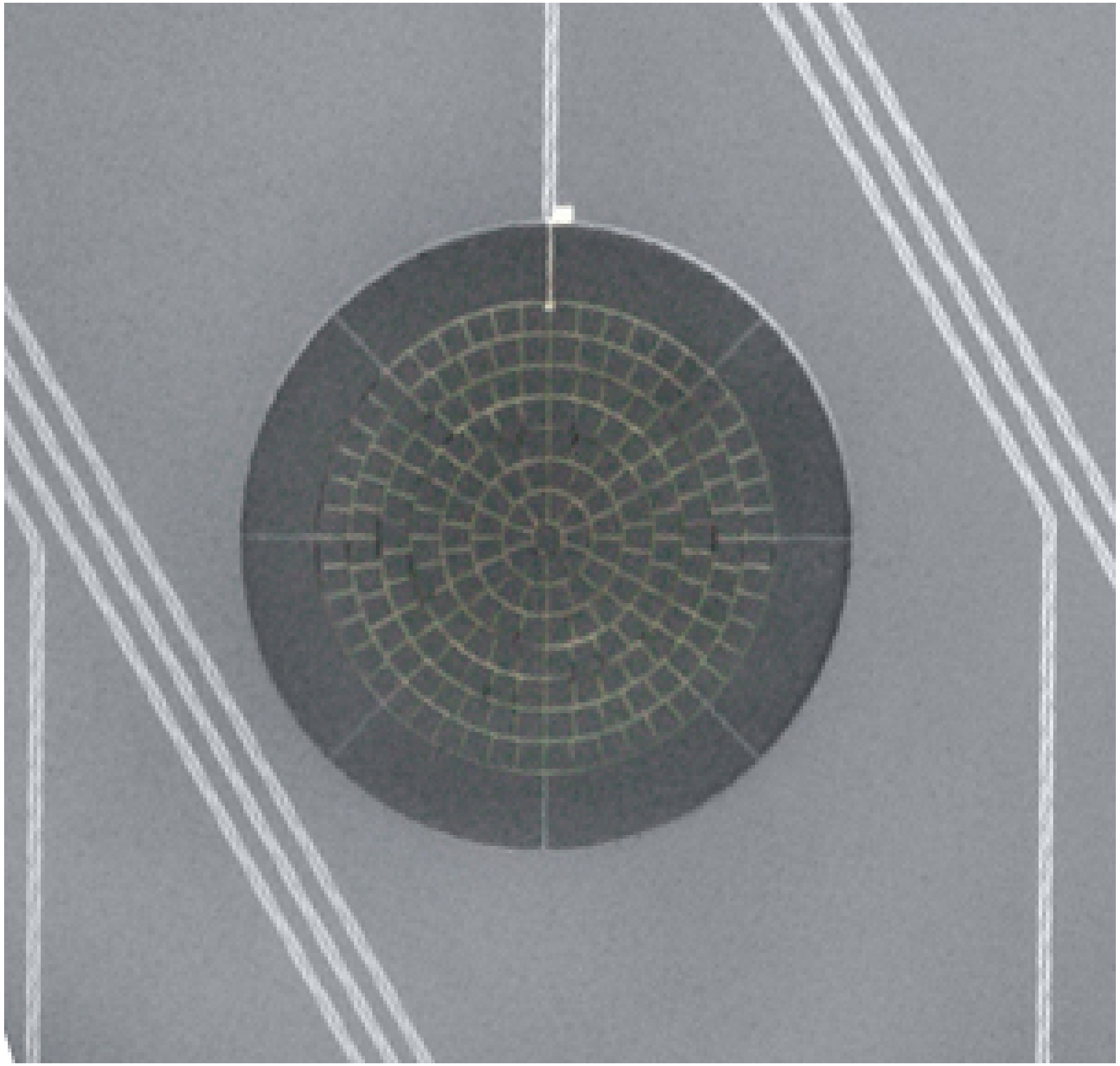

Antenna-Coupled Prototype Pixel for Polarization Measurements (Mike Myers)

Microstrip Transmission Lines

Bandpass Filters (217 GHz, 40% BW)

Focal Plane Wedge

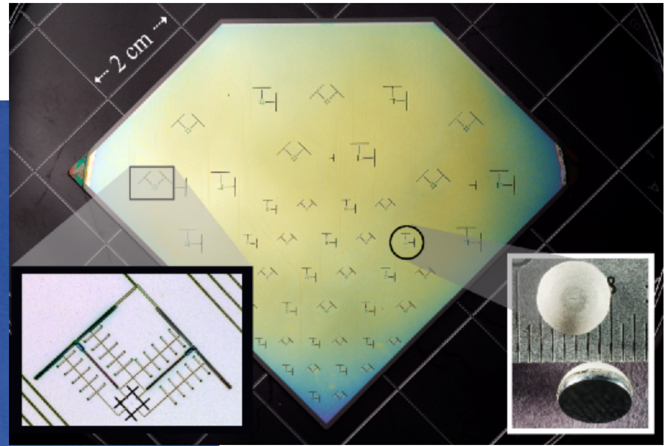

Kam Arnold

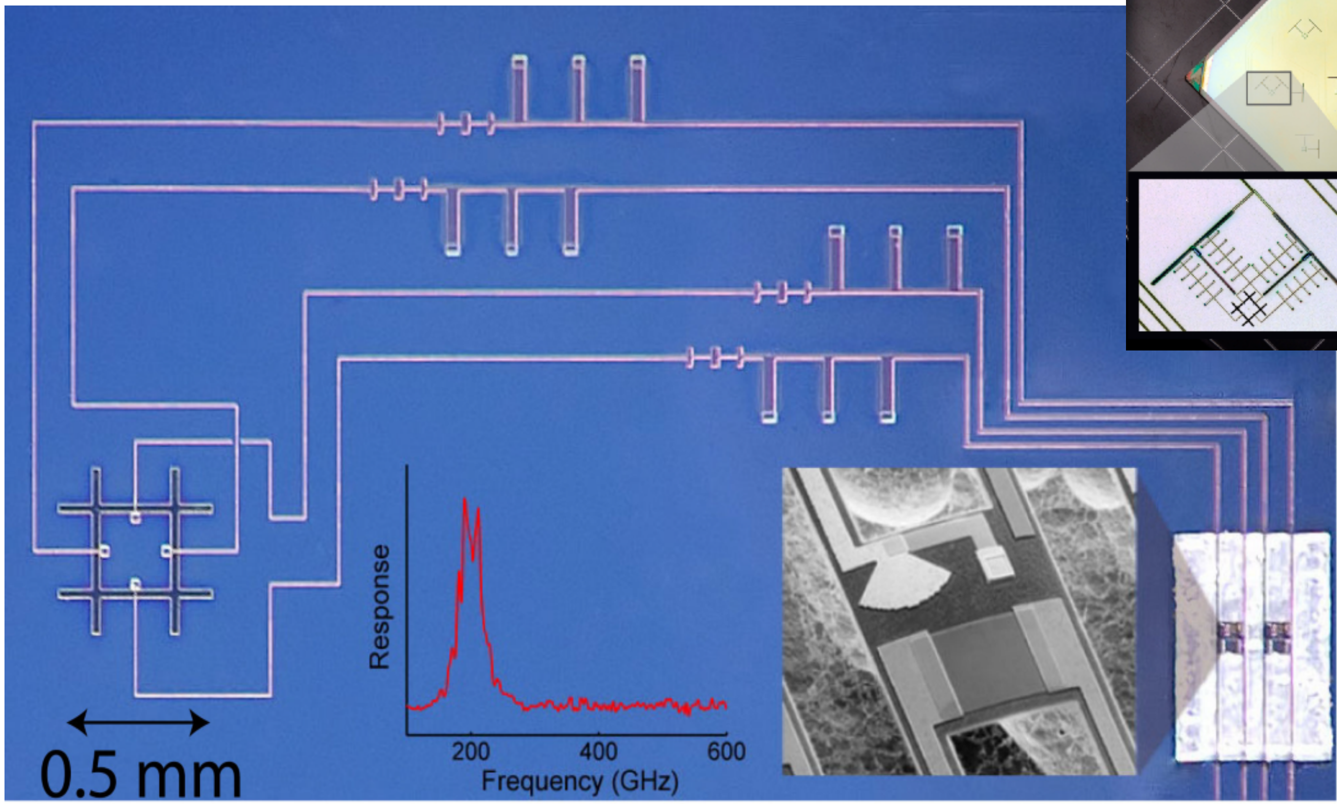

Microstrip terminated on a Si-nitride suspension.

Power measured with TES

Double-Slot Dipole Antenna

Readout

- Constant voltage bias requires that readout impedance $\ll$ bolometer resistance

  bolometer resistance $\approx 1\ \Omega$

  bias resistance $\approx 20\ \mathrm{m}\Omega$

  amplifier input impedance $\approx 10\ \mathrm{m}\Omega$ at 1 MHz

  1st amplifier stage: SQUID at 4K in shunt feedback configuration.
  High-frequency feedback loop includes SQUID +
  warm electronics (300K).

- Typical bolometer bias power: 10 – 40 pW
- Power Budget on 0.25K stage: <10 μW
- Heat conduction through wires to 4K stage acceptable up to ~300 bolometers

  $\Rightarrow$ Larger arrays require multiplexing

- Novel development:

  Frequency-Domain MUX with ZERO additional power on cold stage

Principle of Frequency-Domain Multiplexing

1. High-frequency bias (~100 kHz – 1 MHz)

   Each bolometer biased at different frequency

2. Signals change sensor resistance

   ⇒ Modulate current

   ⇒ Transfer signal spectrum to sidebands adjacent to bias frequency

   ⇒ Each sensor signal translated to unique frequency band

3. Combine all signals in common readout line

4. Retrieve individual signals in bank of frequency-selective demodulators

⇒ High-frequency bias provides greatly reduced sensitivity to microphonics

Modulation Basics

If a sinusoidal current $I_0 \sin \omega_0 t$ is amplitude modulated by a second sine wave $I_m \sin \omega_m t$

$$I(t) = (I_0 + I_m \sin \omega_m t) \sin \omega_0 t$$
$$I(t) = I_0 \sin \omega_0 t + I_m \sin \omega_m t \sin \omega_0 t$$

Using the trigonometric identity $2 \sin \alpha \sin \beta = \cos(\alpha - \beta) - \cos(\alpha + \beta)$ this can be rewritten

$$I(t) = I_0 \sin \omega_0 t + \frac{I_m}{2} \cos(\omega_0 t - \omega_m t) - \frac{I_m}{2} \cos(\omega_0 t + \omega_m t)$$

The modulation frequency is translated into two sideband frequencies

$(\omega_0 t + \omega_m t)$ and $(\omega_0 t - \omega_m t)$

symmetrically positioned above and below the carrier frequency ω_0.

All of the information contained in the modulation signal appears in the sidebands; the carrier does not carry any information whatsoever.

The power contained in the sidebands is equal to the modulation power, distributed equally between both sidebands.

Modulation Waveforms and Spectra

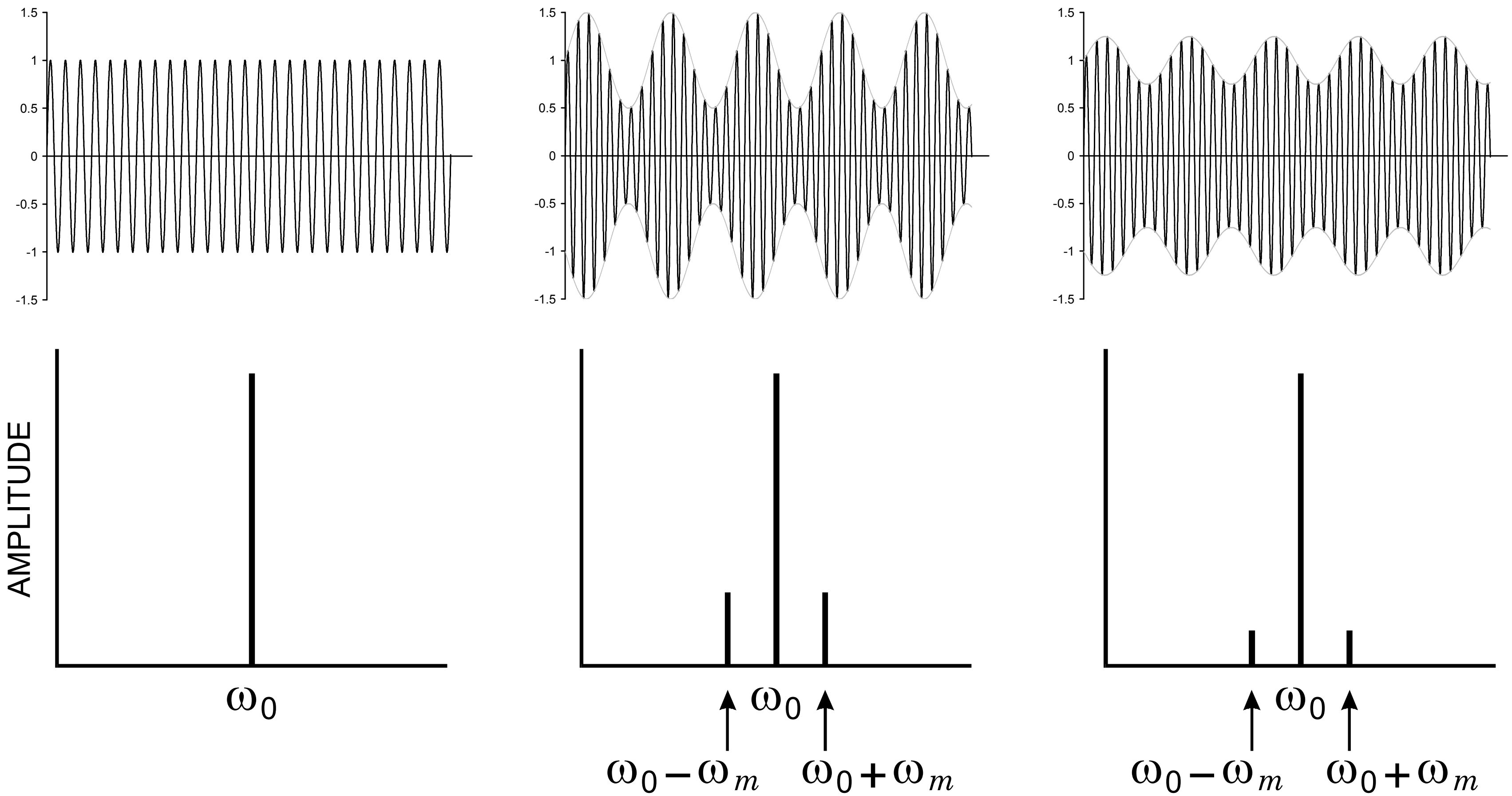

Carrier amplitude remains constant! All signal information in the sidebands.

MUX circuit on cold stage

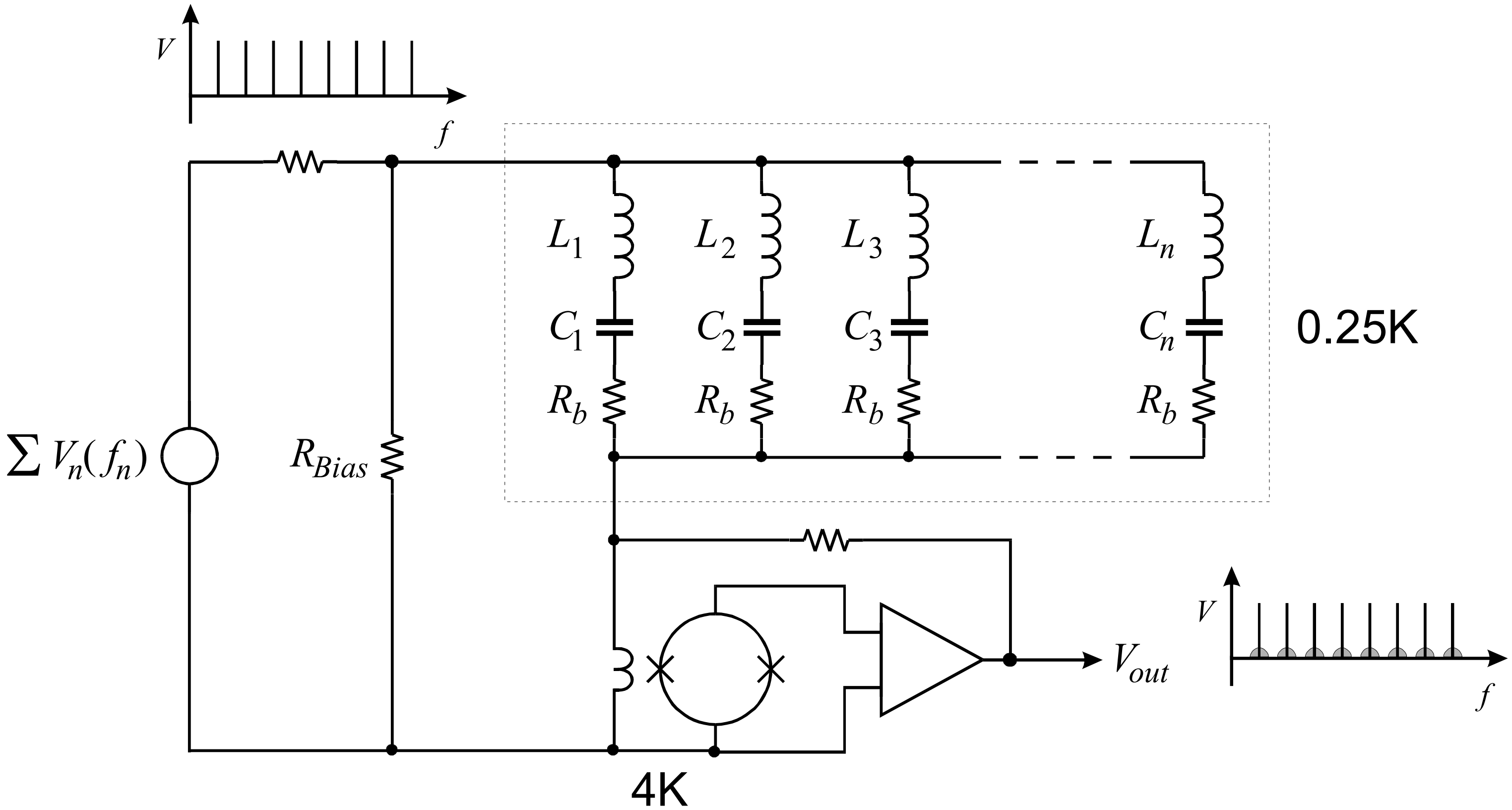

- “Comb” of all bias frequencies fed through single wire.
- Tuned circuits “steer” appropriate frequencies to bolometers and limit noise bandwidth.
- Current return through shunt-fedback SQUID amplifier (low input impedance).
- No additional power dissipation on cold stage (only bolometer bias power).

Demodulation

The same carrier signal that biases the sensor is used to translate the sideband information to baseband.

The mixer acts analogously to a modulator, where the input signal modulates the carrier, forming both sum and difference frequencies.

In the difference spectrum the sidebands at $f_n \pm \Delta f_S$ are translated to a frequency band

$$f_n - (f_n \pm \Delta f_S) = 0 \pm \Delta f_S .$$

A post-detection low-pass filter attenuates all higher frequencies and determines the ultimate signal and noise bandwidth.

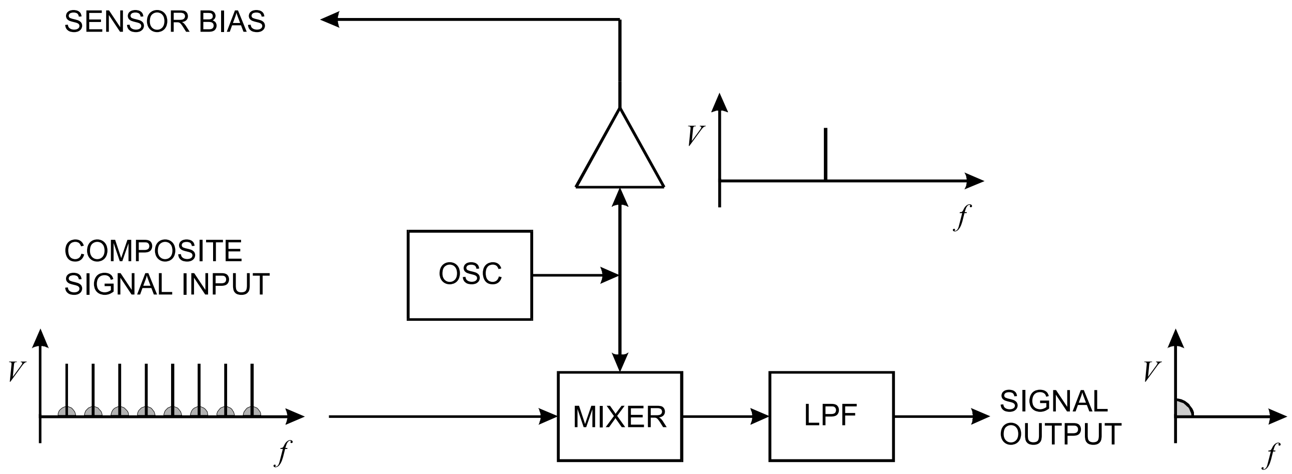

- We use a highly linear sampling demodulator that aliases the high-frequency signal to baseband.

SQUIDs

Superconducting Quantum Interference Devices

Two Josephson junctions connected in parallel to form a superconducting ring.

Two key ingredients:

1. Phase between two tunneling currents in Josephson junction is determined by current.
2. Magnetic flux in superconducting loop is quantized:

$$\Delta\Phi_0 = \frac{\pi\hbar c}{e} = 2.0678 \cdot 10^{-7} \text{ gauss cm}^2$$
$$= 2.0678 \cdot 10^{-15} \text{ Vs}$$

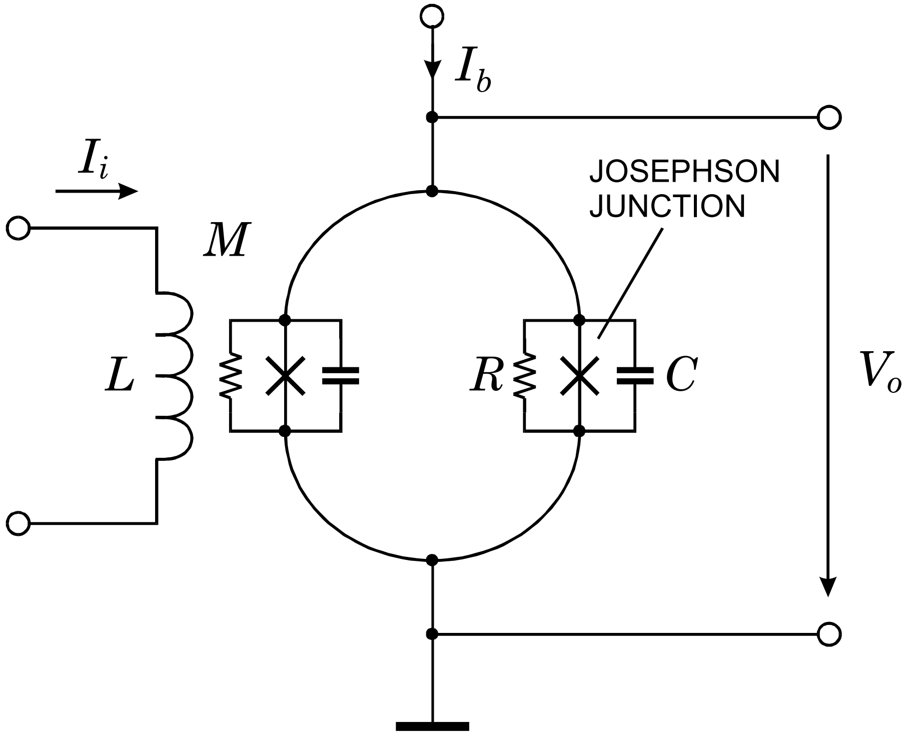

SQUID is biased by current I_b.

- Input signal is magnetic flux due to current through coupling coil L.
- Output is voltage V_o .

Output voltage V vs. magnetic flux Φ/Φ_0 as bias current I_B is increased

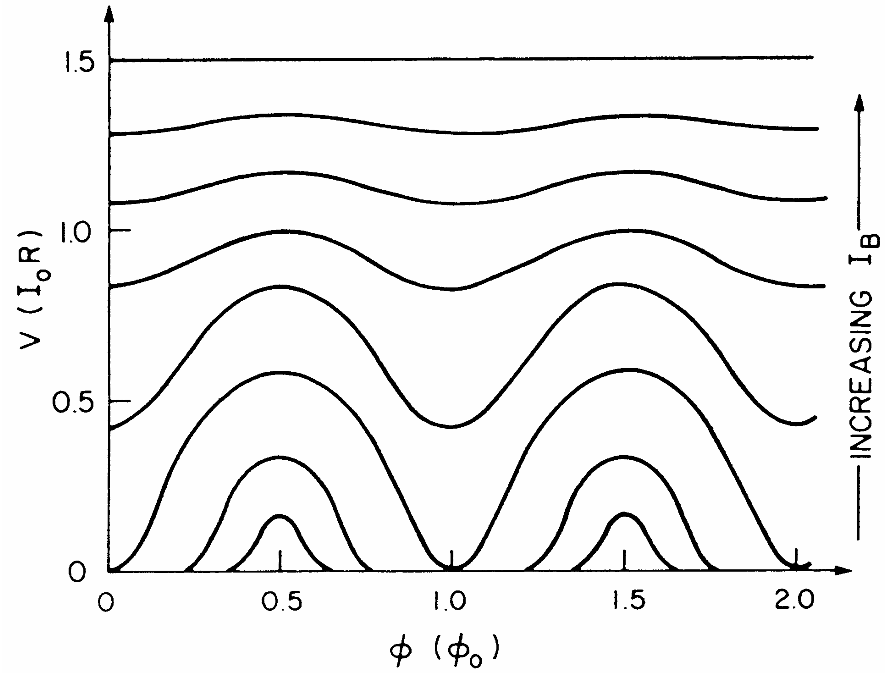

Output voltage is periodic in magnetic flux

$\Rightarrow$ Input signal must be constrained to $\pm\Phi_0/4$

Electronics must provide capability to map SQUID response and set current and flux bias levels.

Feedback

- extends range of input current
- locks flux at proper operating point (flux locked loop)

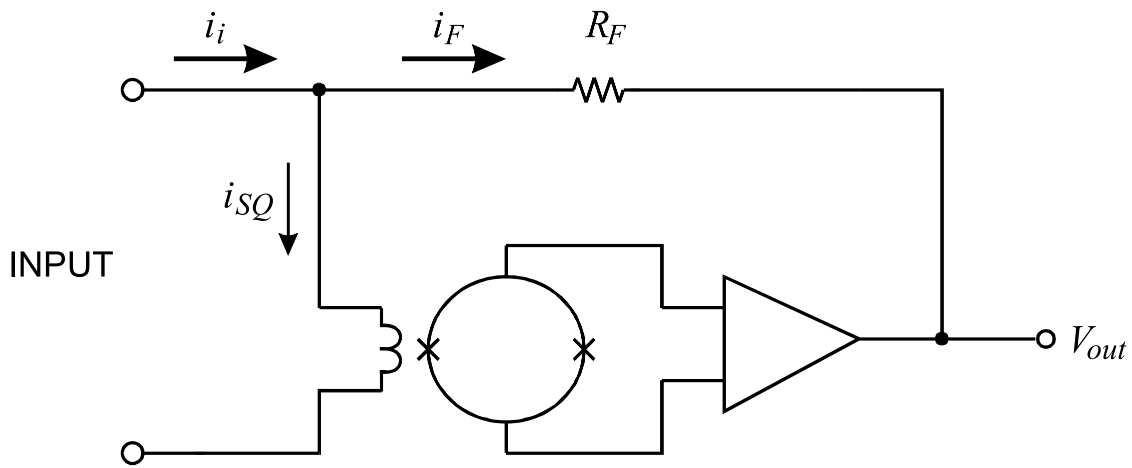

Maximum acceptable signal level grows with increasing loop gain.

Voltage bias requires input impedance ≪ bolometer resistance!

Shunt feedback SQUID amplifier achieves about 10 mΩ at 1 MHz

However: Feedback circuit limits frequency response.

Carrier Nulling

Maximum input signal to SQUID is limited, even with feedback ("flux jumping")

All of the information is in the sidebands, so the carrier can be suppressed to reduce dynamic range requirements.

Low-frequency sideband noise associated with carriers cancels (-110 dBc at 10 Hz)

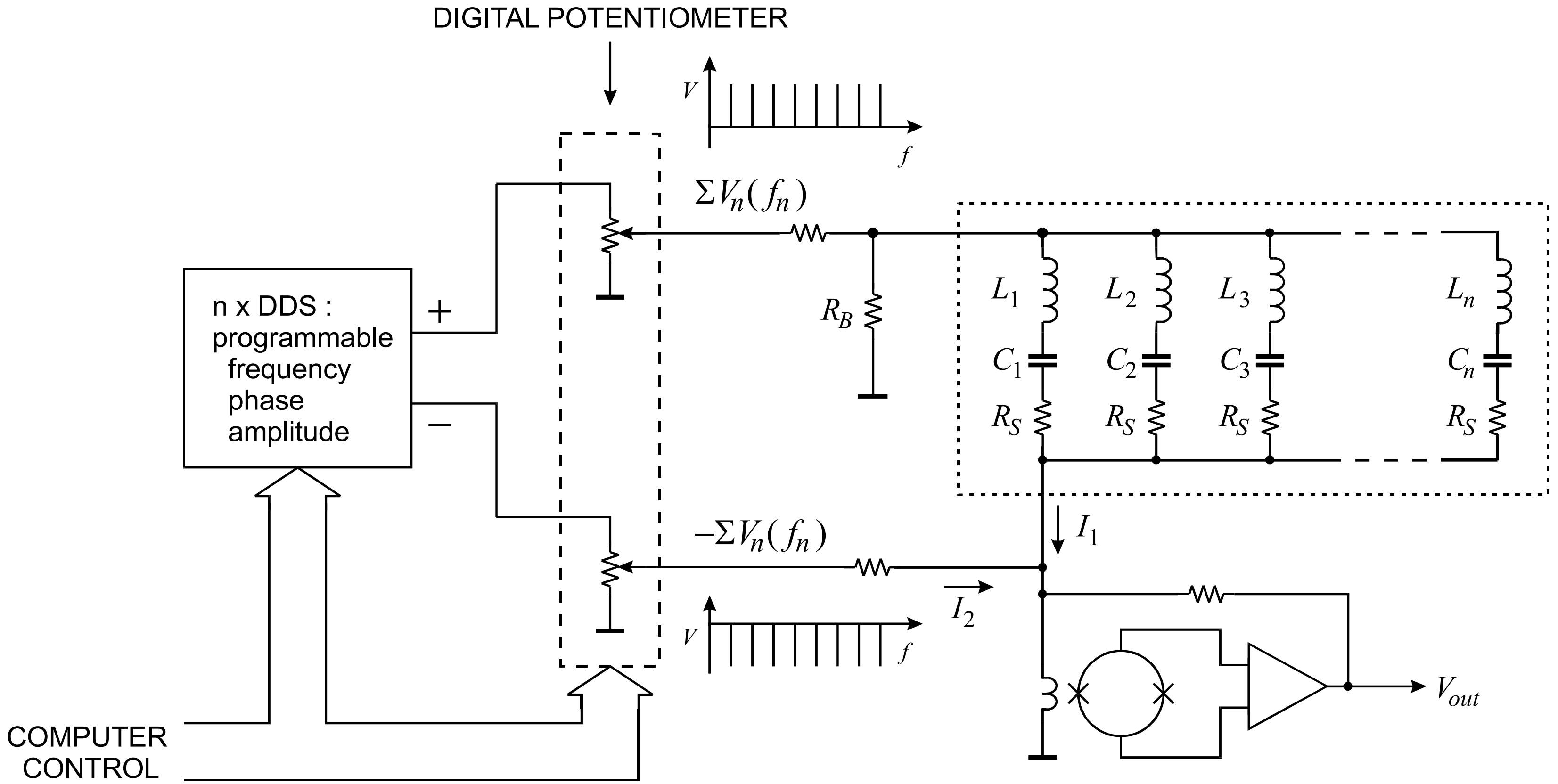

System Block Diagram

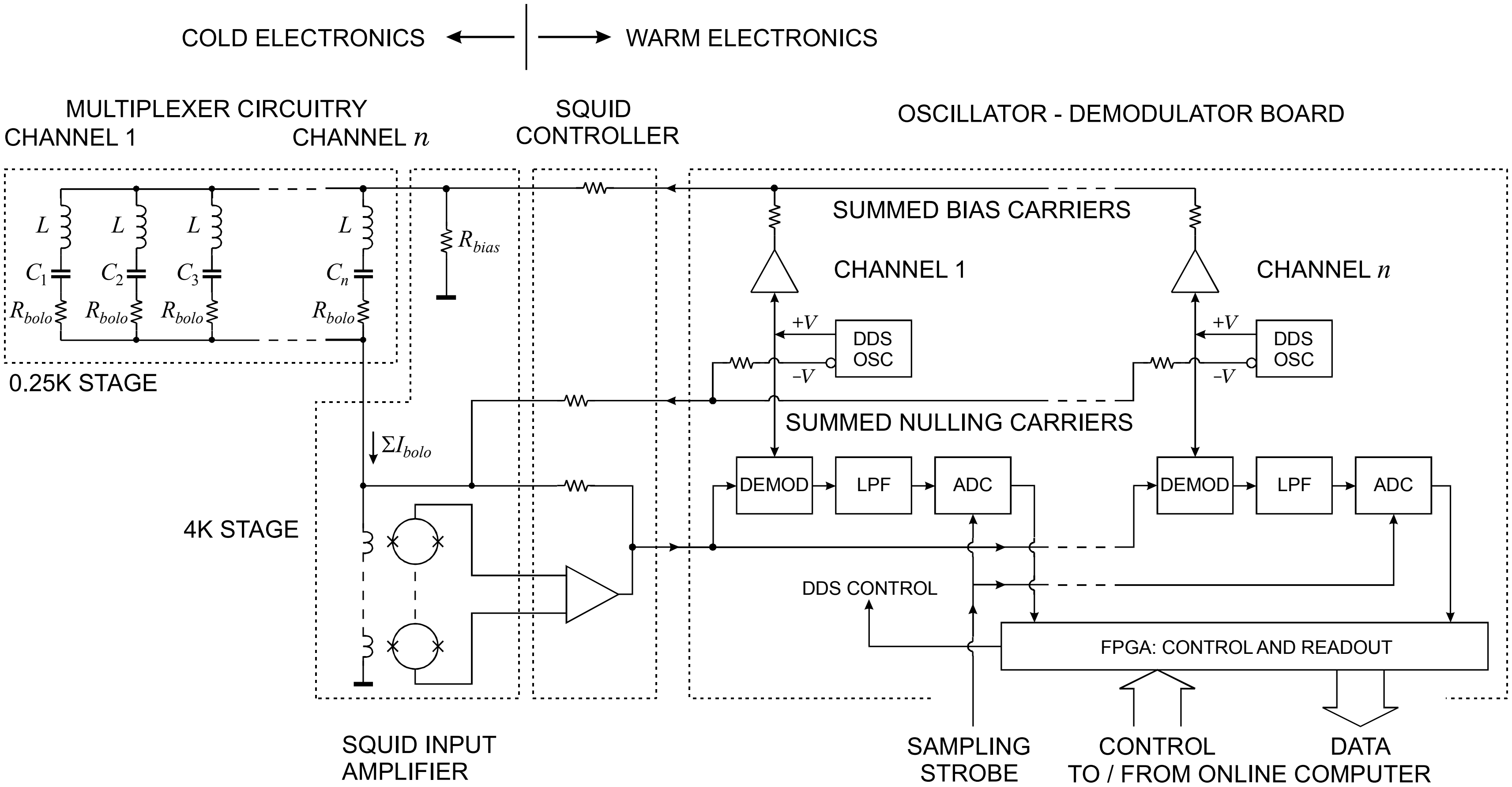

8-channel SQUID Controller

Computer-controlled (FPGA)
SQUID diagnostics
Open/closed loop
Switchable gain

SQUIDs VERY sensitive to pickup (up to GHz), so local shielding of digital circuitry is crucial.

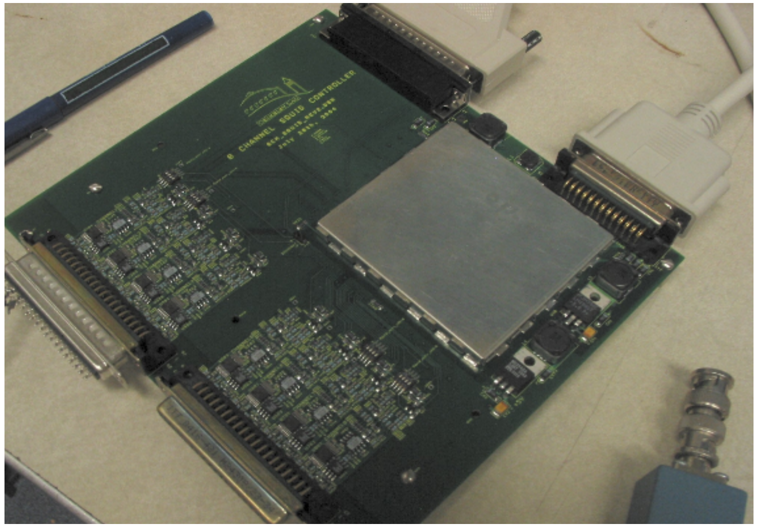

16-channel Demodulator Board

16 individual demodulator channels
1 DDS freq. generator per channel
On-board A/D
Opto-isolated computer interface

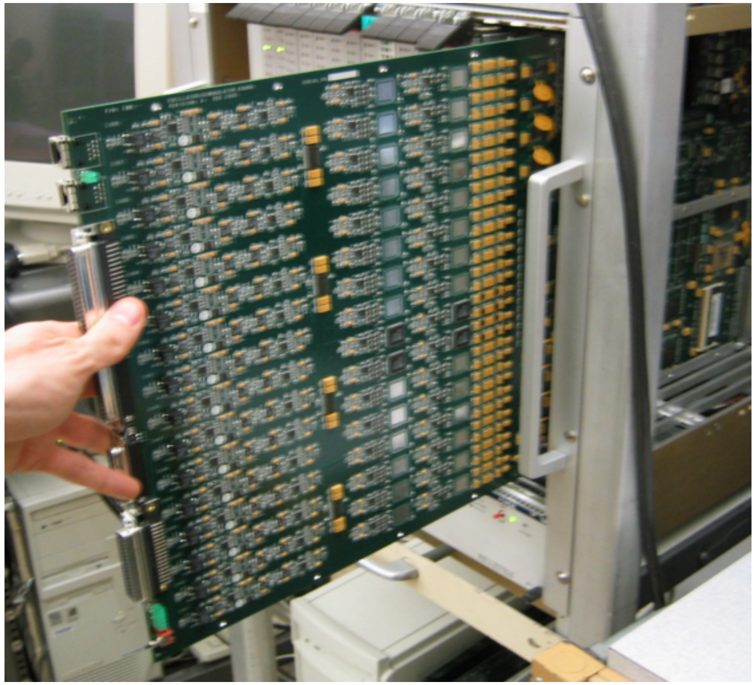

Design and prototyping at LBNL
(M. Dobbs, J. Joseph, M. Lueker, C. Vu)

Measured MUX Noise Spectrum at SQUID Amplifier Output
(Trevor Lanting)

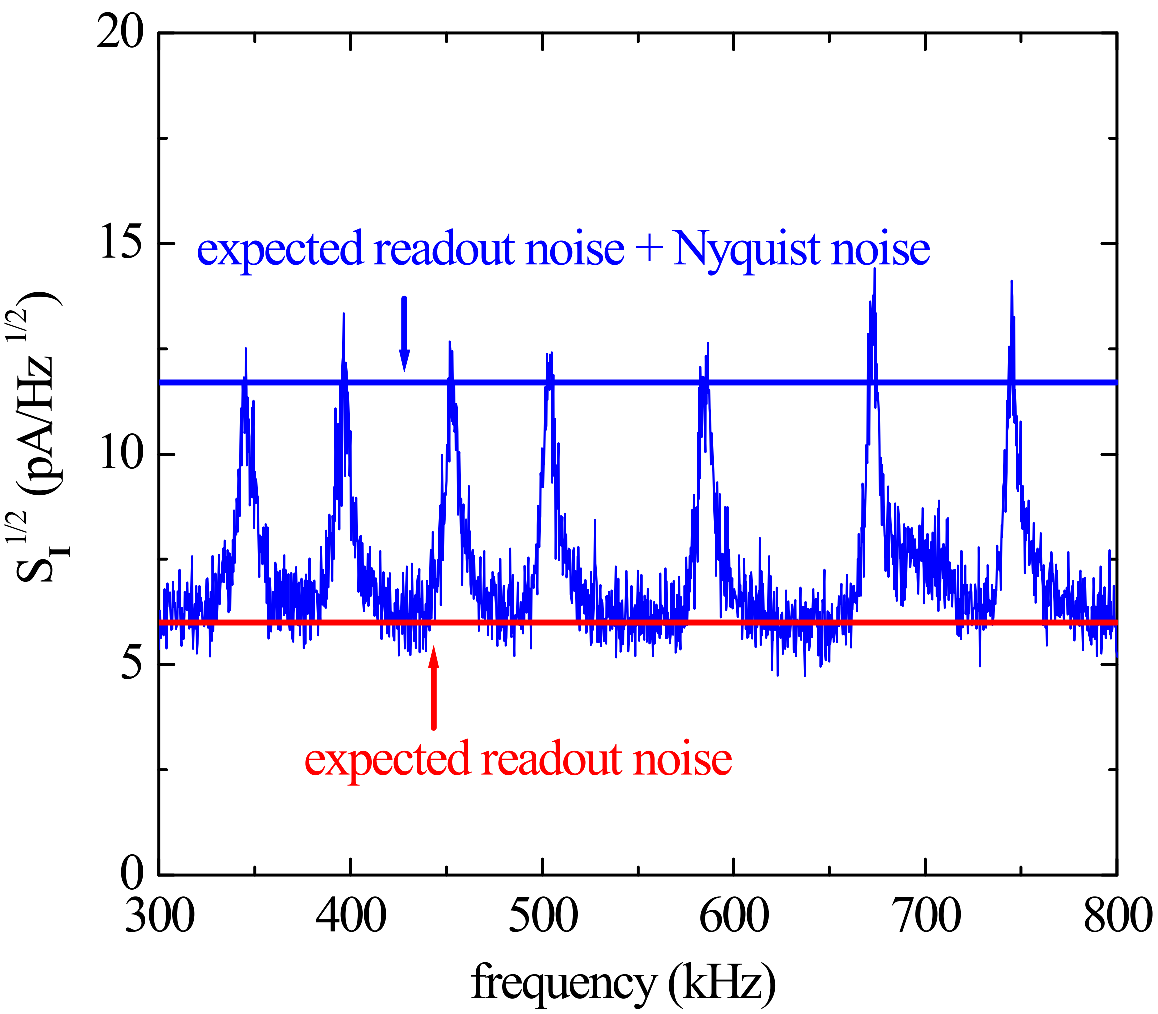

Measured Noise Spectrum in 8-Channel MUX System

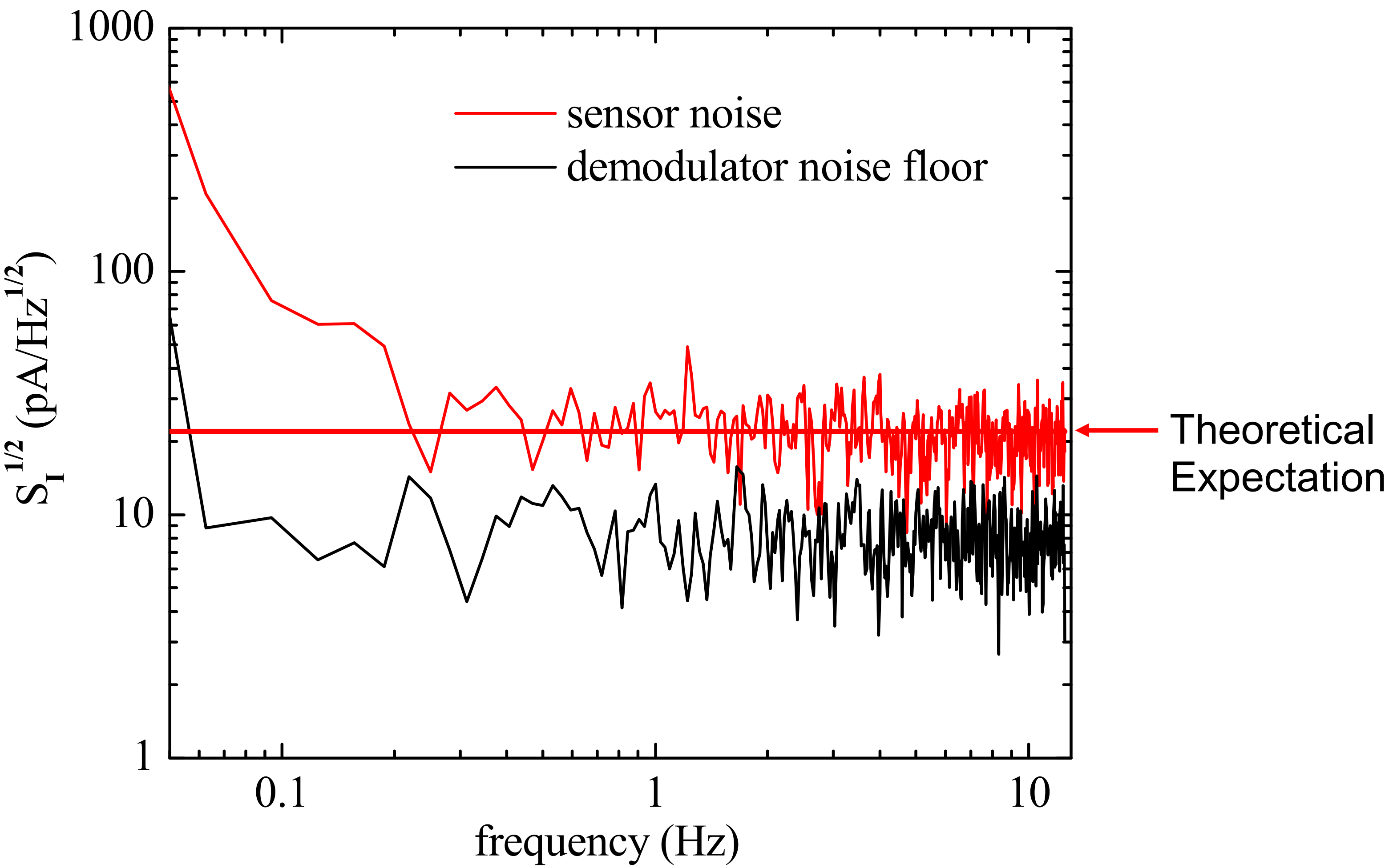

Sensor noise white above 0.2 Hz

(Trevor Lanting)

Cross-Talk < 1%

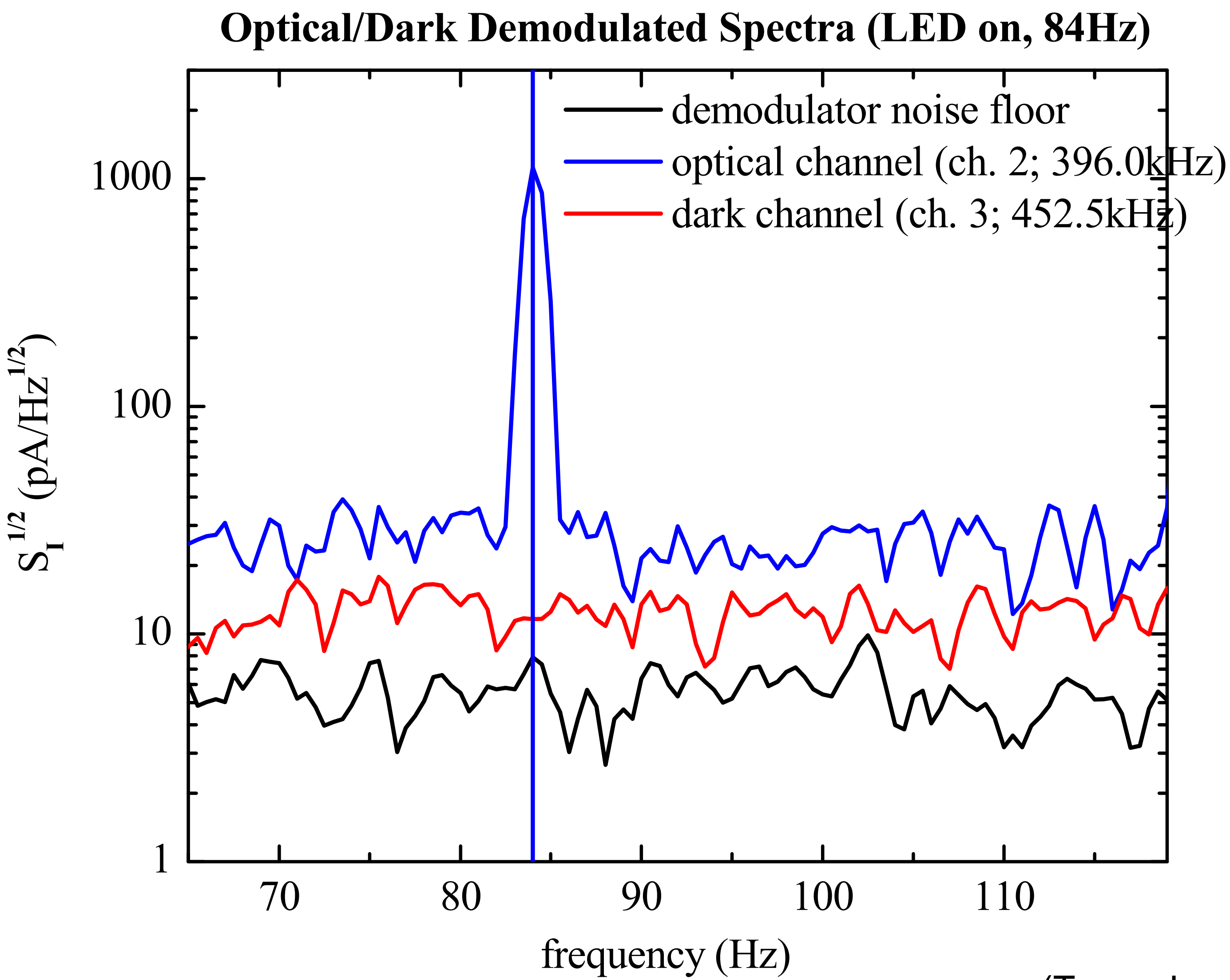

(Trevor Lanting)

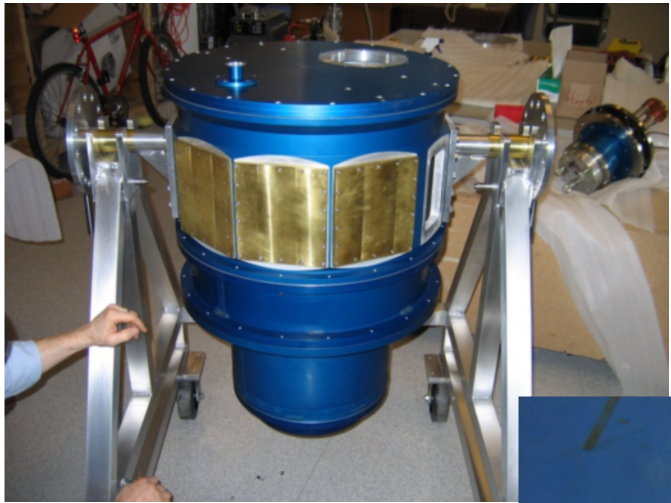

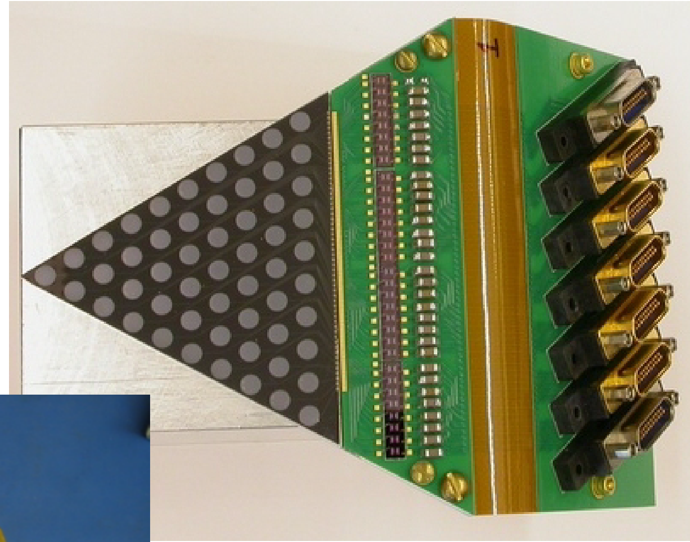

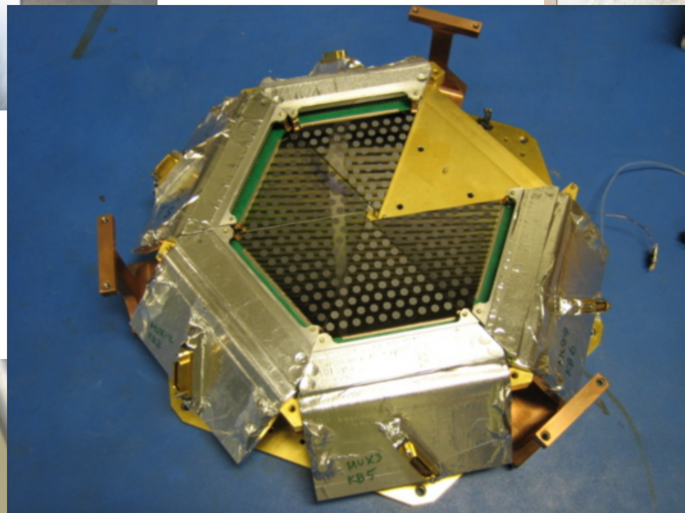

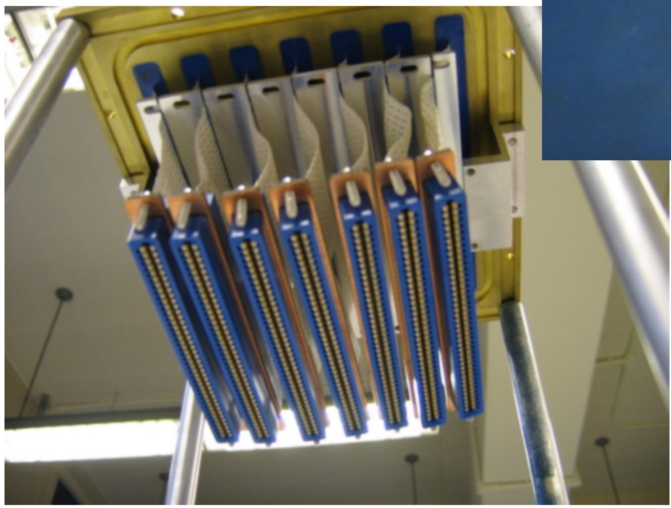

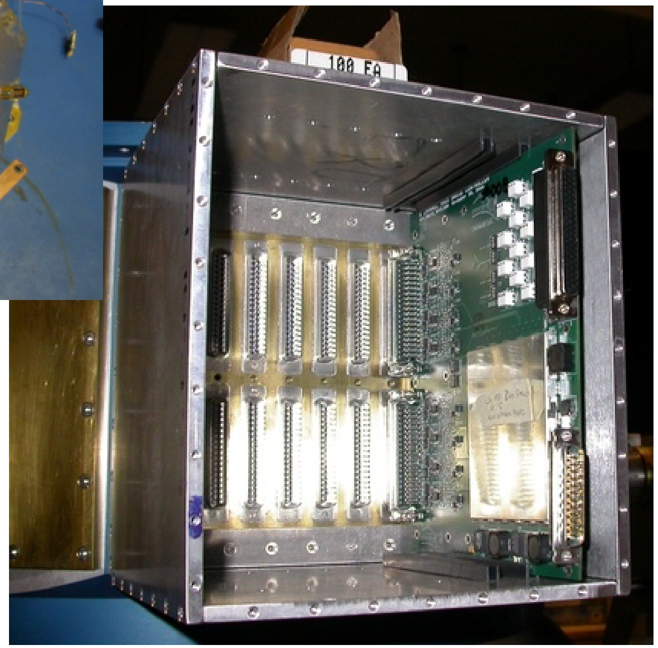
100 EA

Frequency-Domain MUX Demonstrated with Gamma-Ray Micro-Calorimeters

LLNL/UCB/LBNL collaboration

Time domain

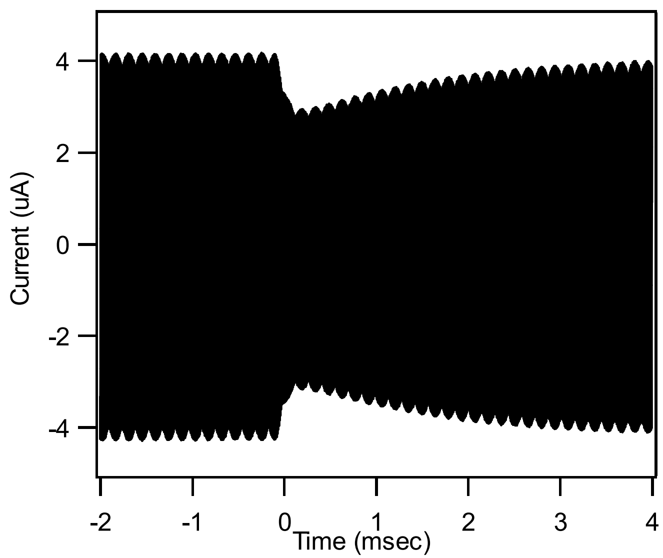

Frequency Domain

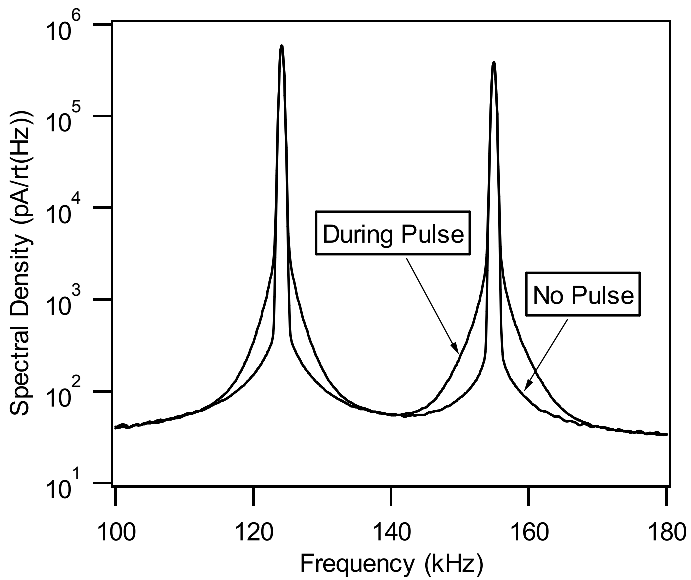

Energy resolution of 60 eV FWHM at 60 keV unaffected by multiplexer.

J. N. Ullom et al., IEEE Trans. Appl. Superconductivity **13/2** (2003) 643-648

MUXing $\Rightarrow$ increase active area, overall rate capability

Major Transition in CMB Instrumentation

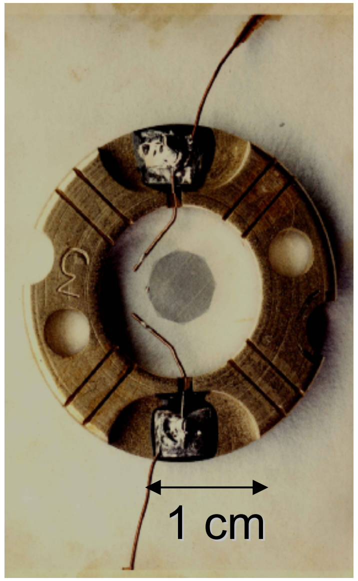

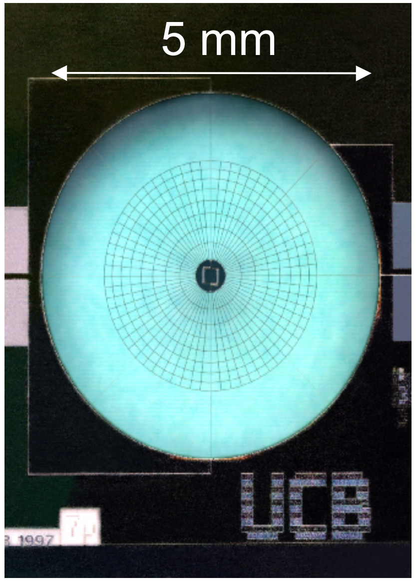

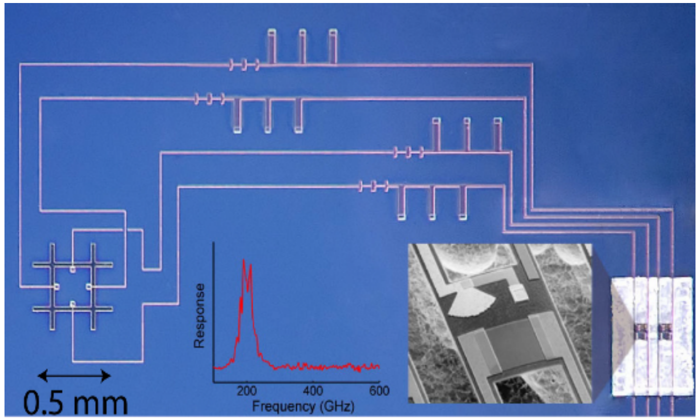

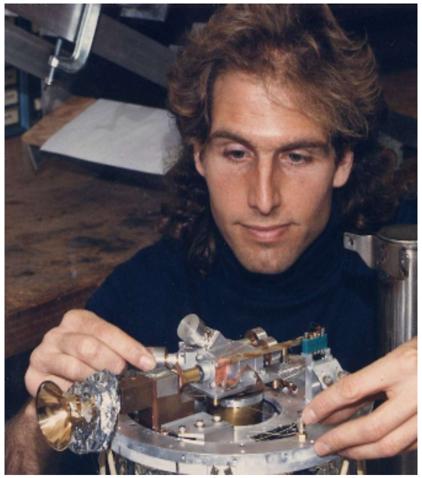

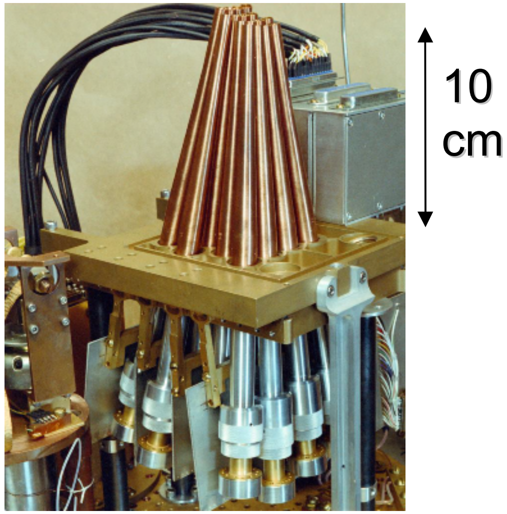

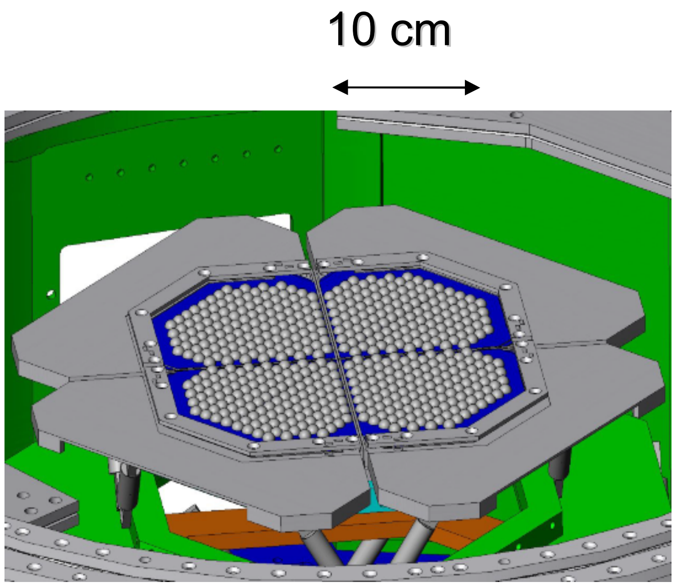

1980s

1990s

2000s

Summary

- Next-generation CMB experiments require 10^2 – 10^3 fold improved sensitivity
- Monolithic fabrication technology provides wafer-scale TES kilopixel arrays
- Antenna-coupled arrays provide polarization discrimination
- Frequency-domain MUXing demonstrated

    Zero power dissipation at 0.25K focal plane
    <1% cross-talk
    Very insensitive to vibration
    Negligible increase in noise
    Conceptually simple, but many crucial details

- System incorporates techniques from

    Cryogenics and superconductivity
    RF communications (old and new)
    Low noise analog electronics
    High Energy Physics

- Team effort between University and National Lab essential